Enhancing immune checkpoint blockade and cancer immunotherapy via tissue targeting and biomaterial nanoparticles

A Dissertation
Presented to
The Academic Faculty

By

David Francis

In Partial Fulfillment
of the Requirements for the Degree
Doctor of Philosophy in BioEngineering

Parker Petit Institute for Bioengineering and Biological Sciences
Georgia Institute of Technology

Enhancing immune checkpoint blockade and cancer immunotherapy via tissue targeting and biomaterial nanoparticles

Approved by:

Dr. Susan N. Thomas, Advisor
Department of Mechanical Engineering
Georgia Institute of Technology

Dr. Krish Roy
Department of Biomedical Engineering
Georgia Institute of Technology

Dr. Julie Champion
Department of Chemical and Biomolecular Engineering
Georgia Institute of Technology

Dr. Ned Waller
Winship Cancer Center
Emory University

Dr. Mark Prausnitz
Department of Chemical and Biomolecular Engineering
Georgia Institute of Technology

Date Approved: June 9, 2020

ACKNOWLEDGEMENTS

First, I would like to thank Dr. Susan Thomas, my advisor and mentor over the past five years. I enjoyed working with Susan every day and am extremely grateful to have had the opportunity to work in her lab. Susan provided a tremendous amount of support during the tough times I endured during graduate school, while supporting my scientific curiosity and experimental designs. Susan was an amazing scientist to work with as she has a unique background and deep understanding of scientific literature that is unmatched with anyone else I have met. Working directly with Susan over the last five years led to my development as both a scientist and person.

Next, I would like to thank both current and past members of the Thomas lab whom I've had the distinct pleasure of working with on a daily basis and now call friends. Susan's ability to recruit the highest quality students to join her lab made my time in graduate school amazing and helped me grow, both from an intellectual and personal standpoint.

Finally, I would like to thank all of those that I have had the honor of directly collaborating with on the various projects I have worked on: Maggie Manspeaker who I worked with on the first aim of my thesis who endured my style of research and continually pushed through failed experiments, with her help, we were able to extended our findings into breast cancer models which led to my first paper; Dr. Nathan Rohner who guided me greatly in my initial years in graduate school including animal work, experimental design, and everyday experiences, I am tremendously grateful to have met Nate and he had a direct influence on my overall development as a scientist; and lastly Dr. Alex Schudel who is a gifted scientist and great friend, working with him led to scientific discussions nearly every day that helped me grow as a scientist and led to the success of both my first and second paper.

Table of Contents

LIST OF FIGURES

SUMMARY

Enhancing immune checkpoint blockade and cancer immunotherapy via tissue targeting and biomaterial nanoparticles

Immune checkpoint blockade (ICB) has emerged in recent years as one of the most promising new cancer therapies. However, a significant majority of patients receiving these therapies 1) do not respond, 2) experience adverse side effects, or 3) respond initially but relapse. Overcoming these limitations is therefore a critical hurdle in improving these treatments. Checkpoint pathways are active in both the tumor microenvironment and lymphoid tissues where they prevent T cell cytotoxic function and activation, respectively. While improving tumor and lymphoid delivery of these therapies offers a promising approach to advance the efficacy of ICB, clinical applications of ICB have so far only relied on systemic administrations, which often result in poor tumor and lymphoid accumulation. Additionally, administration of combination immunotherapies outside of ICB is challenging as many of these drugs are short-lived *in vivo,* are insoluble in aqueous solvents, and are not targeted to the cells of interest leading to off-target side effects. Given the current state of ICB therapy, the focus of this thesis work is to address the drug delivery barriers associated with conventional systemic administrations and non-targeted delivery of immune modulators. This work explored two unique delivery strategies: one which proposes drugging tumor draining lymph nodes with ICB therapies by way of lymphatics using local rather than systemic administrations to enhance anti-tumor efficacy; and the second which proposes a novel drug-eluting ICB platform by engineering an antibody-nanoparticle conjugate system for improved T cell targeting and sustained delivery of small molecule immunotherapies.

CHAPTER 1. INTRODUCTION

1.1 Motivation

Immunotherapy has emerged as the most promising new treatment approach for an array of advanced malignancies *(1)*. Many of these therapies work directly on T lymphocytes, specifically cytotoxic CD8 T cells, by promoting proliferation and re-invigorating cytotoxic potential by blocking suppressive pathways *(2)*. In particular, immune checkpoint blockade (ICB) using monoclonal antibodies (mAbs) such as anti-Programmed Death 1 (aPD1) and anti-Cytotoxic Lymphocyte Associated Protein 4 (aCTLA) are increasingly utilized as cancer immunotherapeutic agents due to their capacity to specifically recognize cell surface markers on immune cells and modulate their signaling effects to enhance anti-tumor adaptive immunity. Furthermore, many other immune pathways have been identified and targeted for drug modulation using traditional small molecule drugs by way of inhibitors or antagonists including the transforming growth factor beta (TGFβ) and adenosine pathways *(3, 4)*. The use of these cancer immunotherapies and others has generated unprecedented improvements in survival including complete, durable responses unseen with chemotherapies.

Although many immunotherapies generate robust and durable responses, a majority of patients do not respond to such treatments or respond initially but experience relapse after initial response *(5, 6)*. Moreover, treatment associated toxicities are prevalent due to systemic accumulation of therapies leading many patients to stop these therapies *(7)*. Thus, there is an urgent need to better elucidate these therapies and look for ways to improve their efficacy while reducing side effects. Due to the integral role T lymphocytes have in robust anti-tumor immune responses, there is interest in improving the delivery of immunotherapies to these cells found throughout the

body including lymphoid tissues, where they are primed and activated, and the tumor microenvironment (TME), where they carry out their effector function by way of tumor killing. Modifying administration route represents an interesting approach to modulate mAb pharmacokinetics due to their large and thus unique biodistribution following cutaneous injections. Furthermore, combination of multiple immunotherapies has emerged in recent years as a promising approach to improve efficacy as inhibition of multiple, non-redundant pathways can augment T cell function and prevent secondary relapse. Hence, formulation changes to improve codelivery of mAb and small molecule therapies to the same cell of interest in order to concurrently modulate multiple pathways are of high interest. Despite different administration routes being recently explored for ICB therapies to improve patient compliance *(8)*, the effects on mechanism of action have not been explored. Furthermore, advances in drug formulations have primarily been focused on instant release strategies, rather than sustained drug release.

The overall goal of this work is to investigate the effects of drugging immune checkpoint pathways in tissues where they are active, including the TME and lymphoid tissues while rationally designing a biomaterial platform capable of delivering multiple immunotherapies to cells of interest. We addressed this by utilizing four different administration routes to enable drugging of the TME, spleen, tumor draining lymph nodes (TdLNs), and non-tumor draining lymph nodes (nTdLNs) and monitored the effects on the anti-tumor response and toxicity. In order to drug T cells with multiple therapies simultaneously, we developed an antibody-nanoparticle conjugate (ANC) platform designed to 1) harness the conjugated antibody as both a targeting protein and therapeutic and 2) release small molecule immunotherapies over a prolonged period of time. By employing these two approaches, we demonstrate improved anti-tumor immune responses by way of both efficacy and toxicity which presumably results from enhanced delivery of immunotherapies to tissues and cells of interest *in vivo*.

1.2 Specific Aims

1.2.1 Specific Aim 1: Evaluate the effects of ICB in the TME and TdLNs by different administration routes in multiple mouse tumor models.

My *working hypothesis* is that ICB therapies can be improved by enhancing the delivery of these drugs to the tissues of interest, specifically where these pathways are active, i.e. the TME and TdLN as tumor associated antigen is present in the LNs thereby enabling the activation of tumor specific T lymphocytes. To explore this idea, this aim will focus on different administration schemes including; 1) intraperiterional (i.p.) – current standard in mouse models comparable to intravenous (i.v.) administration done in the clinic that results in systemic mAb distribution with minimal accumulation in the TME and lymphoid tissues, 2) intratumoral (i.t.) – results in high mAb delivery to both the TME and TdLN, 3) ipsilateral forearm (i.l.) – results in high delivery to the TdLN, and 4) contralateral forearm (c.l.) – results in high delivery to a nTdLN. Through the use of *in vivo* mouse tumor models (melanoma and breast cancers), we were able to assess the biodistribution of mAbs following different routes of administration and subsequently investigate the effects on the anti-tumor immune response, specifically the efficacy and immune related adverse events (iRAE). We demonstrate that following cutaneous administration routes (i.e. i.t., i.l., and c.l.), we achieve high mAb concentrations in draining lymph nodes (dLNs), specifically the TdLNs following i.t. and i.l. administrations and the nTdLNs following c.l. administration. Furthermore, mAb that accumulates in dLNs has access to the deeper areas of LNs where T cells reside. Similar levels of mAb accumulate in the spleen while only using an i.t. administration results in appreciable tumor concentrations of mAb allowing for careful investigation into drugging different tissues. *In vivo,* we show i.l. administration improves anti-tumor responses comparable to i.t. administration, in other words, drugging the TdLN selectively results in

comparable efficacy to drugging both the TdLN *and* TME suggesting the TdLN has a prominent role in mediating ICB efficacy. To extend our findings, we performed dose titration studies to explore whether lower doses could maintain efficacy, while reducing off-target tissue mAb accumulation and toxicities, a major barrier in ICB therapies. We found i.l. and i.t. administrations could reduce dosing by an order of magnitude while concomitantly reducing mAb accumulation in systemic tissues. These results suggest the importance of TdLNs for generating robust anti-tumor immune responses and that simply modifying the route of administration allows for efficient targeting of these tissues.

1.2.2 Specific Aim 2: Engineer an ANC platform to enable codelivery of mAb and small molecule drugs to augment immunotherapies.

My *working hypothesis* is small molecule immune modulators are ineffective as they are not targeted to their cells of interest and thus can be improved by targeted and sustained delivery to T cells using antibody- or affinity-directed carriers to prolong interaction with T cells leading to improve efficacy. This can be achieved using poly(propylene sulfide) NPs as 1) the hydrophobic core of the NP allows for encapsulation and sustained release of small molecule drugs and 2) the versatile corona can be derivatized to conjugate mAbs to the surface to act as both targeting and therapeutic proteins. This aim first focused on synthesizing an ANC platform that retains the binding ability of the mAb and whether encapsulated drug molecules into the core of the NPs could sustain drug modulation. The second part of this aim focused on applying the ANC platform to *in vivo* mouse tumor models to improve cancer immunotherapy applications. To engineer ANCs, we employed a very mild synthesis scheme in order to maintain the antigen binding fragment (Fab) affinity which was done using a reducible disulfide chemistry in aqueous conditions. Using this scheme, we show control over the degree of mAb thiolation and thus can control mAbs per NPs while maintaining binding affinity to T cells. Using *in vitro* experiments, we demonstrate the

ANCs can target lymphoma T cells and deliver paclitaxel, a chemotherapeutic, over a prolonged period of time while controlling the drug loading into the ANC thus highlighting the drug eluting potential of this system. These results highlight the feasibility of targeting antigen expressing cells along with sustained drug modulation to target cells requiring no stimuli other than time related diffusion. We further demonstrate the capability of this platform using combination therapy with ICB mAbs and encapsulated small molecule immune modulators, specifically using a (TGFβ) inhibitor and adenosine receptor antagonist (ArA) to target non-redundant pathways. We demonstrate targeted (PD1 or CTLA4) ANCs afford an improved therapeutic outcome compared to non-targeted isotype-ANCs by way of reduced tumor burden and prolonged animal survival. These results highlight the versatility of this ANC platform to deliver a range of both mAbs and small molecule drugs to target cells as well as suggest the enhancement of immunotherapies may lie in the co-delivery of multiple modulators to T cells.

1.3 Significance

The work presented herein provides insight on various immunotherapies, specifically the mechanisms of action for two ICB mAb therapies at the tissue level and innovations in drug delivery strategies to co-deliver therapies to checkpoint expressing cells for improving anti-tumor response rates. First, this work identifies TdLNs as a therapeutic tissue of interest for ICB immunotherapies, an idea mentioned in the field, but scarcely explored. To this end, drugging TdLNs augments the efficacy and reduces toxicities; a concept that has not been thoroughly explored to our knowledge. Second, this work has engineered a unique drug delivery carrier capable of sustained delivery of small molecule therapeutics without requiring a stimulus to release cargo, a major barrier for prolonged drug delivery to T lymphocytes.

Specific Aim 1. While much research has gone into understanding how and why checkpoint therapies work in some cancer patients and not in others, most of this research has primarily focused on exploring systemic effects from the blood, with emerging literature exploring the TME. Few studies have gone into understanding how these therapies work in the TdLN or the priming phase of the adaptive immune response. However, lymphoid tissues, specifically the spleen, have emerged in recent years as important tissues for ICB efficacy in chronic infections *(9, 10)*. In the context of cancer, the TdLN may be a more appropriate tissue as it is bathed in tumor associated antigen and tumor specific T cells may be generated here. Furthermore, TdLNs are important in controlling cancer dissemination. Utilizing local, cutaneous administration routes to target the TdLNs allows for an order of magnitude increase in mAb exposure relative to a systemic administration routes (i.p./i.v.), and thus dose sparing with reduction of accumulation in systemic tissues that contribute to iRAEs. Utilizing a local administration also enables mAb to access 100% of LN-resident T cells by 24 hours after injection, a phenomenon not thought possible due to the size restriction barriers within the LN. This approach provides broad insight into the mechanisms of action for ICB in the cancer setting, specifically that ICB provides assistance in activation and proliferation of tumor specific lymphocytes outside of the TME and has potential for translation into the clinic and other ICB mAb therapies.

Specific Aim 2. Drugging multiple signaling pathways in T cells has the ability to improve anti-cancer immune responses as monotherapies consistently fail patients due to upregulation and exploitation of other pathways by cancer cells. However, many small molecule therapeutics have short circulation times, accumulate nonspecifically in blood rich systemic tissues leading to toxicity and side effects due to their pleiotropic effects, and the scarcity of tumor and blood resident T cells make the probability of drug interaction unlikely following administration. This has spurred the development of targeted delivery platforms including antibody-drug conjugates (ADCs) as

they enable targeted delivery to the cognate ligand of the Fab sequence. However, many small molecule therapeutics are hydrophobic making them challenging to conjugate and keep soluble post conjugation to mAbs. Furthermore, chemical modifications of small molecule drugs can diminish drug activity by changing the drug structure and binding to target proteins. Amphiphilic polymer nanoparticles are alternative drug carriers that overcome the aforementioned solubility and circulation time barriers. However, delivery to T cells is challenging due to their lack of phagocytosis/pinocytosis. To overcome this barrier, we engineered an ANC that has the ability to target non-phagocytic T cells based off the conjugated mAb Fab specificity, and does not require chemical modification of the drug, but instead relies on encapsulation to retain the drug efficacy. Therefore, using an ANC can improve interaction of small molecule drugs with T cells while concurrently blocking the cognate pathways to the Fab specificity (i.e. anti-PD1 can target PD1 expressing cells while also blocking ligand binding to PD1). Moreover, this ANC system enables encapsulated drug to slowly diffuse out of the NP core based off the molecular weight and logP of the molecule, meaning the NP does not require a stimulus (e.g. intracellular lysosomal degradation or enzyme presence) to release and allow drug cargo to act on target, an ideal feature when targeting inert cells like T lymphocytes. Furthermore, this platform allows for dramatic increases in drug loading; most ADCs are limited to 2-10 drugs/mAb *(11)* whereas this ANC can encapsulate ~100-500 drugs/NP or mAb pending the mAbs per NPs. Therefore, a drug depot or drug eluting ICB platform results since drug release from the ANC is sustained and time dependent which allows for a wide variety of T cell immunotherapeutic applications including; teasing out the effects of dual targeting of independent pathways in the same cell vs multiple interventions not designed to target the same cell can impact drug efficacy.

CHAPTER 2. BACKGROUND AND LITERATURE REVIEW

2.1 Cancer Immunotherapy

Cancer immunotherapy has emerged in recent years as one of the most promising new types of therapy and is providing a paradigm shift for cancer treatment. Unlike traditional cancer interventions (i.e. surgery, radiation, chemotherapy), immunotherapy works with the patient's immune system through a variety of ways including reinvigoration of T cells and has immense potential for generating long-term responses against the primary tumor, metastatic tumors, and recurring tumors after initial therapy. In order for immune cells to eliminate cancer cells, a series of steps must be carried out, known as the cancer immunity cycle. This cycle requires; 1) tumor associated antigen to be released in the TME, 2) uptake of this antigen by APCs, 3) activation of naïve lymphocytes – generally in lymphoid tissues like the TdLN, 4) trafficking of activated lymphocytes from the TdLN to the TME, and 5) recognition and elimination of cancer cells by lymphocytes *(12)*. When this cycle is compromised, cancer cells evade immune destruction and continue to grow. One way cancer cells have evolved to evade immune destruction is by harnessing immune checkpoint pathways, which are generally surface receptors found on both cancer and immune cells. Upon engagement of these proteins, immune cells are generally suppressed, either at the tumor killing stage or the activation stage in the case of T cell checkpoint pathways. Thus, therapies to block these particular inhibitory pathways have been developed to reinvigorate immune cells and enable an effective anti-cancer immune response, known as ICB therapy. In addition to ICB, many other immunotherapies have been discovered that contribute to immune suppression and thus cancer progression. Two rather interesting pathways that differ from immune checkpoints, but have interactions are the TGFβ and adenosine pathways which promote immune exclusion in the TME and suppress T cell function.

This background will discuss further details on immune checkpoint pathways including their roles, expression, effects on the anti-cancer immune response, and ICB therapies. The TGFβ and adenosine pathways will also be discussed further delineating their role on immune suppression and current therapies targeting these pathways.

2.1.1 Checkpoint pathways and mAb inhibitor therapies

Cytotoxic T-lymphocyte-associated protein 4. CTLA4 is a transmembrane receptor found on a variety of T cells including activated, memory, cytotoxic, and regulatory cells as well as B cells *(13)*. In contrast to CD28, a stimulatory co-receptor, CTLA4 acts as an inhibitor of T cell activation promoting an anergic phenotype similar to TCR stimulation alone (Fig. 1) *(14)*. Although counterproductive to cancer therapy, CTLA4 is vital for homeostasis as deletion of Ctla4 in mice leads to a fatal, rapidly progressive lymphoproliferative disease causing death by 3-4 weeks of age in mice suggesting a role in lymphoid tissues *(15)*. The expression of CTLA4 is induced following TCR stimulation and is thus rarely found on resting T cells, in fact CTLA4 expression is enhanced by CD28 costimulation *(16)*. Following TCR engagement, CTLA4 is trafficked from intracellular vesicles to the cell surface *(17, 18)*. Maximum protein expression of CTLA4 is around 24-48 hours post-TCR stimulation and decreases thereafter, however antigen experienced memory CD4 and CD8 T cells as well as regulatory T cells (Tregs) constitutively express CTLA4 *(19)*. While CD4h, CD8, and Tregs all express CTLA4, it appears to be most important on Tregs as it promotes their suppressive function and is constitutively expressed at high levels *(20)*. One of the main ways CTLA4 inhibits T cell function is by out-competing CD28 for the B7 ligands found on APCs leading to inadequate T cell stimulation *(21)*. CTLA4 has a higher affinity and avidity for B7 ligands allowing it to exert inhibitory functions at lower expression levels compared to CD28 which is critical as this generates a threshold for activation to limit low-affinity and self-reactive T cell activation. In addition to competing with CD28 for B7 ligands,

CTLA4 expressing cells have been shown to acquire B7 ligands from APCs by a trans-endocytosis process leading to degradation of B7 ligands in lysosomes of T cells *(22)*. This process leads to lower B7 ligand expression and availability on APC surfaces providing another explanation for the suppressive effects of CTLA4.

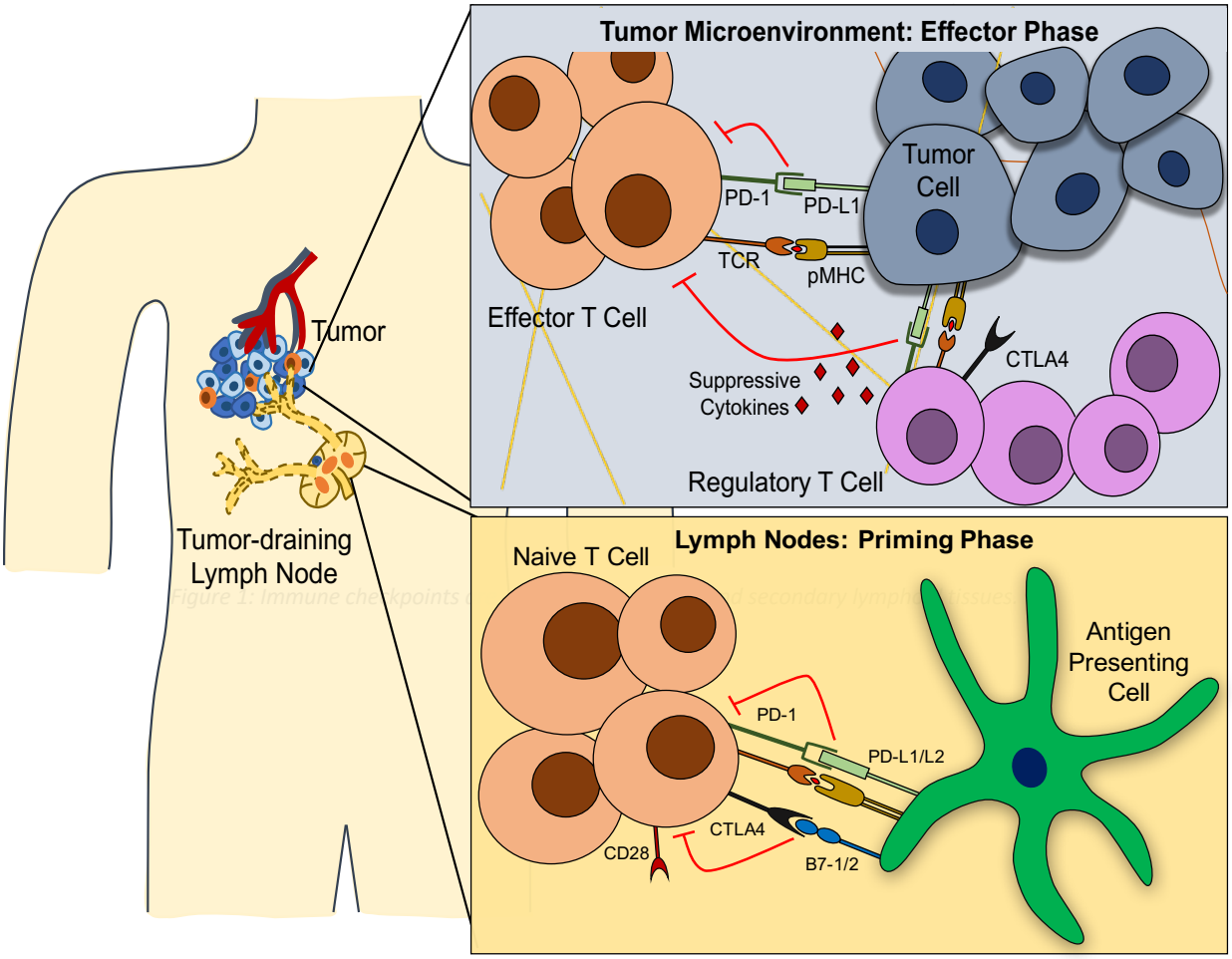

Figure 1: Immune checkpoints are active within tumors and secondary lymphoid tissues. Top: In the TME, effector T cells primarily express PD1 and become exhausted upon chronic engagement with PDL1 by tumor cells. Tumor resident Tregs express PD1 and CTLA4 and upon engagement with cognate ligands may secrete suppressive cytokines (e.g. TGFβ) leading to tumor progression. Bottom: In LNs, T cells undergoing activation by APCs rapidly express both PD1 and CTLA4 post TCR engagement dampening T cell activation via exhaustion or anergy leading to cancer progression.

Programmed Death-1 & Programmed Death-Ligand-1/2. Similar to CTLA4, PD1 is an inhibitory transmembrane receptor found primarily on activated T cells with minimal expression

on resting immune cells restrained primarily to activated cells including T, B, NK, NKT cells, DCs, and macrophages *(23, 24)*. In studies exploring the role of PD1, knockout PD1 mice leads to a delayed-onset tissue specific autoimmune disease after 6 months of age suggesting the role for PD1 to be at peripheral tissues *(25)*. Further studies of PD1 have been in the context of chronic infections where blockade of the PD1 pathway restores T cell function and thus helps protect the host from tissue destruction in a chronic antigen stimulation setting *(26)*. Furthermore, it has been shown PD1 is highly expressed on dysfunctional T cells during chronic infections, but not expressed on resting memory T cells in an acute infection *(27)*. PD1 has two known ligands, PD-ligand 1 (PD-L1) and PD-ligand 2 (PD-L2) where PD-L1 is broadly constitutively expressed on hem atopoietic cells (T, B, DCs, and macrophages) and nonhematopoietic cells (endothelial and epithelial cells) whereas PD-L2 has a more restricted expression found on DCs, macrophages, and mast cells (Fig. 2) *(24, 28)*. Both ligands are inducible by inflammatory signals including type I and II IFNs and TNF-alphas for PD-L1 and IFN-gamma, GM-CSF, and IL-4 for PD-L2 highlighting the importance of this pathway in regulating effector T cell responses in both peripheral and lymphoid tissues *(28)*. In addition to inhibiting effector T cells, PD1 plays an important role development, maintenance, and function of Tregs. PD-L1 on APCs has been shown to induce Treg differentiation and helps to maintain their suppressive capabilities *(29)*.

Clinical checkpoint inhibitor therapies. As these pathways emerge and become better understood, drug development has explored ways to block these inhibitory pathways and restore effector function and inhibit regulatory T cells for cancer immunotherapy. This has primarily been through the use of mAbs that are nonstimulatory and bind to different epitopes than endogenous ligands leading to blocked interactions.

Anti-CTLA4 in Cancer. Due to the widespread expression of the inhibitory receptor, CTLA4 on activated T cells, it became a prime target after it was discovered *(30)*. In immunogenic

tumor models, it demonstrates delayed tumor growth and rejection of implanted tumors *(30)*. Moreover, aCTLA4 can promote immune memory leading to subsequent rejection of a second tumor without any additional anti-CTLA4 *(31)*. In less immunogenic tumors, combination of aCTLA4 with another agent is usually required including radiation, chemotherapy, or a cancer vaccine – these all suggest that any method of providing a tumor associated antigen in combination with aCTLA4 will lead to synergy by rejecting T cell tolerance to these antigens leading to enhanced anti-tumor efficacy *(32–35)*. On a mechanistic level, aCTLA4 can mediate its effect on both the regulatory and effector T cell compartments *(36)*. Numerous studies have shown aCTLA4 when injected in the TME leads to the elimination of tumor resident Tregs by an analogous method to antibody dependent cellular cytotoxicity where aCTLA4 will coat constitutively CTLA4 expressing Tregs and tumor resident macrophages will subsequently eliminate these decorated Tregs *(37–39)*. This is due to the Fc region of the aCTLA4 clone used as some clones will bind to Fc gamma receptors found on macrophages whereas some will not. However, studies have shown isolated blockade on the Treg or effector cell compartment does not lead to anti-tumor efficacy and concurrent blockade of both compartments is necessary *(36)*. As previously mentioned, CTLA4 has roles in preventing activation of lower affinity TCRs, however the use of aCTLA4 has been shown to broaden the tumor specific CD8 T cell repertoire while not affecting the numbers of pre-existing tumor specific T cells prior to therapy *(40)*. This data suggests a role for aCTLA4 not only in the TME, but also in lymphoid tissues where CTLA4 expressing CD8 T cells are prevented from activation until CTLA4 blockade occurs.

Anti-PD1 and Anti-PDL1 mechanism. From early studies in chronic infections, especially viral infections, the PD1:PD-L1 pathway become an exciting target in cancers *(41)*. PD1 is expressed by many tumor-infiltrating lymphocytes (TILs) and PD-L1 by numerous cancers and tumor resident myeloid cells suggesting a role in tumor progression *(42, 43)*. Many studies have

explored blocking this pathway in hopes to restore reinvigorating exhausted T cells *(44–46)*. PD1 blockade has been shown to enhance T cell cytokine production thereby restoring some of the cytotoxic capabilities which may lead to anti-tumor efficacy *(47)*. Interestingly, it has also been shown that the PD-1 pathway also has a role during the naïve-to-effector activation and differentiation in lymphoid tissues motivating the modulation of this pathway here *(48)*. Furthermore, literature has shown PD1 blockade acts on an exhausted stem cell like CD8 T cell in lymphoid tissues that promotes proliferation of these cells leading to effector like CD8 cells and reductions in viral loads *(9, 49)*. Similar to aCTLA4 mAbs, the specific clone of aPD1 and aPDL1 mAbs appears to have an effect in anti-tumor efficacy. Based on the Fc region of the IgG clone used, differential affinities for Fcγ receptors can enhance or diminish the response thereby warranting careful consideration of the clone used in therapeutic experiments *(50, 51)*. These literatures suggest a role of PD1 blockade in both the TME (effector phase) and also the lymphoid tissues (priming phase) motivating the hypothesis of enhanced delivery to the TME and TdLN.

Dosing effects on ICB efficacy and toxicity. The dosage of mAb administered is an important criterion that can greatly affect therapeutic response. Accordingly, clinical studies have established a dose-toxicity relationship for anti-CTLA-4 therapy indicating that higher doses lead to better response rates but with concurrent increases in iRAE. In a study with patients with advanced melanoma, anti-CTLA-4 mAb ipilimumab was administered at doses of 0.3, 3, or 10 mg/kg with the highest tested dose resulting in better overall response rates as well as higher total lymphocyte counts, a measurement used as a biomarker for anti-CTLA-4 therapy efficacy/pharmacodynamics *(52)*. In that same study, as the dose was increased, blood serum concentration of ipilimumab and iRAE also increased in a linear fashion, however at all three doses, manageable safety profiles were achieved *(52)*. From a mechanistic standpoint, it has been shown in both preclinical and clinical models that CTLA-4 blockade leads to proliferation and activation of both regulatory and

effector T cells, however, at lower doses in patients, regulatory T cells appear to be more sensitive to anti-CTLA4 treatment and therefore higher doses may be needed to affect effector T cells to result in anti-tumor immunity *(53, 54)*.

In contrast to CTLA-4, there are conflicting reports on the dose effects on the clinical efficacy and toxicity of PD-1 blockade. In patients with prostate, lung, and advanced melanoma, doses of anti-PD-1 nivolumab up to 10 mg/kg were well tolerated with no signs or indications of a dose-efficacy or dose-toxicity relationship *(55, 56)*. However, in another trial in patients with advanced melanoma, a dose of 10 mg/kg anti-PD-1 mAb lambrolizumab every two weeks resulted in a superior rate of response (52%) compared to those achieved by lower doses (2 mg/kg every three weeks) or the same dose, just on a less frequent schedule (10 mg/kg every three weeks) (25% and 27% respectively) *(57)*. However, these dose-related improvements in response rates were accompanied by higher frequencies of iRAE, 23% for the group receiving 10 mg/kg every two weeks compared to 4% and 9% for the groups receiving 10 mg/kg every 3 weeks and 2 mg/kg every three weeks, respectively *(57)*. Similarly, in a preclinical study using the B16F10 melanoma model, improvements in tumor reduction were seen with increasing dose of mAb blocking PD-1 *(58)*.

In contrast to checkpoint blockade with anti-CTLA-4 mAb and the conflicting reports on checkpoint blockade with anti-PD-1 mAb, the rate of patient response and frequency of iRAE with anti-PD-L1 treatment appears to be relatively dose independent. In a study involving patients with various advanced cancer types, clinical activity was seen with a dose as low as 1 mg/kg, although there appeared to be an improvement in response at higher doses, albeit not to a statistically significant level *(59)*. However, like anti-PD-1 mAb, preclinical studies have indicated a slight improvement in survival and tumor suppression with increasing anti-PD-L1 mAb dose *(58, 60)*, although toxicity effects have not to our knowledge been well studied in rodent models.

Other consistent themes seen in clinical testing are the dose-dependent blood pharmacokinetics and dose-independent blood pharmacodynamics or blood lymphocyte PD-1 or PD-L1 occupancy rates *(55, 57, 59)*. Specifically, as the dose of administered mAb increases, serum mAb concentration also increases in a direct manner. However, PD-1/PD-L1 expressing blood lymphocytes appear to be saturated at the lowest of tested dose (0.3 mgs/kg) suggesting that as the dose of mAb is increased and the serum concentration increases, unwanted accumulation in off-target tissues may result, leading to higher likelihoods of iRAE.

With these monotherapy studies in mind, the potential for combination therapy with anti-CTLA-4 and anti-PD-1 mAb drugs to achieve improved effects using lower doses compared to monotherapy was evaluated. In a study in patients with advanced melanoma, escalating doses of both nivolumab and ipilimumab were concurrently administered *(61)*. Doses at or above 3 mg/kg of nivolumab and 3 mg/kg of ipilimumab surpassed the maximum tolerated dose *(61)*. However, when reduced to 1 mg/kg nivolumab and 3 mg/kg ipilimumab, iRAE were reduced to acceptable levels while still achieving substantial rates of favorable responses (53%) *(61)*. In fact, all nine of the patients who responded to combination therapy exhibited tumor regression of 80% or more compared to less than 3% of patients who received nivolumab or ipilimumab monotherapy at a dose of 3 mg/kg *(61)*. These phase I results suggest that combination therapy with nivolumab and ipilimumab can achieve high rates of patient response while maintaining manageable safety profiles depending on dose.

2.1.2 TGFβ and adenosine inhibition for cancer immunotherapy

While ICB has advanced cancer medicine tremendously in recent years, targeting additional pathways to treat additional cancer and improve response rates may be necessary as cancer utilize a myriad of pathways to go unnoticed by the immune system. TGFβ and adenosine

have been recently identified as active pathways in clinical and preclinical cancers providing potential pathways to modulate in combination with ICB.

TGFβ in Cancer. Transforming Growth Factor-β (TGFβ) is a pleiotropic cytokine that can act as a potent growth inhibitor shown to be overproduced in a variety of cancers. TGFβ is produced by a variety of cells including epithelial, endothelial, fibroblast, and various immune cells including macrophages *(62)*. It is critical in maintaining tissue homeostasis, and prevents early stage tumors from progressing to malignant tumors by limiting proliferation and survival while also regulating the TME (angiogenesis, ECM growth, etc.) *(63)*. However, as cancer cells mutate and evolve over their lifespan, they begin to become immune to the suppressive effects of TGFβ and begin to utilize it in malignant progression and metastasis *(64)*. For these reasons, TGFβ inhibition has not been considered a universal approach for cancer immunotherapy as dosing and scheduling must carefully be considered. As tumors progress, it is thought they utilize TGFβ through three broad ways 1) epithelial to mesenchymal transition, 2) tumor proliferation by affecting stromal fibroblasts, angiogenesis, and the ECM, and 3) dampening the immune surveillance ability *(3)*. One way the immune system is limited is by TGFβ signaling on type 1 differentiated neutrophils, macrophages, and T cells that stimulates the release of pro-tumorigenic cytokines including IL-17 and more TGFβ *(65, 66)*. In addition to suppressing T cells in the tumor, TGFβ has been shown to suppress anti-tumor immune responses in TdLNs where it can inhibit proliferation and function of DCs and T cells while increasing Treg accumulation leading to metastasis to the LNs *(67, 68)*.

Adenosine in Cancer. Adenosine signaling is a key signaling molecule involved in a variety of metabolic pathways including immunosuppression. ATP and adenosine are present at very low extracellular levels during homeostasis, however during inflammation and cancer, ATP is released from apoptotic and lysed cells *(69)*. In cancer, as cells incessantly grow and undergo death, ATP

is released leading to higher extracellular levels and acts as a Danger-Associated Molecular Pattern (DAMP) that trigger both innate and adaptive immune responses *(70)*. However in cancer, ATP is constantly dephosphorylated by ectonucleotidases, primarily CD39 and CD73, leading to the formation of adenosine *(71)*. In contrast to ATP, extracellular adenosine acts as an immunosuppressant on effector cells while promoting regulatory cell function *(72)*. Both CD39 and CD73 are found on a variety cells in cancer including tumor, stromal, endothelial, and infiltrating immune cells *(71)*. Adenosine acts on several known G-protein-coupled receptors including A2a and A2b which are upregulated following immune cell activation, however A2a has much higher affinity that A2b *(73)*. Following adenosine binding to A2a, which is found on monocytes, DCs, T, and NK cells, intracellular cAMP is produced leading to a variety of effects on these cells *(74)*. This includes reduction of cytokine production and costimulatory molecules in CD4 cells along with reduced proliferation and cytotoxicity in effector CD8 cells while also increasing Treg survival *(75, 76)*. Furthermore, it should be noted that A2a signaling can trigger the expression of immune checkpoints including CTLA4 and PD1 *(71)*. However, adenosine is also involved in a variety of other homeostatic metabolic pathways, therefore selective targeting of adenosine to specific cell subtypes is a crucial aspect of successful is desirable for cancer immunotherapy.

TGFβ inhibition and ICB in Cancer. Based off the wide range of pro-tumorigenic effects of TGFβ, there are many therapeutic targets to reverse these effects including ligand traps, small molecule receptor kinase inhibitors, peptide aptamers, and antisense oligonucleotides *(3)*. This work focused primarily on small molecule receptor kinase inhibitors to inhibit the activity of soluble TGFβ and its downstream suppressive functions. Since small molecule inhibitors directly block receptor signaling compared to ligand traps and oligonucleotides, they have a distinct advantage in this area. However, these molecules are pharmacokinetically unstable and thus are

challenging to study *in vivo*. Nevertheless, several studies have explored the combinatorial effects of TGFβ blockade and ICB due to TGFβ strong suppressive activities against effector immune cells and demonstrated superior effects to either therapy alone *(77–79)*. As previously mentioned, TGFβ plays a role in immunosuppression in dLNs, therefore this dual blockade may be improved by targeting the TdLN *(67)*.

Adenosine antagonists and ICB in Cancer. Adenosine blockade through A2AR has been reported as a promising strategy for cancer immunotherapy applications *(80)*. There are currently 4 agents in clinical Phase 1 trials targeting the A2a receptor for cancer immunotherapy *(4)*. These agents work by outcompeting endogenous adenosine to the A2a receptor and thereby can negate the pro-tumorigenic effects. A variety of studies have explored the effects and potential synergies of combining A2a blockade and ICB due to the non-redundant pathways *(81, 82)*. Adenosine has been shown to increase PD1 expression, but not CTLA4 expression on CD8 TILS*(82)*, while PD1 blockade has been shown to increase A2A receptor expression on CD8 TILs *(81)*. Moreover, dual blockade of A2a and PD1 increase IFNγ and Granzyme B expression leading to improved anti-tumor efficacy *(81)*. These results suggest that targeted delivery of adenosine antagonists to PD1 expressing cells can augment cancer immunotherapy.

2.2 Considerations and strategies for drug delivery in cancer immunotherapy

2.1.1 Introduction

Drug efficacy is in part due to drug reaching its target site of interest at the bioactive dose where it can then mediate its effect. In the context of the aforementioned immunotherapies, the desired tissues include the TME and the lymph nodes. Furthermore, T cells are a specific cell of interest as many drugs administered directly act on extra- and intra-cellular receptors. Thus, formulations and administration routes that improve access to the tissues and cells is of great

interest for improving therapy. This background will discuss the relevant concepts and barriers related to drug delivery to the TME and lymph node, specifically the physiologies of both tissues and how that dictates drug access, administration routes related to mAb pharmacokinetics and biodistributions, formulations that have advanced targeting of drugs and improved outcomes of therapeutic interventions, and the challenges associated with these immunotherapies.

2.1.2 Limitations of immunotherapies.

mAb drugs. Currently, ICB therapy is administered systemically through i.v. and i.p. routes in the clinical and preclinical setting respectively. As a result, transport of mAb to target tissues is based primarily on convective transport in the blood followed by diffusion and transcytosis through vascular epithelial cells out of the blood and into the target tissues *(83)*. The enhanced permeability and retention effect (EPR) suggests mAbs should accumulate in tumors. However, the EPR effect has been questioned and combined with the large size of Abs, ~150 kDa, diffusion is limited, especially considering the density of cells and ECM in the TME, discussed further below *(84)*. Combined with the selective permeation of the high endothelial venules in LNs, very little of mAb therapies accumulate in the TME and TdLN *(85)*. Once mAb arrives in the TME, it is often restricted to the peri-vascular space due to its large size, and also its deposition to cells expressing its target and thus occupies only a small volume of the tumor *(84)*. Most administered mAb instead accumulates in blood rich systemic organs where it is degraded following either non-specific pinocytosis or target-mediated drug disposition facilitated either by the constant fragment (Fc) or antigen binding fragment (Fab) *(86)*. However, the circulation times of mAbs are very long, on the order of weeks due to Fc neonatal receptor (FcRn), a receptor important in protecting Abs from lysosomal degradation by binding to the Fc region in early endosomes and recycling them back into the extracellular space *(87)*. As a result, this increases the chance of target tissue accumulation, but can also mediate immune related adverse events (IrAEs) associated with checkpoint therapies.

Small molecule drugs. Unlike mAb therapies, most small molecule drugs are limited by short circulation times and are rapidly filtered and excreted by the kidney or catabolized in the liver. Most small molecules are administered orally as they are stable toward gastrointestinal protease activity and are permeable to intestinal linings. Following this administration, a fraction of the drug will enter the circulatory system where most drug is cleared in <24 hours thereby leading to low tumor accumulation (generally <1%) while even a smaller amount will accumulate in LNs *(88)*. As a result, therapeutic efficacy is low and multiple dosing is required to reach the therapeutic threshold leading to toxicities associated with small molecule therapies. Small molecule drugs can also be injected in the peripheral skin, however due to their small size and permeability, they are cleared quickly from the injection site almost exclusively by the blood vasculature into the circulatory system *(89)*. Thus, formulations to improve small circulation time and/or bias their clearance into lymphatics are required.

Monotherapies. Although ICB has exhibited great promise for advancing cancer therapy, most patients receiving these therapies do not respond (~70%) and one-third of patients that do respond initially experience relapse. These data suggest that multiple non-redundant pathways are activated during therapy and thus warrant further understanding of checkpoint blockade mechanisms for novel combinatorial drug approaches. For example, CTLA4 monotherapy has not resulted in significantly enhanced response rates in various cancer types and may in part be explained due to increased PD-L1 expression. Therefore, the combination of aCTLA4 and aPD1 has been widely explored leading to improved therapeutic efficacy compared to either monotherapy. However, this dual therapy is still ineffective in some patients warranting exploration into other combination with other immune modulators targeting TGFβ, adenosine, and other ICB targets.

2.1.3 Tissue physiology and effects on drug transport

LN physiology. A significant fraction of the total immune cells in the body are located in several hundred lymph nodes, in which lymphocyte accumulation, activation and proliferation are organized. Therefore, targeting lymph nodes provides the possibility to directly deliver drugs to lymphocytes and lymph node-resident cells and thus to modify the adaptive immune response. However, owing to the structure and anatomy of lymph nodes, as well as the distinct localization and migration of the different cell types within the lymph node, it is difficult to access specific cell populations by delivering free drugs.

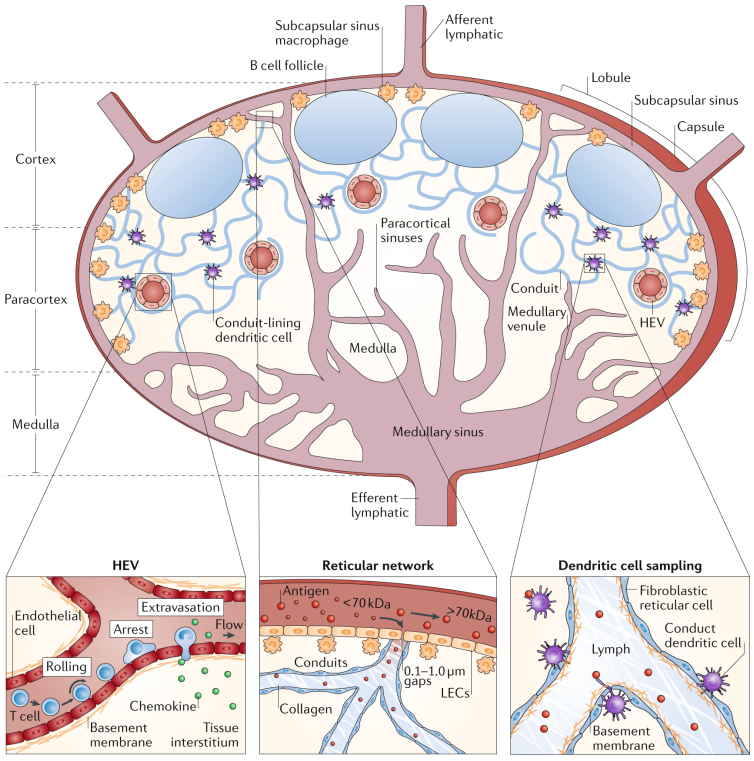

Figure 2: Lymph node structure and physiology. A cross section of a lymph node is shown. The architecture of the lymph node can be divided into distinct areas: fluid-filled lumen structures (lymphatics, high endothelial venules (HEVs), capillaries and sinuses), cellular locations (B cells in follicles, dendritic cells and T cells in the paracortex and macrophages in the subcapsular sinus and medulla) and structural units (cortex, paracortex and medulla). Lymphocyte extravasation occurs in the HEVs. The distribution of antigens within the reticular structure is regulated by hemodynamic size and molecular weight by the capsule and conduit. Circulating lymphocytes enter through the vasculature and exit through the efferent lymphatics. Dendritic cells sample the conduit and conduit structures. LEC, lymphatic endothelial cell.

The lymph node provides a specialized microenvironment to connect peripheral immunological information (antigens and other immune-modulatory molecules and cells) and circulating lymphocytes. Lymph nodes are composed of basic units called lymphoid lobules, each of which is drained by a single afferent lymphatic vessel sampling lymph from different drainage basins (Fig. 2) *(90)*. The base of the lobule consists of slender cords that are anchored by vascular roots and form part of the lymph node medulla, in which the arterioles, high endothelial venules and paracortical sinuses reside. The apex of the lobule is separated from the surrounding lymph node capsule by the subcapsular sinus *(91)*. The lobule is structurally supported by the reticular network, which is a fibrous sponge-like tissue composed of fibroblastic reticular cells and their reticular fibers. The reticular network provides a 3D scaffold for the interaction and migration of lymphocytes, APCs and macrophages (Fig. 2) *(92)*. Within this mesh, conduits of the reticular network are formed by extracellular matrix (ECM) proteins, with a central core composed of the interstitial matrix molecules collagen types I and III and a surrounding basement membrane-like structure ensheathed by a layer of fibroblastic reticular cells *(93)*.

Within each lobule, B and T cells home to separate locations (Fig. 2). B cells reside in follicles, in which they primarily interact with follicular dendritic cells. Once activated, B cells proliferate and undergo clonal expansion within the follicle, which leads to the formation of germinal centers containing proliferating B cells and areas of displaced resting B cells, called the secondary follicles *(94)*. By contrast, T cells migrate to the deeper interfollicular cortex and paracortex of the lobule, where they interact with migratory dendritic cells from peripheral tissues or lymph node-resident dendritic cells to become activated and proliferate *(95)*. Therefore, the reticular network, the lobular blood vessels and the sinuses are key components of the lymph node providing the specific structure that enables the relatively small number of lymphocytes to efficiently circulate and monitor antigen in the lymph node network *(96)*.

Solutes, biomolecules and cells can enter the lymph node by afferent lymphatics, lymph node blood capillaries or high endothelial venules (Fig. 2), resulting in a specific distribution of molecules and cells within the lymph node *(97)*. The distribution depends on the interfaces of the entry pathways with the other structural components and resident cells of the lymph node. Therefore, the specific structure and location of the different lymph node components are important design factors for materials targeting specific lymph node-resident cell types. Thus, materials need to be designed to leverage the different entry pathways to lymph nodes to enable targeted lymph node drug delivery: diffusive or convective delivery through the afferent lymphatics or capillaries, active cell-mediated migration from the peripheral tissue interstitium, transport in the circulating vasculature and entry through the blood capillaries and high endothelial venules, or direct injection.

Tumor physiology. The TME is composed of not only malignant cells, but many other nonmalignant cells including immune cells, as well as proteins and vasculature *(98)*. Since many cancer types express proteins of interest for immune modulation (e.g. PDL1) and lymphocytes reside in the TME prior to therapy, the TME represents a potential tissue target for immunotherapies. Tumor tissue differs greatly from healthy tissues in many physiological aspects (in addition to genetic abnormalities) including blood vessel development and architecture, lymphatic function, and extracellular matrix composition which is interest for drug delivery considerations *(99)*. During tumor progression, cancer cells rapidly proliferate and thus require constant nutrient and oxygen supply thus promoting rapid formation of blood vessel networks. However, blood vessel growth and distribution in tumors is very tortuous and heterogenous which gives rise to hypoxic areas within the tissue due to 1) lack of oxygen and nutrient delivery and/or 2) blood vessel collapse due to pressure from proliferating cancer cells resulting in necrotic areas *(100)*. Of the blood vasculature that does form and function properly, it has a leaky and permeable

characteristic which allows for improved macromolecule entry or exit. The lymphatics within tumors may be greatly impaired which can affect drug distribution. In healthy tissue, lymphatics play a vital role in regulating interstitial fluid pressure (IFP) by regulating osmotic balance and clearing larger molecules from the extracellular space. However, when lymphatics function improperly, as is the case in many tumors, fluid pressure builds up leading to retention of macromolecules and solutes in the extracellular space of tumors. Between the increased leakiness of tumor blood vessels and improper drainage function of lymphatics this contributes to the aforementioned EPR effect *(101)*. The EPR effect is primarily related to larger compounds (<40 kDa) which has motivated the development of many nano-formulations to improve small molecule delivery to tumors. However, as a result of impaired lymphatic function leading to increased IFP, reduced macromolecule extravasation may occur counteracting the leaky vasculature advantage. With constant cancer cell proliferation, the tumor environment is composed of densely packed cells which reduces diffusivity of macromolecules. Furthermore, the increased cell density leads to increased production of extracellular matrix (ECM) macromolecules including proteins (e.g. collagen) and polysaccharides (e.g. hyaluronan) providing further physical resistance to drug transport by way of diffusion *(98)*. Taken together, these hallmarks of cancer pose serious challenges for efficient for drug delivery vehicles and drug distribution within tumors.

2.1.4 Entry routes for drugging LN and TME resident T cells

Drug entry into the LNs and TME range from passive transport via lymphatics and the blood vasculature to active targeting utilizing affinity via mAbs to bind to tissue and cell antigens. Furthermore, targeting of circulating or adoptively transferred lymphocytes or APCs to backpack into the tissues is another approach to enable LN and TME accumulation. Modification of administration is also an approach including intra -LN and -tumoral injections and cutaneous administrations upstream from dLNs and adjacent to tumors which enables high drug

concentrations in the tissue targets. This section will highlight these principles further including discussion in the transport phenomena and intrinsic barriers with each approach.

Drugging LN resident T cells

Lymphatic uptake. Unlike the circulatory system, which contains a central pump, the lymphatics operate on a local level *(102)*. Fluid uptake and transport in the interstitium of a tissue are thought to be driven by expansion and compression of the initial lymphatics: expansion leads to percolation of interstitial fluid through the endothelial microvalves, which causes filling of the initial lymphatics. The lymphatics are then compressed by the surrounding tissue, triggering the transport of the fluid (now termed lymph) to the large collecting lymphatics *(103)*.

The initial lymphatics are blind-ended and composed of non-fenestrated overlapping endothelial cells with filaments anchoring them to the surrounding ECM, which provides mechanical support against the low pressure inside the initial lymphatic vessel lumen *(104)*. Owing to permeability differences between the non-fenestrated vascular capillaries and the lymphatics, only molecules with a certain size (10–100 nm in hydrodynamic radius) can efficiently convect into the lymphatics, which has important ramifications on drug formulation and delivery to the lymphatics *(105)*.

In the collecting lymphatic vessels, lymph is propelled by the synchronized movement of lymphatic vessel compartments called lymphangions, which contain one-way valves to propel the lymph in a unidirectional manner *(106)*. Once the lymph arrives at the draining lymph node through one of the afferent lymphatic vessels, it enters the subcapsular sinus (Fig. 2) *(107)*. The lymph then spreads into the subcapsular sinus and moves through the transverse sinuses, covering each lobule before finally exiting into the medullary sinuses, which merge from all lobules into a single efferent lymphatic vessel that may filter through subsequent lymph nodes in the same chain, before the lymph eventually returns back to the blood through the thoracic duct (Fig. 2).

Within each lymph node, the lymph flowing over the lobules through the subcapsular sinus is sampled by percolating through the conduits created by the reticular structure *(108)*. The reticular network restricts the access of lymph-borne material to the paracortex, which is important for preserving the naive state of the lymphocyte microenvironments and for controlling immunogenic molecules that adversely affect the immune response in the cortex, for example, exosomes from tumors or soluble products produced by microbial infections (Fig. 2) *(109–111)*. The efficiency of this barrier depends on the size of the lymph-borne molecules with high molecular weight (>70 kDa) molecules being virtually excluded from conduit and cortex access by the subcapsular sinus thus making T cell drugging via lymphatics a challenging task. Conversely, lower molecular weight species are gradually excluded, with molecules <70 kDa having some access to the conduits *(110, 111)*. Permeation of low molecular weight molecules from the conduits to the lymphocytes within the paracortex is mostly restricted. For immune challenges with low antigen concentration, this restriction poses a significant barrier to the generation of a robust adaptive immune response. However, higher antigen concentrations could enable direct lymphocyte access on a physiologically relevant scale.

To be transported to lymph nodes in the afferent lymph, drug delivery systems must overcome barriers, such as vasculature clearance, penetration of the epithelium of the skin and traversing the mucosa and gut barriers. In the tissue interstitium, where afferent lymphatic access is maximized, transport is restricted by the gel-like ECM, which is composed of fluid, solutes, fibrillar proteins and proteoglycans, which inform the design parameters for size, shape and charge of the drug delivery system as drug delivery systems that prevent adsorption and entrapment within the ECM show improved diffusivity through the interstitium and therefore better lymphatic uptake *(112)*.

Blood Vasculature. The blood vasculature provides an alternative transport pathway to the lymph nodes. The infiltration of circulating lymphocytes into the lymph node is controlled by high endothelial venules, which are specialized tissues lined with high (full rounded shaped) cuboidal endothelial cells with receptors that facilitate intravascular lymphocyte transmigration through the endothelial layer into the reticular meshwork (Fig. 3). Therefore, owing to the fact that the blood capillaries perform filtration functions, materials can be designed to leverage the diffusive and convective transport through these vascular structures to target cells in the lymph node.

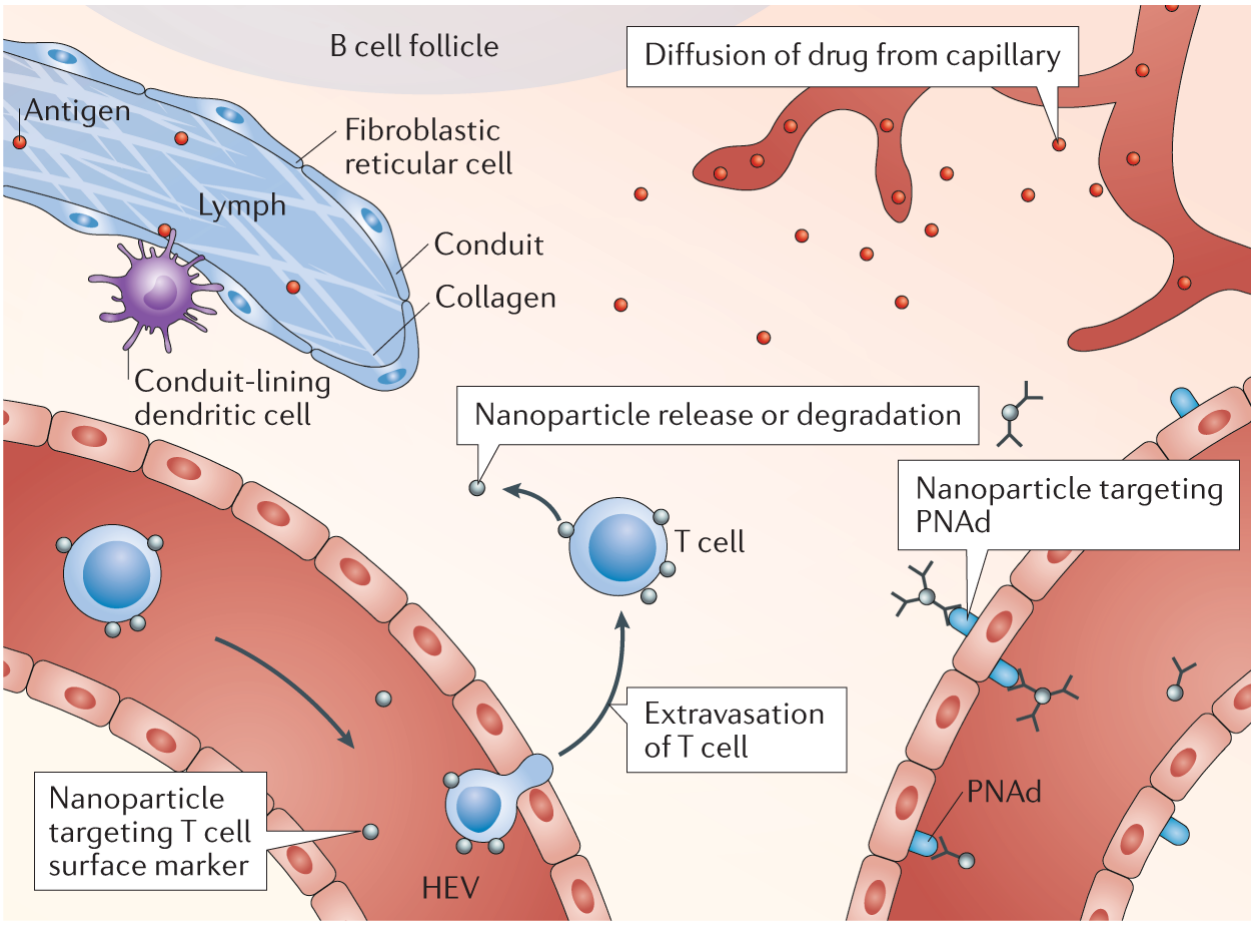

Figure 3: Canonical outlook for targeting T cells. Conduit-lining dendritic cells sample antigen for subsequent presentation to proximal T cells. Circulating T cells can be targeted for T cell-mediated nanoparticle trafficking into the lymph node T cell zone. Lymph node blood capillaries that are leaky as a result of disease allow for diffusion-mediated transport to lymph node T cells. Microparticles and nanoparticles can be actively targeted to high endothelial venules (HEVs) using anti-peripheral node addressin (PNAd) antibodies, such as MECA-79, followed by diffusion of the delivered agent into the lymph node.

T cells primarily reside in the paracortex near the blood capillaries, and thus the blood vasculature is an attractive potential route to target LN-resident T cells (Fig. 3), for example, by mimicking homeostatic T cell trafficking from the blood to the lymph node through high endothelial venules (Fig. 3). The entry of lymphocytes through high endothelial venules is initiated by the homing receptor L-selectin (CD62L), which recognizes peripheral node addressin (PNAd), which is expressed on high endothelial venules in lymph nodes and upregulated at sites of chronic inflammation. This natural homing process can be explored for drug delivery by functionalizing carrier formulations with the 6-sulfo-sialyl Lewis X-targeting antibody MECA-79, which binds to PNAd. The functionalized particles accumulate in draining lymph nodes downstream from rejected transplants following intravenous injection, as draining lymph nodes have higher expression levels of PNAd than non-draining lymph nodes owing to chronic inflammation, enabling selective targeting *(113)*. Therefore, drugs can be selectively delivered to draining lymph nodes, where they can then be delivered to T cell populations compared with free drug or drug-loaded microparticles without targeting ligands.

Circulating lymphocytes. Antigen-specific T and B cells are rare, and the vast majority of naive lymphocytes are circulating between lymph nodes and the lymphatics, spending less than half an hour in circulation before homing to a lymphoid organ, where they take a few hours or days to find their cognate antigen *(114)*. Lymphocytes primarily migrate into lymph nodes along the entire length of HEVs, and exit through efferent lymphatics, with T and B cell trafficking being substantially increased during lymph node inflammation *(115)*. Following a tightly orchestrated adhesion cascade, adhesive ligands and chemokines direct lymphocyte diapedesis through the inter-endothelial junctions of the high endothelial venules. Once inside the lymph node, T and B cells home to their respective areas in the paracortex and to the follicles, guided by chemokine cues *(116, 117)*.

Cell homing to the lymph node can be exploited to target T cells in the lymph node by using cells for 'backpacking', that is, drug- loaded nanoparticles or carriers are covalently or non-covalently bound to T cells and thus shuttled to lymph nodes (Fig. 3) following adoptive transfer. For example, this method can be used to prolong autocrine stimulation of transferred T cells, triggered by conjugated nanoparticles that are tethered with anti- CD45 antibodies and release IL-15 superagonist (IL-15Sa). This approach can be applied to support the antitumor activity of therapeutic T cells and increase their lymph node accumulation *(118)*. Active targeting by cell homing can also be used for the treatment of lymphomas in lymph nodes. For example, T cells can be functionalized ex vivo with nanocapsules loaded with a chemotherapeutic, which is then delivered to the lymphoma *(119)*. By engineering the T cells to be resistant to the chemotherapy, high- payload delivery to lymph nodes can be achieved, which ultimately leads to a decrease in tumor growth rate compared with traditional systemic dosing.

Intra-Lymph Node injections. Administration of drugs in peripheral tissues or intravenously achieves low yet sustained levels of LN delivery, mediated by convection and active cell-mediate trafficking. Alternatively, drugs can be directly injected into the lymph node, a method that has been used for over half a century to treat lymph node metastasis *(120)*. Direct lymph node injection is invasive and often used only if delivery via the lymph or blood is not sufficient to achieve the required drug levels in the lymph nodes. Usually, the draining lymph node is identified by administration of lymph-draining chromogenic colloid in peripheral tissues. The use of intra-LN injections has been expanded in addition to treating LN metastasis to improve vaccine potency in several disease indications including cancer and autoimmunity *(121–123)*.

Drugging tumor resident T cells

Blood vasculature. Systemic administration by way of i.v. injections are the most common route to target drugs to the TME. Following i.v. administration, drug will circulate through the

blood via convection and may pass through the tumor tissue, upon which it must extravasate out of the blood and into the tumor tissue itself where diffusion will carry drug into deeper areas of the tumor away from vasculature *(99)*. In order for drug to accumulate within tumors, the systemic concentration gradient of drug must stay above what it is in the tumor, thus clearance rates of drugs are an important factor in determining drug accumulation in tumors. Drug clearance rates are determined by the size of the molecule *(84)*. Generally small molecules stay in the extracellular space in the plasma and are cleared via the renal system or are broken down in the hepatic system. Conversely, mAbs are taken up intracellularly by cells via both non-specific and receptor mediated uptake and subsequently degraded within lysosomes. Furthermore, drug interactions with receptors disseminated throughout the body, specifically FcRn and Fc-gamma receptors are important factors in determining drug clearance rate *(83)*.

Once drug extravasates into the tumor, permeability throughout the tumor is an important consideration. For small molecule drugs, even with the densely packed tumor, these molecules can diffuse relatively easy throughout *(124)*. However, for larger molecules like mAbs and drug carriers, diffusion is greatly restricted, thus convection generally dominates this transport and has led to direct modulation of the TME to improve drug diffusion within tumors. By normalizing the tumor matrix using extracellular matrix-degrading enzymes such as collagenase or extracellular matrix antagonists, increased diffusivity and penetration of agents within the tumor results *(125–127)*. Normalization of the tumor microvasculature using anti-angiogenic therapies can also reduce tumor interstitial hypertension and matrix remodeling, leading to improved drug entry and penetration *(128)*. It should also be noted that affinity of the mAb plays a role in drug distribution as lower affinity mAbs have more homogenous distribution within tumors as low affinity mAbs dissociate from target antigens after binding and subsequently diffuse deeper into the tissues. Unfortunately, lower affinity mAbs can more easily leave the tumor tissue reducing tumor mAb

concentrations. Diffusion and permeation of tumors using higher affinity mAbs is characterized by mAb rapidly binding to target antigen, thus mAb is rapidly depleted as it fills up available antigen-binding sites and only once complete saturation of initially encountered cells occurs can mAbs diffuse farther into the tissue. Since endocytic uptake occurs simultaneously, complete saturation of target antigens by mAb diffusion within tumors from blood vasculature can be hard to achieve and has spurred the development of intratumoral administrations (discussed below).

Intratumoral delivery. An alternative to systemic administration, direct injection of immunotherapies into the tumor is an emerging option in the clinic as immune cells expressing the targets of emerging drugs are present within the TME *(129)*. This is not a new concept as intratumoral delivery of pathogens has been described since the late 1800s by Dr. William Coley and has grown with our advanced understanding of the immune system *(130)*. Using this approach, a single injection in one tumor site can generate a systemic antitumor immune response and is capable of triggering a more potent response while causing less off-target toxicity. Using an i.t. injection results in a much higher drug concentration in the TME compared to a systemic infusion while also lowering the total dose administered reducing drug concentrations in off-target tissues. This strategy has been performed with various drugs in both the clinical and preclinical setting including; mAbs to eradicate tumor resident Tregs *(131)*, mAbs and cytokines (interleukin-2) to stimulate cytotoxic T cells *(132)*, and toll-like receptor agonists to activate antigen presenting cells *(133)*. While promising, i.t. administration has some limitations including accessible tumor sites and ones which are of sufficient size for injection.

2.1.5 Drug delivery vehicles for immunotherapies

Many formulations have been engineered to improve drug delivery to the TME and/or LNs including dendrimers *(134)*, synthetic polymer nanoparticles *(135)*, lipid-based drug delivery vehicles *(136)*, inorganic particles *(137)*, and proteins including albumin *(138)* and mAbs *(84)*.

Formulation changes are engineered with drug entry mechanisms in mind (mentioned above) including passive transport via vasculature, but also allow for active targeting, enhanced retention at injection sites, and sustained or bolus drug release platforms. These systems work in a variety of ways including increasing the size of their cargo to reduce excretion rates/increase circulation time, modulate biodistribution, and improve solubility of hydrophobic drugs *(139)* and have improved delivery of various therapeutics including chemotherapeutics, oligonucleotides, and peptides *(140)*.

Poly(propylene sulfide) NPs. One particular formulation to achieve improved drug delivery is via micelles composed of block copolymers that self-assemble to various sizes in the nano-range (10-300 nm). Micelles composed of block copolymers including poly(propylene sulfide) have key features that make them attractive for delivering mAbs and small molecules to specific tissues. Due to self-assembly, the size of the NPs can be controlled based off polymer ratios allowing for NPs in the 30-300 nm size range *(141)*. Furthermore, the hydrophobic core is a suitable environment for encapsulation of hydrophobic molecules and peptides which allows the drug to; 1) do not need to be chemically modified, a common requirement for other ADCs, 2) can be encapsulated at very high levels <90%, and 3) dramatically increase the solubility and alleviate the need to administer these drugs in organic solvents. For example, Thomas et al explored the ability to encapsulate paclitaxel (PTX) into the hydrophobic core of these NPs *(142)*. PXL was loaded into the NPs with over 95% efficiency and released approximately 50% of PXL over the first 50 hours post encapsulation while maintaining the size and stability of the NPs. Furthermore, the encapsulated and released PXL retained its immune stimulatory activity comparable to that of the free PXL drug. The corona of these NPs is composed of a carboxy terminus that is 1) anti-fouling, ideal for preventing protein deposition *in vivo*, and 2) the carboxy terminus allows for derivatization with functional groups including a pyridyl disulfide (PDS) chain that has a

reduction-sensitive disulfide bond which can be displaced by thiol containing compounds. Van der Vlies et al explored the ability to derivatize PDS-NPs with several different thiolated compounds including a thiol containing- biotin, peptide, and ovalbumin protein *(143)*. Using this synthesis approach allowed for mild reaction conditions keeping the conjugated compound intact and has the ability to be applied to many thiol-containing proteins. These features highlight the potential of poly(propylene sulfide) NPs for improving the co-delivery of small molecules and mAbs to the same target cell.

While this NP system provides ideal characteristics for both encapsulation of small molecule drugs and surface derivatization with mAbs thereby allowing codelivery to the same target cell, the ability to interact with T lymphocytes remains a challenge due to their lack of pinocytosis. For example, Kourtis et al explored the ability to drug different immune cell compartments *in vivo* using this NP system by fluorescently labeling the NPs and monitoring their cellular access and uptake *(144)*. While monocytes and granulocytes displayed distinct population shifts following NP uptake, B and T lymphocytes exhibited minimal shifts in NP fluorescence over time *in vivo* suggesting little uptake in these compartments. This was explored further *in vitro* with cultured splenocytes and biotinylated NPs to address whether NPs were located extracellularly or intracellularly on various compartments. While monocytic compartments displayed both external and internal NP signals via a micropinocytosis method, B and T cells had only extracellular staining associated with interaction with the plasma membrane. Furthermore, the level of surface interaction of NPs with T cells was below 1 and 5 % for CD8 and CD4 T cells respectively. These results highlight the challenge in targeting T cells *in vivo* as they perform minor levels of pinocytosis and phagocytosis.

T cell and ICB targeting platforms. Drug delivery systems that do target T cells efficiently have been developed in recent years and rely on targeting strategies, including mAbs with affinities

to T cell surface proteins both *ex vivo* and in *vivo*. For example, Tang et al developed a thiol sensitive degradable protein carrier composed of therapeutic cytokines that was functionalized with surface anti-CD45 *(145)*. Using this system, they were able to incubate the carrier with CD8 T cells *ex vivo* and adoptively transfer *in vivo* where the carrier slowly degraded as T cells became activated and increased their surface thiol content thereby degrading and releasing the cytokines. Similarly, Zheng et al engineered a antibody-liposomal carrier by covalently linking the Fab to the surface of liposomes using an irreversible maleimide crosslinker *(146)*. Following lymphodepletion *in vivo*, they adoptively transferred this drug carrier and showed effective binding to T cells *in vivo* demonstrating the ability to target the cells of interest. Platforms to more selectively target T cells of interest have also recently been developed. For example, Schmid et al developed a NP composed of poly(lactic-co-glycolic acid) (PLGA) and polyethylene glycol (PEG) which was functionalized with the Fabs of aPD1 to target PD1 expressing T cells *(147)*. *In vivo* studies demonstrated these PD1 targeted NPs were able to target ~6% of PD1 expressing T cells vs ~1% for non-targeted NPs within B16F10 tumors 1 hour post iv administration. These results emphasize the potential for targeted NPs to interact with T cells and thus deliver drug cargos.

Due to iRAE and the requirement for repeated dosing in clinical ICB therapeutic protocols, drug delivery platforms that improve mAb delivery to the tumor and achieve sustained release have garnered recent interest. To this end, microparticle-based formulations aiming to prolong the retention of therapeutic agent at the site of injection have emerged as an attractive strategy since increasing carrier size enhances and prolongs retention at the site of injection *(89, 148)*. Material systems can additionally be engineered to control the release of agent from its carrier in order to prolong its therapeutic effects. For example, Rahimian *et al*. engineered microparticles ~10-25 μm in diameter composed of a biodegradable poly(lactic-co-hydroxymethyl-glycolic-acid) polymer that could be modified to vary mAb release kinetics and loading efficiency *(149)*. The formulation

the authors deemed optimal allowed for a burst release of about 20% of loaded mAb followed by a sustained release of the remaining 80% of mAb over approximately 30 days *(149)*. When compared to the same dose of mAb formulated in an incomplete Freund's adjuvant formulation, the mAb-loaded microparticle system resulted in serum mAb levels that were significantly lower (5-10 fold) than the mAb administered in incomplete Freund's adjuvant. Microneedle (MN)-based platforms may be an appealing administration strategy to improve mAb retention due to its ease of administration on superficial tumors such as those of the skin, and potential to more homogenously distribute therapeutic agent throughout the target tissue. Wang et al. and Ye et al. utilized MN to deliver nanoparticles composed of hyaluronic acid or dextran-alginate that encapsulate anti-PD-1 mAb and other small molecule therapeutics *(150, 151)*. In this engineered MN system, the release of anti-PD-1 mAb from the nanoparticles was stimuli responsive to either hyaluronidase, an enzyme overexpressed in the tumor microenvironment *(152)* or glucose-triggered reductions in local pH. These MN-based approaches resulted in sustained anti-PD-1 mAb retention within the tumor, leading to a more robust immunotherapeutic response indicated by enhanced T cell infiltration into the tumor, reductions in tumor growth, and prolonged animal survival *(150, 151)*. Another approach is the use of hydrogel-based platforms to improve release kinetics of delivered mAb. Wang et al. recently demonstrated that a s.c. injected alginate hydrogel improved the anti-tumor activity of both celecoxib and anti-PD-1 mAb when used individually or combined *(58)*. It is interesting to note that this system did not lower the serum concentration of anti-PD-1 mAb compared to an i.p. injection of free mAb *(58)*. However, the accumulation within the B16F10 melanoma was much higher compared to i.p. infusion *(58)*. Another approach developed to improve immune checkpoint mAb accumulation within tumors and resulting therapeutic effects is piggybacking on the intrinsic capacity of platelets to accumulate at wound sites, such as those created with tumor resection *(153, 154)*. Wang et al. decorated platelets via a

bifunctional maleimide linker and demonstrated the release of anti-PD-L1 mAb via platelet-derived microparticles following platelet activation or adhesion *(155)*. This approach improved survival and tumor suppression compared to i.v. injection of free anti-PD-L1 mAb in both melanoma and breast cancer models *(155)*. Taken together, these drug delivery approaches show great promise in improving checkpoint blockade by enhancing payload delivery without the need for repeated injections and potential for reducing systemic toxicity.

CHAPTER 3. BLOCKADE OF IMMUNE CHECKPOINTS IN LYMPH NODES THROUGH LOCOREGIONAL DELIVERY AUGMENTS CANCER IMMUNOTHERAPY

3.1 Introduction

Immune checkpoint blockade (ICB) using monoclonal antibodies (mAbs) specific to cytotoxic T lymphocyte antigen 4 (CTLA4) and programmed cell death 1 (PD1) or its ligands has emerged as one of the most promising new approaches in cancer immunotherapy to invigorate anti-tumor immunity *(156–159)*. CTLA4 is a transmembrane receptor found constitutively on regulatory T cells (Tregs) and is limited in its expression by CD4 and CD8 T cells immediately following engagement of the T cell receptor. CTLA4 directly competes with CD28 for B7 ligand binding on antigen-presenting cells (APCs), consequently leading to T cell anergy *(160)*. Similarly, surface expression of PD1 is broadly induced following T cell activation and PD1 is thought to function in peripheral tissues through its binding interactions with programmed death ligands (PDL1 and PDL2) found on many cell subtypes including predominantly, but not limited to, tumor cells and APCs, respectively. Following PD1:ligand engagement, T cell function is dampened; an effect that protects the host during viral infection from immune-mediated tissue destruction leading to T cell exhaustion *(161)*. By blocking these inhibitory pathways using function blocking mAbs, activation and cytotoxic capabilities of T cells can be restored *(156, 161)*.

Although the canonical view on ICB therapy effects is that they are mediated primarily within the tumor microenvironment (TME) by restoring anti-tumor functions of infiltrating T cells, evidence of the pleotropic effects of ICB mAbs continues to amass. Specific isotypes of anti-CTLA4 (aCTLA4) (IgG2a) mediate the depletion of tumor resident Tregs (trTregs) via antibody dependent cellular cytotoxicity, although other isotypes (IgG1) do not *(37–39)*. Additionally, while

anti-PD1 (aPD1) has been shown to restore the effector functions of CD8 and CD4 T cells *(2)*, CD28 stimulation is required for aPD1 efficacy, suggesting a role of B7-expressing APCs *(162)*. aPD1 has also been shown to modulate a stem-like CD8 T cell population capable of proliferating and giving rise to T cells of a tumor killing effector-like phenotype *(9, 10, 163–166)*. Furthermore, PDL1 expression on tumor cells is not required for disease progression and aPD1 efficacy in certain cancer types *(167–169)*. Both aCTLA4 and aPD1 therapy have also been shown to broaden the repertoire of tumor specific CD8 T cell clones *(40, 170–172)*, which is associated with improved clinical outcomes *(173, 174)*. Solely blocking checkpoint pathways in the TME may thus not be sufficient to generate high response rates following ICB therapy.

To this end, appreciation for lymphoid tissues as critical in the generation of effective immunotherapy responses is increasing *(175, 176)*. $CD103^+$ APCs transport antigen to tumor draining lymph nodes (TdLNs) where they can prime naïve CD8 T cells *(177, 178)*. Moreover, TdLNs are involved in mediating the effects of aCTLA4 *(179)* and aPD1 therapy *(180)*. The presence of the aforementioned stem-like CD8 T cell compartment has been observed in mouse and human LNs, in addition to the TME, suggesting these tissues as a potential source of tumor infiltrating lymphocytes (TILs) *(181)*. However, the TME and TdLNs are poorly accessed using systemic drug administration *(83, 182, 183)*, the predominant route used in both preclinical tumor models and human patients, which may limit drug effects. Clinical studies have reported dose-efficacy relationships of aCTLA4 and aPD1 therapies *(52, 57)*. Increasing the availability of ICB mAb within target tissues, including the TME and lymphoid tissues that are enriched in tumor-specific T cells, thus has the potential to improve ICB therapy.

Previous reports have described improvements in anti-tumor responses using intratumoral (i.t.) administration routes compared to traditional systemic administration *(132, 184, 185)*. However, less is known about the anti-tumor effects of ICB modulation in LNs, although peri-

tumoral administration has previously been investigated *(179, 186)* and subcutaneous (s.c.) administration is being explored in the clinic *(8)*. It is of interest to note that mAbs are large molecules (150 kilodaltons) and thus are transported differently than traditional small molecule drugs or other smaller biologics. Specifically, injection of compounds similarly sized to mAbs into the interstitium of peripheral tissues usually results in clearance from the injection site via the initial lymphatics and thus accumulation of such compounds in draining LNs *(144)*. We hypothesized that mAbs would behave similarly and therefore utilizing direct administration into peripheral tissues would improve LN delivery of mAbs allowing for improvement of ICB therapeutic effects. Our results in three preclinical solid tumor models (utilizing melanoma and breast cancer cell lines) support the hypothesis that modulation of immune checkpoint pathways in (Td)LNs using locoregional administration of ICB mAbs leads to enhanced anti-tumor efficacy, enables dose-sparing, and has the potential to reduce treatment-induced toxicity compared to systemic drugging.

3.2 Results

3.2.1 Tumor-directed ICB augments therapeutic responses locally

To evaluate whether augmenting the accumulation of administered mAb drug within target tissues can improve the effects of ICB, survival studies were performed in a poorly ICB responsive tumor model (B16F10 melanoma) using both aCTLA4 and aPD1 mAbs and comparing intraperitoneal (i.p.) versus i.t. routes of administration. Modest reductions in tumor growth were induced by i.p. administration of ICB mAb, however administration i.t. instead resulted in profound reductions in tumor growth (Fig. 4A). To explore the potential effects on priming and expansion of T cells in response to endogenous tumor antigen, the systemic response of untreated tumors in the contralateral (c.l.) dorsal skin was concurrently monitored. Strikingly, untreated tumors were found to be dramatically reduced in animals treated i.t. with ICB therapy (Fig. 4B).

The net effect was a substantial prolonging of mouse survival with i.t. compared to i.p. administration of ICB mAb (Fig. 4C). These data demonstrate the capacity of tumor-localized ICB therapy to elicit a systemically functional anti-tumor immune response that exceeds the effects of systemically administered ICB therapy.

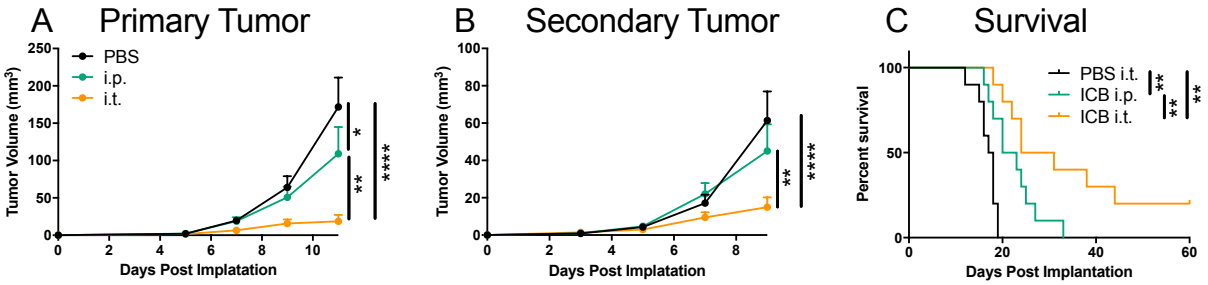

Figure 4: Intratumoral administration of ICB promotes systemic antitumor immunity. Following B16F10 implantation, mice were administered 150 μg of aPD1 and aCTLA4 (9H10) on d 5, 7, and 9 post tumor implantation i.p. or i.t.. (**A**) Tumor growth curve of primary tumor (d 0 tumor implant, i.t. treated tumor). (**B**) Tumor growth curve of secondary tumor (d 2 tumor implant, non-treated i.t. tumor). (**C**) Survival curves of mice. Combined data of two independent repeats (total n=10, mean + SEM). Statistical analyses were done using ANOVA with Tukey's test. Log-rank (Mantel-Cox) test for survival curves. *p < 0.05, **p < 0.01, ***p < 0.001, ****p < 0.0001.

The immunological mechanisms underlying the therapeutic responses seen with i.t. and i.p. ICB therapy (aCTLA4 and aPD1 in combination) were explored. T cell phenotypes in i.t. saline (control) or ICB treated animals bearing single B16F10 tumors were analyzed 12 d post tumor implantation. Administration i.t. led to a dramatic reduction in tumor burden (Fig. 5A) and was associated with a reduction in trTregs frequencies (Fig. 5B), which can attributed to the particular aCTLA4 clone used *(37–39)*. As is well characterized in many preclinical melanoma models and human patients, ICB therapy was associated with an increase in CD8 TILs, although this effect was limited to i.t. administration here (Fig. 5C). Interestingly, of these $CD8^+$ TILs, the levels of granzyme B producing (Fig. 5D) and effector ($KLRG1^+$) cell frequencies (Fig. 5E) were similar between i.p. and i.t. administration, suggesting effective therapy is associated with increased frequencies of CD8 TILs rather than reinvigoration of exhausted TILs. To explore the source of

CD8 TILs, the levels of proliferation through Ki-67 expression were measured. Cycling CD8 T cells frequencies were found to be elevated in the TME and TdLN using i.t. administration with comparable increases observed in the spleen between i.p. and i.t. administration as well as minimal changes in the non-TdLNs (nTdLNs) (Fig. 5F-G). Frequencies of CD8 T cells within each tissue compartment exhibiting stem-like ($PD1^{+}Tcf1^{+}Tim3^{-}$) versus effector-like ($PD1^{+}Tcf1^{-}Tim3^{+}$) CD8

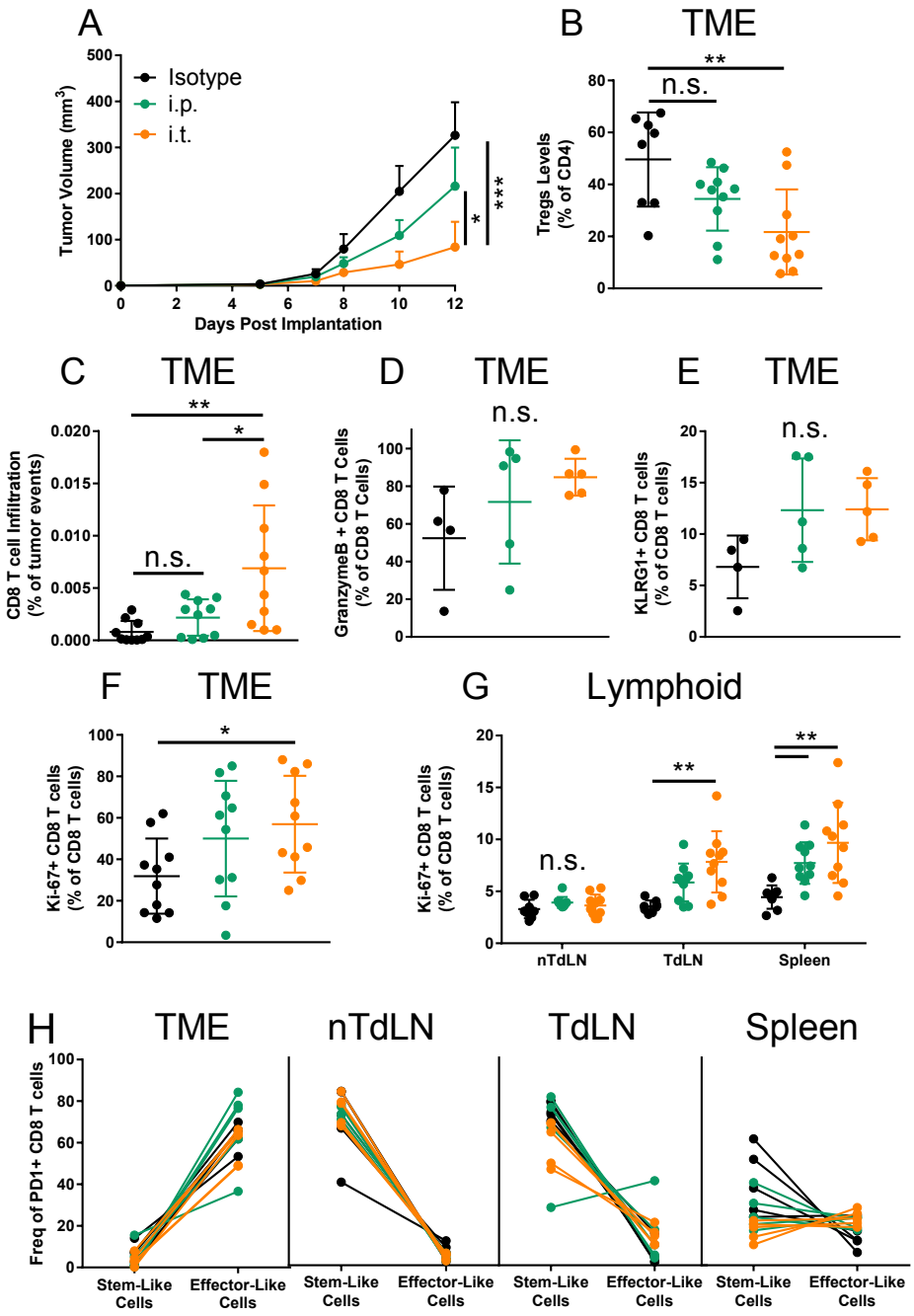

Figure 5: Tumor-bearing mice administered ICB intratumorally exhibit unique T cell changes in TME, TdLN, and Spleen. (**A**) B16F10 tumor growth over first 12 d with 150 μg of ICB mAb [combination of aPD1 and aCTLA4 (9H10) administered on d 5, 7, and 9 post tumor implantation. (**B**) Frequencies of CD4+ FoxP3+ T cells. (**C**) Frequencies of CD8+ T cells in TME. Frequencies of granzymeB+ (**D**) and KLRG1+ (**E**) CD8+ T cells in TME. Frequencies of Ki-67+ CD8+ T cells in TME (**F**) and lymphoid tissues (**G**). (**H**) Frequencies of "stem-like" ($Tcf1^{+}Tim3^{-}$) vs "effector-like" ($Tcf1^{-}Tim3^{+}$) CD8 T cells, pregated on $PD1^{+}$, in the TME, nTdLNs, TdLNs, and spleen. Data represent one or two independent experiments (n=4-10, mean ± SD) Statistical analyses were done using ANOVA with Tukey's test. *p < 0.05, **p < 0.01. n.s., not significant.

T cell phenotypes were also assessed. The phenotypes of activated ($PD1^{+}$) CD8 T cells were found to predominately be effector-like in the TME compared to stem-like in the LNs with a balance in between in the spleen regardless of therapy or route of administration (Fig. 5H).

Similar trends for Ki-67^{+} frequencies were also observed in the CD4 T cell compartment (Fig. 6).

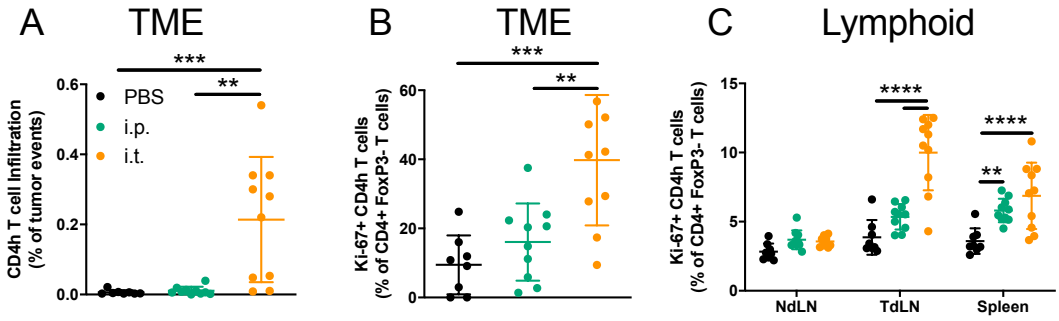

Figure 6: Changes in CD4 T cell compartment resulting from ICB. (A) Frequencies of CD4h (CD4+ FoxP3-) TILs. (**B**) Frequencies of Ki-67+ CD4+ FoxP3- TILs. (**C**) Frequencies of Ki-67+ CD4+ FoxP3- T cells in lymphoid tissues. Data represent two independent experiments (n=8-10 mice, mean ± SD), n.s., not significant relative to each group in each tissue. Statistical analyses were done using ANOVA with Tukey's test. **p < 0.01, ***p < 0.001.

Of note, *ex vivo* staining confirmed that therapeutic aPD1 mAb did not block the binding of aPD1 mAb used for flow cytometry staining (Fig. 7). These data support the concept that ICB

efficacy is in part mediated by increasing the frequencies of TILs that may originate from the TME or peripheral tissues including the TdLN or spleen.

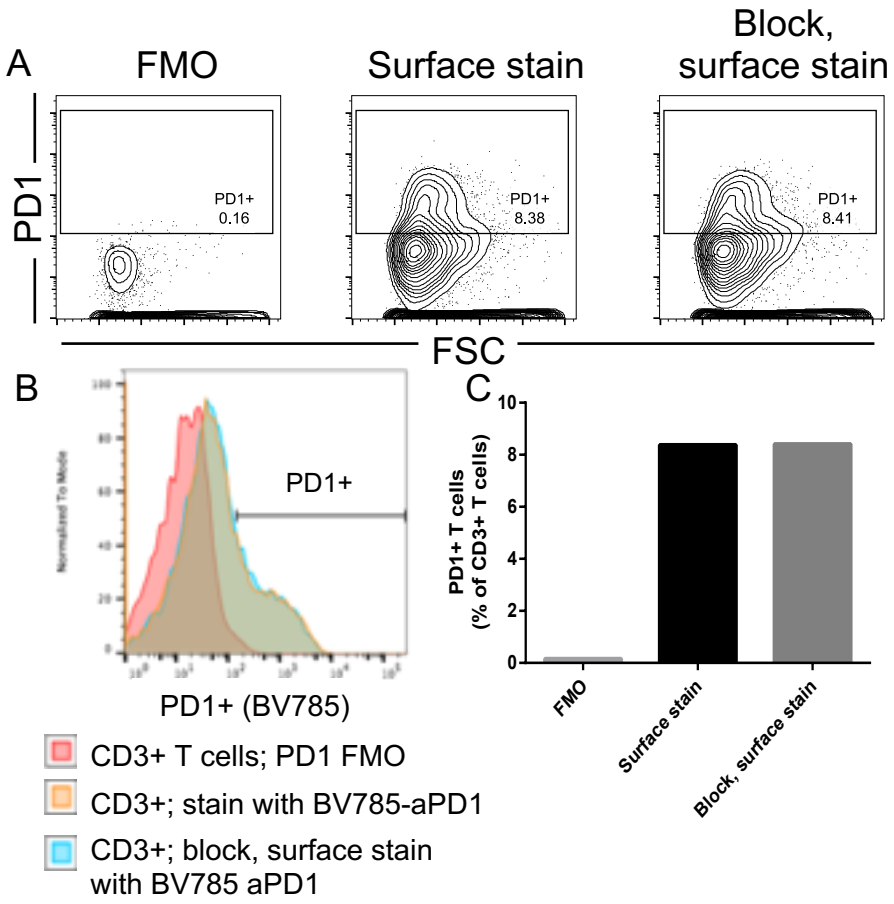

Figure 7: Therapeutic and staining aPD1 antibodies can simultaneously stain PD1-expressing T cells. (**A**) Representative flow cytometry plots of splenocytes from each staining group gated on live cells. (**B**) Histogram and quantification of PD1 expression on CD3+ T cells following activation with ionomycin+PMA using no stain (FMO), BV785 labeled aPD1 (Biolegend, clone: 29F.1A12) stain, or incubation with non-fluorescent aPD1 (BioXCell, clone: RMP1-14) followed by BV785-aPD1 (Biolegend, clone: 29F.1A12) stain. (**C**) Quantification of B. Data represents staining performed on splenocytes from one C57Bl6 animal.

3.2.2 Administration route affects mAb biodistribution

Considering responses were observed in secondary lymphoid tissues in addition to the TME following i.t. administration, the effect of route of administration on levels of mAb accumulation within the spleen, LNs (tumor-draining or non-draining), and TME as well as other

systemic tissues was assessed. Levels of AlexaFluor647 labeled aPD1 or aCTLA4 mAb (Fig. 8A) were measured following a single dose using four different administration routes; i.p., in the forelimb contralateral to the tumor (c.l.), in the forelimb ipsilateral to the tumor (i.l.), and i.t. 5 d post B16F10 tumor implantation (Fig. 9A). Tumor mAb levels were found to be sustained over 24 h using an i.t. injection but were near the limit of detection using other administration routes (Fig. 9B-C). Levels of mAb in the blood and spleen were equivalent between administration routes (Fig. 9C-D). When assessing mAb levels in LNs, i.p. administration resulted in minimal accumulation in any measured LN, whereas c.l. administration led to accumulation within nTdLNs (Fig. 9E-F). Using an i.l. and i.t. administration led to detectable levels of mAb accumulation solely within

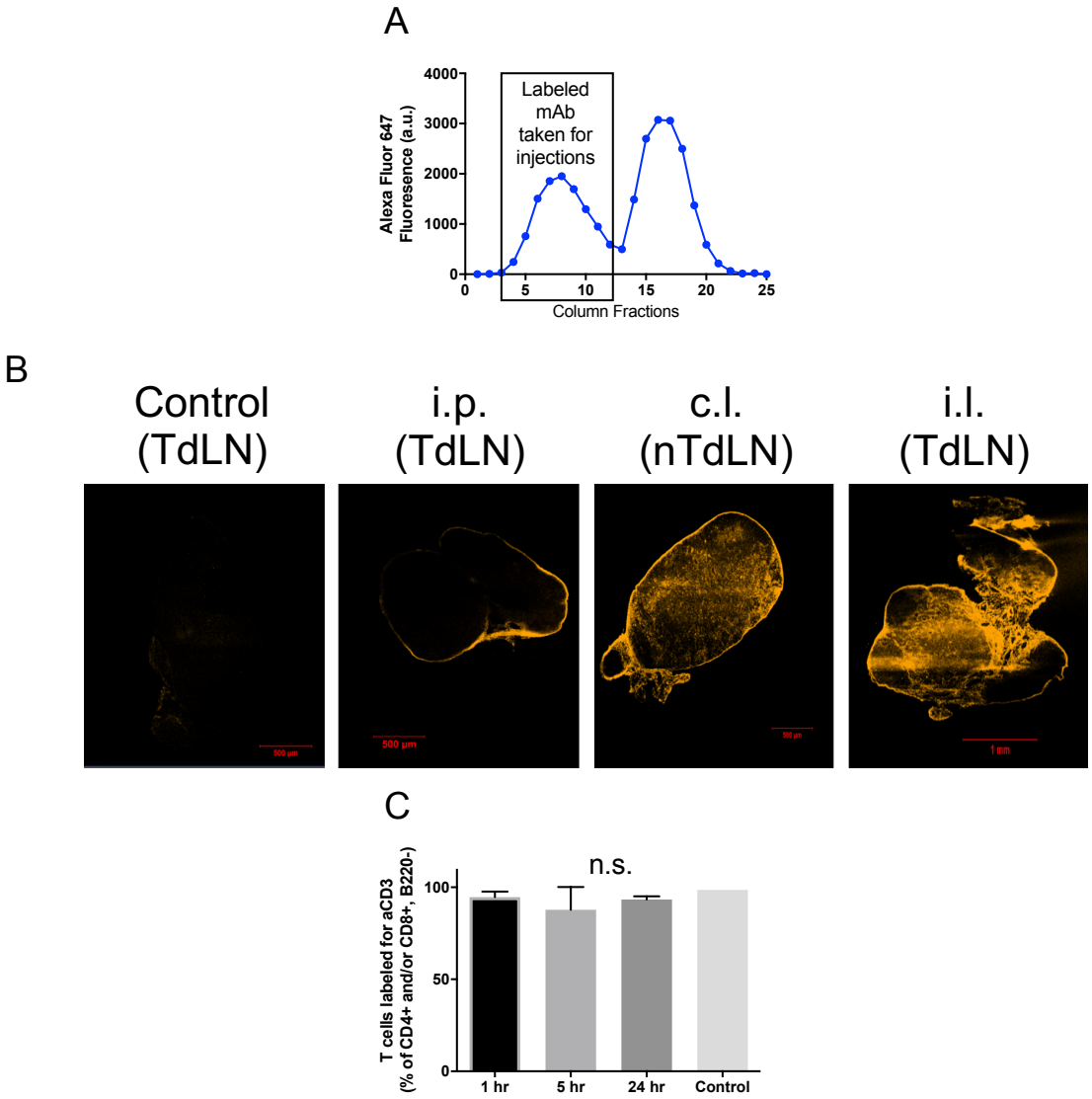

Figure 8: Characterization of mAb labeling and accumulation within LNs and binding of LN T cells after administration. (**A**) Representative size exclusion chromatography curve of Alexa Fluor 647 labeled antibody elution from sepharose CL-6B. Box indicates collected fractions that were concentrated for *in vivo* use. (**B**) LN distribution of unlabeled aCTLA4 (9H10) mAb 24 hr post injection and stained *ex vivo* with fluorescently conjugated secondary antibody (TdLN from uninjected animals as control, TdLN from i.p. or i.l injected animal, nTdLN from c.l. injected animal). (**C**) Quantification of aCD3 binding to CD3 expressing T cells at different time points following collagenase D treatment and LN mechanical disruption. Data represents one experiment (total n=2, mean ± SD)). n.s., not significant. Statistical analyses were done using ANOVA with Tukey's test. n.s., not significant.

TdLNs (Fig. 9E-F). These locoregional administration routes allowed for reduced dosing while maintaining mAb accumulation within TdLNs (Fig. 9G-H). Accumulation of mAb in dLNs was

not an effect of dye labeling as administered non-fluorescent mAb was observed to accumulate within dLNs as with AlexaFluor647 tagged mAb (Fig. 8B). Using these four different routes of administration allowed for subsequent studies to explore the effects on drugging particular tissues of interest and their effects on ICB therapeutic efficacy.

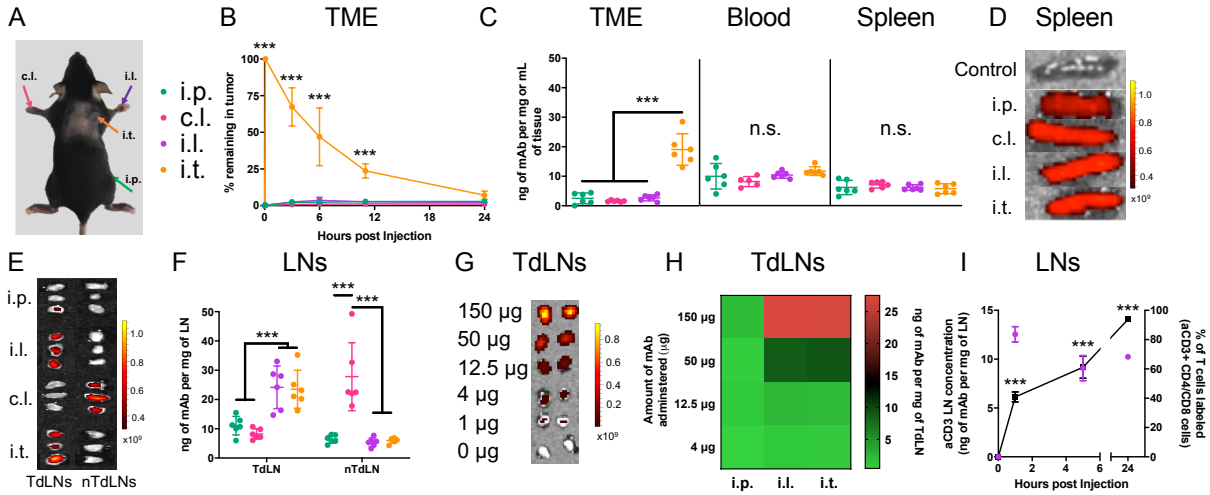

Figure 9: Directed mAb delivery to various tissues with different routes of administration. Measured tissue levels of AF647-labelled aPD1 or aCTLA4 (9H10) mAb. (**A**) Injection sites and color scheme. (**B**) mAb signal (IVIS quantification) in TME over 24 hr post injection. (**C**) mAb concentration in tumor, blood, and spleen 24 hr post injection. (D-E) Representative IVIS images of mAb levels in spleens (**D**) and LNs (**E**). (**F**) mAb concentrations in LNs 24 hr post injection. (G-H) Measured levels of AF647-labelled aPD1 or aCTLA4 in TdLNs using different mAb doses. (**G**) Representative IVIS images of mAb levels in TdLNs. (**H**) Quantification of G. (**I**) Concentration of aCD3 (purple – left axis) and frequencies of T cell labeling of injected aCD3 (black – right axis) in LNs draining forearm i.d. injection. Data represent two independent experiments (total n=5, mean ± SD). Statistical analyses were done using ANOVA with Tukey's test. ***p < 0.001, n.s., not significant.

To explore whether lymph-delivered mAb had access to LN T cells, aCD3 (in place of immune checkpoint targeting) mAb was administered in the forelimb to target LN-resident CD3 expressing T cells. A gradual increase in T cell labeling was observed over 24 hr, with nearly 100% of T cells labeled with AlexaFluor647-aCD3, suggesting a diffusion-limited intra-LN transport process as comparable total LN mAb concentrations were observed within LNs at all time points (Fig. 9I). The measured LN mAb concentration was sufficient to label ~100% of T cells when LNs were mechanically and enzymatically degraded after resection (Fig. 8C). These

results are in line with a recently published study confirming mAb has access to LN cells *(187)*. Overall, these results demonstrate various administration routes can be used as an approach to direct the delivery of mAb to T cells in specific tissues including the TME, LNs, and systemic tissues.

3.2.3 TdLN targeted ICB improves anti-melanoma response

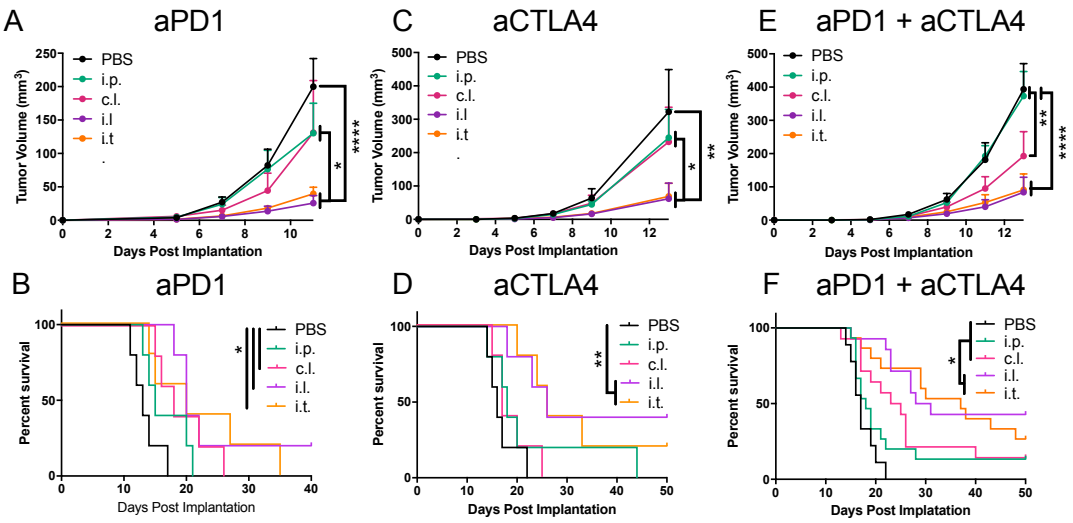

Figure 10: ICB directed towards TdLN potentiates ICB therapeutic effects in melanoma. B16F10 tumor growth (A,C,E) and animal survival (B,D,F) after aPD1 monotherapy (**A-B**), aCTLA4 (9H10) monotherapy (**C-D**), and aPD1+aCTLA4 (9H10) therapy (**E-F**) using 150 µg of each mentioned mAb. Data represent at one, two, or three independent experiments (total n=5-15, mean + SEM). Statistical analyses were done using ANOVA with Tukey's test. Log-rank (Mantel-Cox) test for survival curves. *p < 0.05, **p < 0.01, ***p < 0.001, ****p < 0.0001.

To elucidate the mechanistic effects of modulating immune checkpoints in various tissues on anti-tumor immunity, ICB mAbs were administered in a similar scheme as reported in Fig. 9. This approach allowed the effects of ICB mAb delivery to specific tissues to be elaborated as i.t. administration results in appreciable mAb accumulation within the TME, TdLN, and spleen, i.d. forelimb injections target only the TdLN or nTdLN and spleen, and i.p. administration results in only accumulation in the spleen but not the TME nor LNs. On d 5 following B16F10 melanoma implantation, mice were treated with various ICB therapeutic regimens and treated every other

day, including aPD1, aCTLA4, or the combination of the two, for a total of three doses. When used as monotherapies, aPD1 and aCTLA4 administered i.p. and in the forelimb c.l. to the tumor had minimal effect on tumor growth and animal survival, whereas administration of ICB in the forelimb i.l. to the tumor and i.t. reduced tumor growth during treatment to equivalent extents, which in the case of aCTLA4 monotherapy led to prolonged survival (Fig. 10A-D). However, ICB therapy was less effective in larger sized tumors (Fig. 11). Similar effects were observed when aPD1 was combined with aCTLA4, with c.l. administration resulting in reduced tumor growth during treatment (Fig. 10E-F). Overall, these data suggest that targeting of TdLNs alone (or alone in addition to the spleen) results in the generation of robust anti-tumor immunity much greater than that of systemic administration.

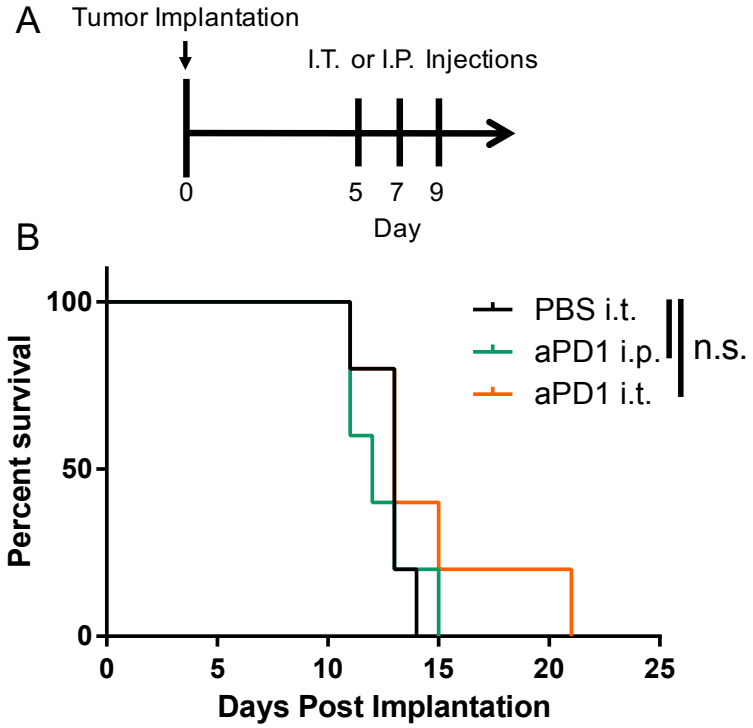

Figure 11: ICB therapy is less effective in larger tumors. (**A**) C57Bl6 mice were implanted with 5 x 10^5 B16F10 cells on d 0 and treated on d 5, 7, and 9 mice with 150 µg of aPD1 mAb i.p. or i.t.. (**B**) Survival curves. Data represents one experimental test (total n=5). Log-rank (Mantel-Cox) test for survival curves. n.s. not significant.

3.2.4 Locoregional ICB improves vaccination therapy

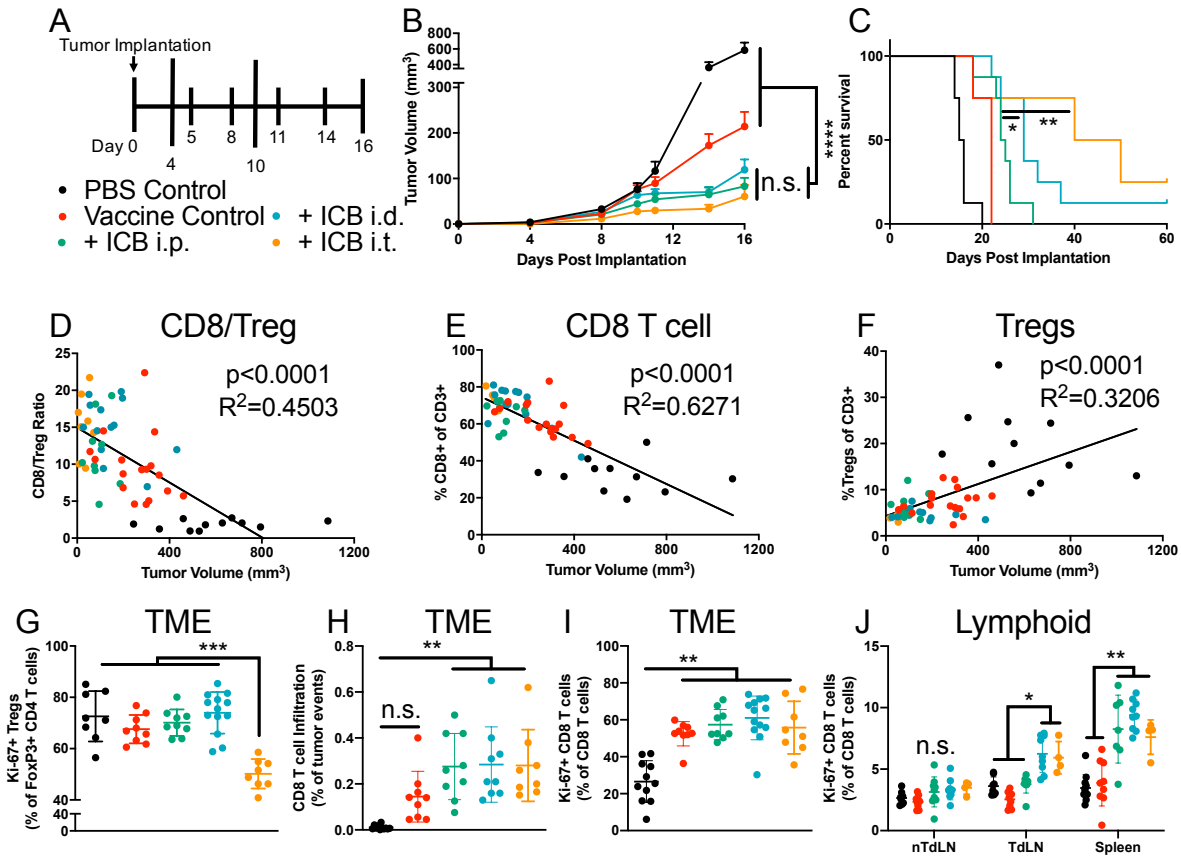

Figure 12: mAb directed to tumor and TdLNs in combination with vaccination improve therapeutic effects of ICB. (A) B16F10-OVA treatment schedule and color scheme. Vaccination was performed by intradermal administration 3 μg of CpG and 10 μg of OVA in each limb d 4 & 10. 150 μg of ICB mAb [aPD1 and aCTLA4 (9H10) in combination] using indicated administration routes d 5, 8, 11, & 14. (**B**) Tumor growth during treatment window. (**C**) Animal survival curves. (**D-F**) Tumor volume (x-axis) versus T cell infiltration levels (y-axis): (**D**) CD8+/CD4+FoxP3+ TIL ratio, (**E**) CD8+ frequency of CD3+ TILs, (**F**) CD4+ FoxP3+ frequency of CD3+ TILs. (**G**) Frequencies of Ki-67+ CD4+ FoxP3+ in TME. (**H**) Frequencies of CD8+ T cells in TME. Frequencies of Ki-67+ CD8+ T cells in TME (**I**) and lymphoid tissues (**J**). Data represent one, two, or three independent experiments (total n=4-14, mean ± SD). Statistical analyses were done using ANOVA with Tukey's test. Log-rank (Mantel-Cox) test for survival curves. *p < 0.05, **p < 0.01, ***p < 0.001.

We next explored administration effects using ICB therapy in combination with a model tumor vaccine. The rationale was to first develop and expand a robust anti-tumor CD8 T cell pool in tumor-bearing animals prior to modulation of T cell activation and effector functions resulting from ICB. Mice bearing B16F10 melanomas expressing ovalbumin (OVA) were vaccinated i.d. in

each limb with OVA protein as tumor antigen with CpG oligodeoxynucleotide (CpG) as an adjuvant 4 and 10 d post tumor implantation prior to ICB administration (aPD1 and aCTLA4) on d 5, 8, 11, and 14 (Fig. 12A). Irrespective of route of mAb administration, ICB improved vaccine effects during treatment, as measured by tumor outgrowth over the first 16 d (Fig. 12B). After cessation of therapy, ICB administered in the skin (either i.t. or i.d.) conferred improved survival (Fig. 12C) to that of systemically administered ICB (i.p.). T cell phenotyping d 16 post tumor implantation revealed that increased CD8/Treg ratios and CD8 T cell infiltration correlated with smaller tumors (Fig. 12D-E) while increased Treg frequencies correlated with increased tumor size (Fig. 12F). ICB administered i.t. led to reductions in proliferating Tregs ($CD4^+FoxP3^+Ki\text{-}67^+$) within the tumor compared to other ICB administration methods (Fig. 12G), an effect due to the particular aCTLA4 clone used and from higher CTLA4 surface expression on Tregs (Fig. 13).

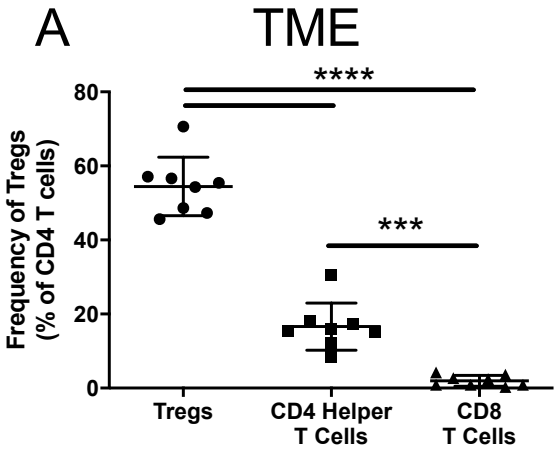

Figure 13: Tregs in TME express CTLA4 at higher levels than helper CD4 and CD8 T cells. (**A**) 16 d following B16F10-OVA implantation and treatment, mice were sacrificed and tumor resident T cells were analyzed for CTLA4 expression. Tregs defined as CD4+ FoxP3+ and CD4h T cells as CD4+ FoxP3-. Data represent one experiment (total n=8, mean ± SD). Statistical analyses were done using ANOVA with Tukey's test. ***$p < 0.001$, n.s., not significant.

Interestingly, when mice were treated with ICB therapy, increased infiltration of CD8 TILs was observed (Fig. 12H). However, similar levels of CD8 TIL proliferation were observed

regardless of therapy or route of administration (Fig. 12I). Instead, increases in proliferation were observed in lymphoid tissues, specifically the TdLN using an i.d. or i.t. administration and the spleen with the addition of ICB therapy (Fig. 12J). Similar to results exploring the cell state of PD1+ CD8 T cells (Fig. 5), the PD1^{+} CD8 T cells within the TME were predominately effector-like cells whereas lymphoid tissues consisted of both effector- and stem-like CD8 T cells (Fig. 14). Furthermore, CD8 T cells generated in LNs and spleen with ICB therapy were functional and capable of responding to tumor antigen upon *ex vivo* restimulation (Fig. 14). Similar trends were observed in the CD4 helper compartment (Fig. 15). Taken together, these results are in line with those from neoadjuvant studies where improved responses are associated with increased CD8 T cell proliferation and tumor infiltration (Fig. 5), which was achieved via concurrent drug modulation of immune checkpoint pathways in the TME and LN.

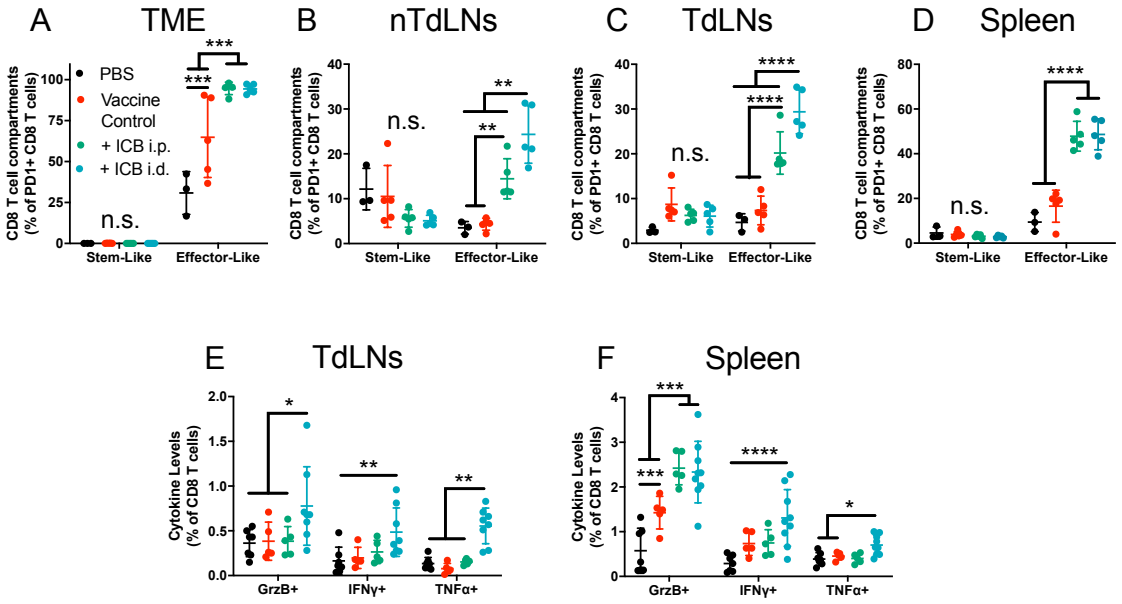

Figure 14: ICB therapy modulates CD8 T cells in various tissues leading to effector cell phenotypes. 16 d following B16F10-OVA implantation, mice were sacrificed and CD8 T cells were analyzed for "stem-like" (PD1+ CXCR5+ CD39-) or "effector-like" (PD1+ CXCR5- CD39+) phenotypes. (**A**) TME. (**B**) nTdLNs. (**C**) TdLNs. (**D**) Spleen. E-F) Frequency of effector molecule producing SIINFEKL specific CD8 T cells in TdLNs (**E**) and spleen (**F**). A-D represents one experiment (n=3-5, mean ± SD). E-F represent two independent experiments (n=8-10, mean ± SD). Statistical analyses were done using ANOVA with Tukey's test. * represents significance, *$p < 0.05$, **$p < 0.01$, ***$p < 0.001$, ****$p < 0.0001$.

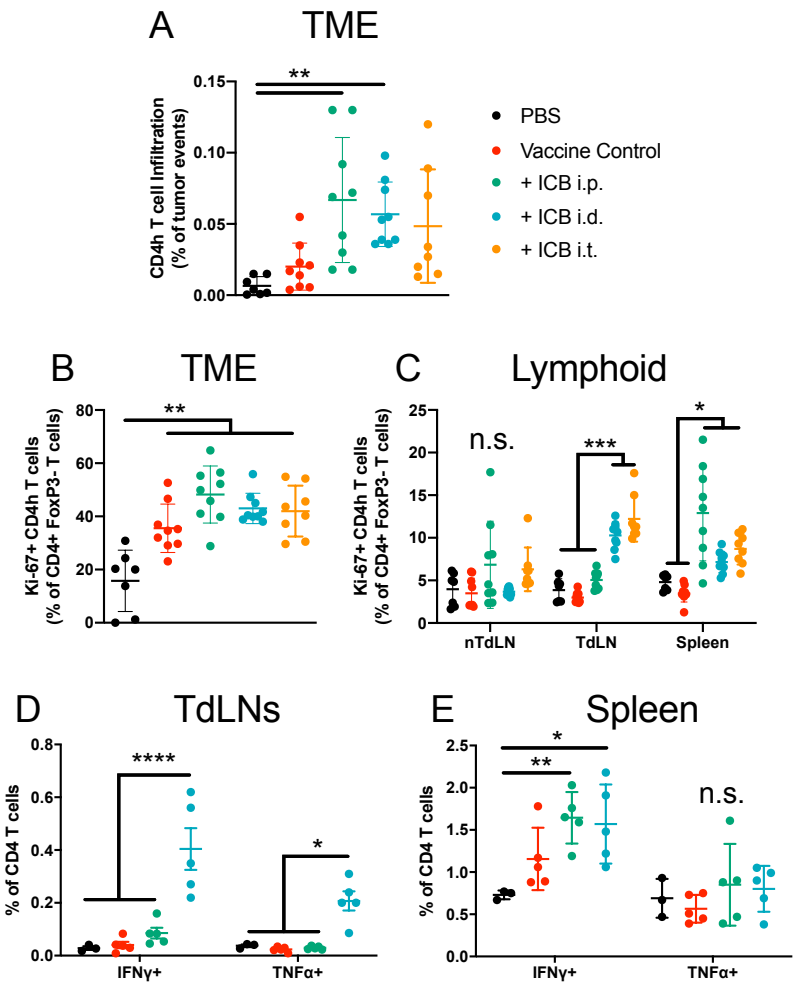

Figure 15: ICB with vaccination promotes CD4h activation in TdLNs. (**A**) Frequencies of CD4+ FoxP3- T cells in the TME. Frequencies of Ki-67+ CD4+ FoxP3- T cells in TME (**B**) and lymphoid tissues (**C**). D-E) Frequency of cytokine producing OVA specific CD4 T cells in spleen (**D**) and TdLNs (**E**). Data represent one or two independent experiments (n=4-10 mice, mean ± SD). Statistical analyses were done using ANOVA with Tukey's test. *p < 0.05, **p < 0.01, ***p < 0.001, ****p < 0.0001, n.s., not significant.

3.2.5 Dose sparing achieved by LN and TME directed ICB

Considering the dose-toxicity relationship of ICB therapy, we assessed ICB efficacy in a dose de-escalation study using aPD1 and aCTLA4 (Fig. 16). Dose-limited therapeutic effects were observed in the case of nTdLN (c.l.) and TdLN (i.l.) drugging while i.t. administration did not display a dose-efficacy relationship (Fig. 16). This may be explained by our observations of

substantial reductions in trTregs levels following i.t. administration (Fig. 5B, Fig. 12G), which is in line with multiple other reports showing that the efficacy of aCTLA4 therapy is due in part to the depletion of trTregs when an IgG2a clone is used. However, Treg depletion by aCTLA4 has not been observed in the clinical setting and instead clones of aCTLA4 used in human patients have been shown to act predominately via CTLA4 receptor blockade and favoring CD28 ligation *(188, 189)*, i.e. without measurable Treg depletion. We therefore investigated the therapeutic effects of CTLA4 blockade using a clone of an IgG1 isotype (4F10) using an identical dosing schedule to those conducted using the Treg-depleting (IgG2a isotype) aCTLA4 clone (Fig. 10). Using this non-Treg depleting aCTLA4 clone (IgG1), i.p. and c.l. administration had minimal anti-tumor therapeutic effects (Fig. 17A-B, E-F). Conversely, both i.l. and i.t. administration elicited robust anti-tumor therapeutic effects even at the lowest tested dose (12.5 μg, Fig. 17C-D, G-H). These data thus demonstrate that the benefits of LN targeting are applicable to multiple aCTLA4 mAb clones with differing immune modulatory mechanisms. More interestingly, these results suggest that the efficacy of ICB directed to the TdLNs alone or in addition to the TME is roughly equivalent, at least at these tested doses in this model, pointing to LNs mediating the expansion of CD8 T cell immunity in response to ICB.

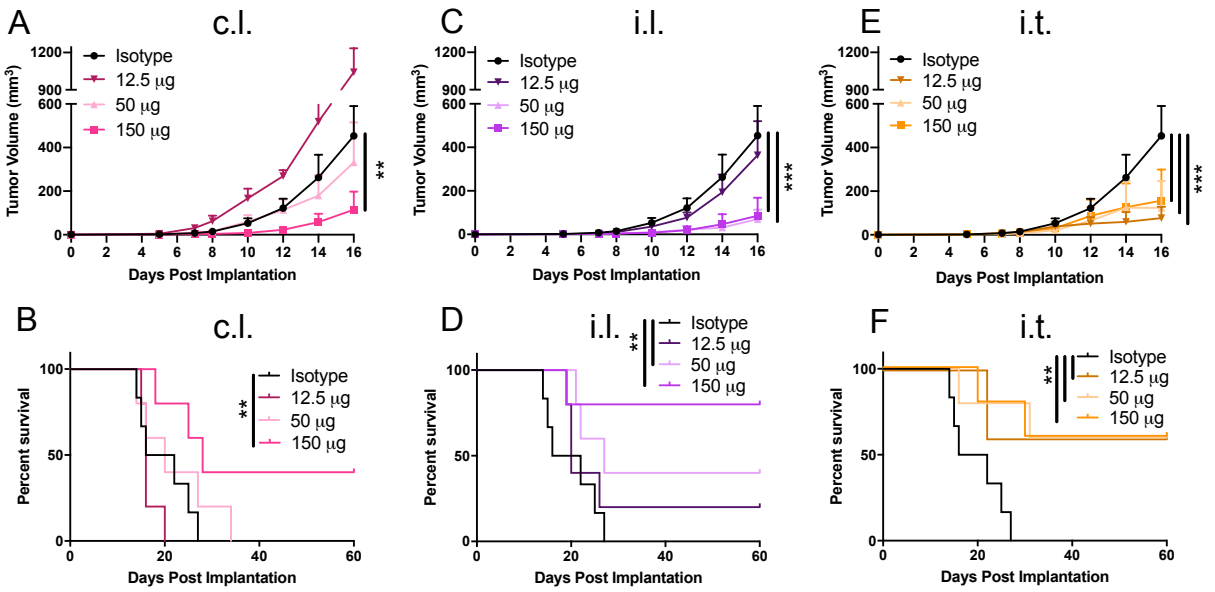

Figure 16: ICB directed to TME and/or TdLN allows for dose reductions. B16F10 tumor growth (A,C,E) and animal survival (B,D,F) using aPD1+aCTLA4 (9H10) mAb therapy at various doses; (**A-B**) c.l. administration, (**C-D**) i.l. administration, (**E-F**) i.t. administration. Data represent one experiment (total n=5, mean + SEM). Statistical analyses were done using ANOVA with Tukey's test. Log-rank (Mantel-Cox) test for survival curves. *p < 0.05, **p < 0.01, ***p < 0.001, ****p < 0.0001.

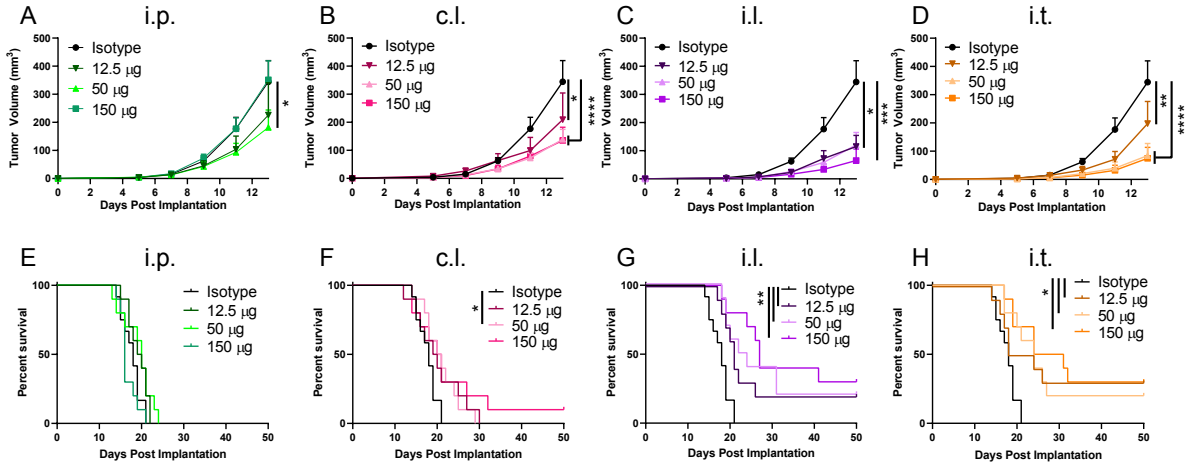

Figure 17: ICB directed to tumor and/or TdLN potentiates ICB therapeutic effects independent of tumor resident Treg depletion. B16F10 tumor growth (A - D) and animal survival (E - H) after ICB therapy using 150, 50, or 12.5 μg of aPD1 (clone: RMP1-14) in combination with aCTLA4 (clone: 4F10); (**A,E**) i.p. administration, (**B,F**) c.l. administration, (**C,G**) i.l. administration, and (**D,H**) i.t. administration. Combined data of two independent repeats (total n=10, mean + SEM). Statistical analyses were done using ANOVA with Tukey's test. Log-rank (Mantel-Cox) test for survival curves. *p < 0.05, **p < 0.01, ***p < 0.001, ****p < 0.0001.

3.2.6 ICB targeted to TdLNs improves therapeutic effects in breast cancer

To extend these results beyond melanoma models, two different mammary carcinoma models, the E0771 and 4T1, were implanted orthotopically in the 4th mammary fat-pad. These implantation sites generate different TdLNs, specifically the ipsilateral inguinal (primary draining) and axillary (secondary draining) LNs. In order to deliver mAb to TdLNs or nTdLNs, mAb administration was performed in the flanks of mice (Fig. 18A) while the systemic i.p. administration was kept the same and i.t. administration is administered to the mammary fat-pad tumor site. Following administration of fluorescently labeled mAb (aPD1), i.t. administration resulted in substantial mAb retention in the TME while other administration routes resulted in low to minimal TME concentrations (Fig. 18B). Levels of mAb accumulation in the spleen were found to be equivalent regardless of administration route (Fig. 18B). Contrastingly, i.l. and i.t administration of mAb (aPD1 or isotype) led to higher TdLN accumulation while c.l. administration led to accumulation within nTdLN (Fig. 18B).

In the context of ICB with aPD1 in the E0771 model, locoregional therapy was found to somewhat hasten responses, in particular with i.l. administration (Fig. 19A-B). However, the effects of aPD1 monotherapy, irrespective of the administration route, were less efficacious in prolonging survival, motivating the exploration of aPD1 use in combination with aCTLA4. To this end, a single dose of aPD1 in combination with aCTLA4 (clone: 9H10) administered i.t., i.l., and c.l. resulted in substantial reductions in tumor growth compared to both no treatment and systemic i.p. administration (Fig. 18C). However, substantial improvements in survival were found for this combination therapy (40-60% overall complete response) and were comparable between all administration routes (Fig. 18D). Dose de-escalation studies demonstrated that survival was highly dose sensitive, but effects were again roughly equivalent between ICB mAb administration route

(Fig. 19C-F). This data demonstrates that the therapeutic benefits of ICB with aPD1 in this model can be substantially augmented by aCTLA4, which is unsurprising given this aCTLA4 clone's pleotropic effects on the anti-tumor immune response.

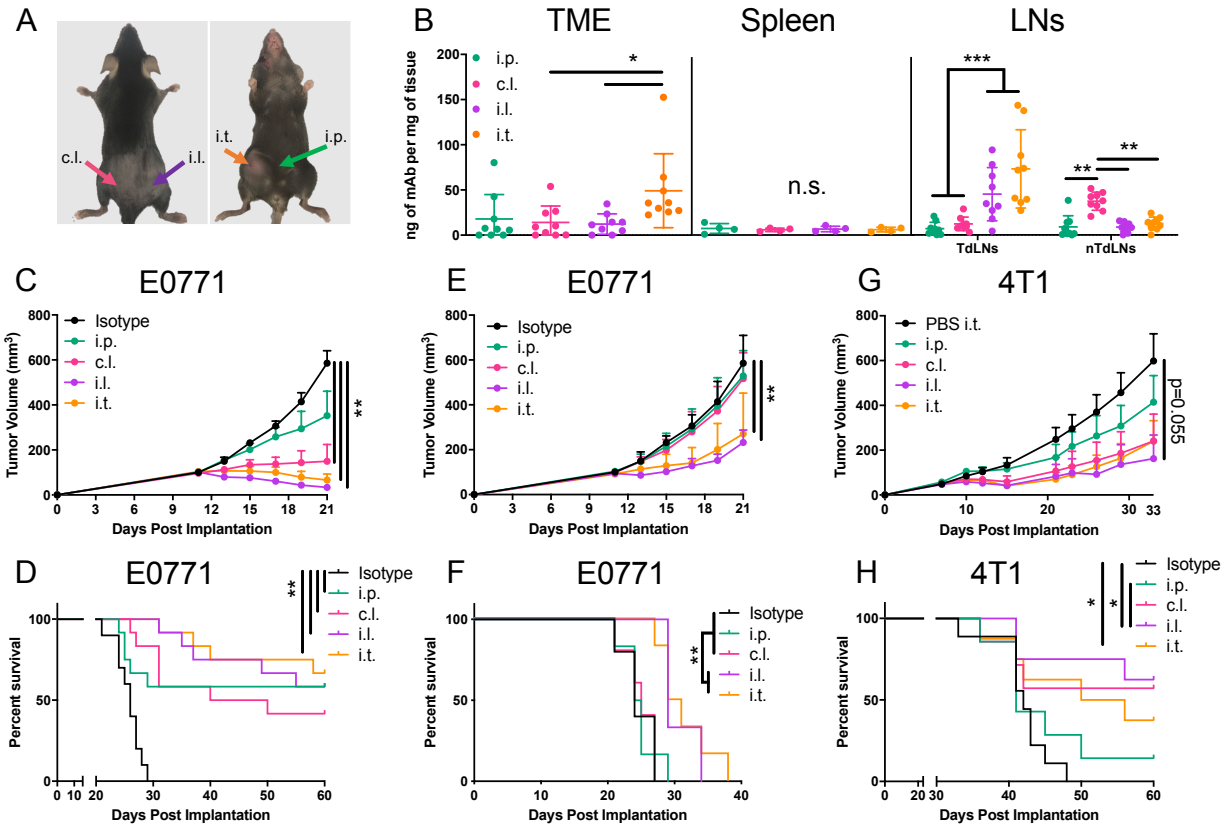

Figure 18: TdLN targeted ICB exhibits robust antitumor therapeutic effects in breast tumor models. (**A**) Image of administration sites and color scheme. (**B**) mAb concentrations in TME, spleen, and LNs in E0771 tumor-bearing animals 24 hr post injection. (**C**) Growth curves of E0771 tumors using single a 100 μg dose of aPD1+aCTLA4 (clone: 9H10) when tumors reached approximately 100 mm^3. (**D**) Survival of animals treated in panel C. (**E**) Growth curves of E0771 tumors with 30 μg aPD1+aCTLA4 (clone: 4F10) therapy on d 10, 14, and 20. (**F**) Survival of animals treated in panel E. (**G**) Growth curves of 4T1 tumors treated with 50 μg aPD1 and aCTLA4 (clone: 4F10) on d 7. (**H**) Survival of animals treated in panel G. B represents one or two independent experiments (total n=4-9, mean ± SD), C/D represent two independent experiments (total n = 11, mean ± SEM), E-H represent one experiment (total n=4-8, mean ± SEM). Statistical analyses were done using ANOVA with Tukey's test. Log-rank (Mantel-Cox) test for survival curves. *p < 0.05, **p < 0.01, ***p < 0.001, n.s., not significant.

To decouple the effects of trTreg depletion versus expansion of CD8 T cell immunity associated with aCTLA4 treatment, the effects of the 4F10 clone of aCTLA4 that does not result in trTreg depletion were evaluated (Fig. 18E-F). Unsurprisingly, anti-tumor therapeutic efficacy in all tested administration routes was found overall to be much less effective, indicative of a major role that Tregs play in the immune physiology of the E0771 model. However, i.l. and i.t. administration did substantially suppress tumor growth as well as prolong survival compared to i.p. and c.l. administration (Fig. 18E-F). Effects of aPD1 in combination with aCTLA4 (clone: 4F10) in the highly metastatic 4T1 model were also tested. Improved responses were observed with c.l., i.l., and i.t. therapy compared to that of systemic i.p. therapy (Fig. 18G-H) with no signs of metastasis in responding mice (Fig. 19G-H). Notably, when the trTreg depleting aCTLA4 clone (clone: 9H10) was used, systemic therapy was just as effective as administration in the skin (both i.l. and c.l., Fig. 19I-J). This data is suggestive of these breast tumor models being highly infiltrated with Tregs that are implicated in tumor progression. Nevertheless, as was found in the B16F10 melanoma model, (Td)LN targeting of mAb improved therapeutic responses to ICB in two breast tumor models compared to conventional systemic administration.

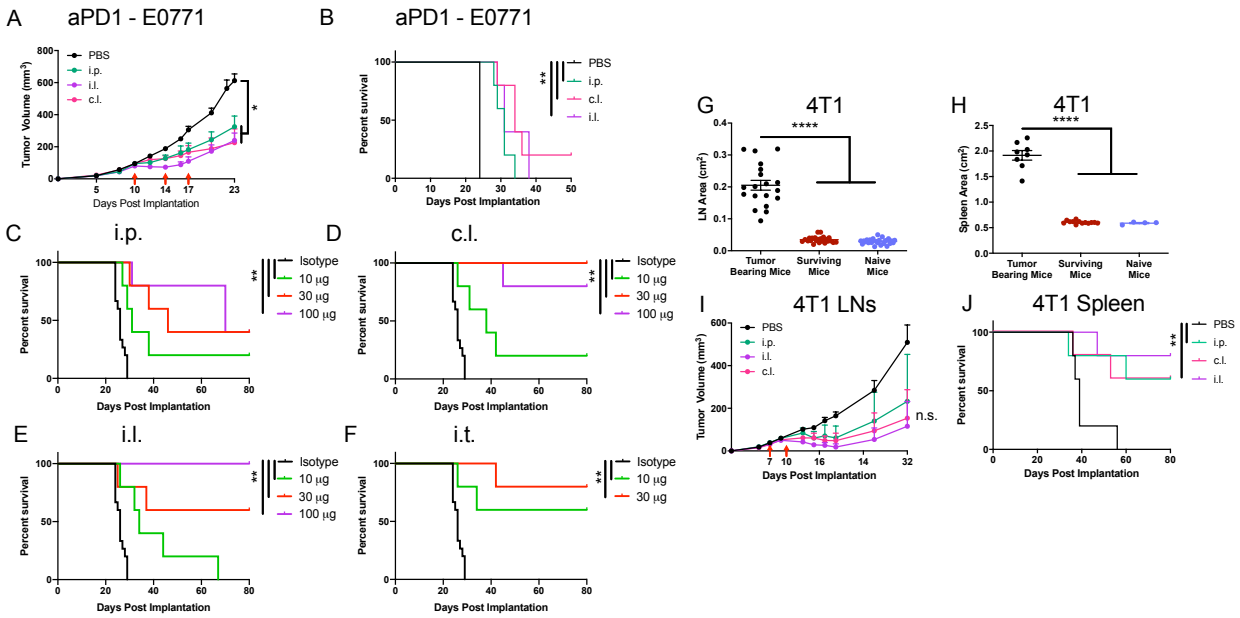

Figure 19: Effective ICB therapy in breast cancers requires aCTLA4. (**A**) Growth curves of E0771 tumors with 100 μg aPD1 monotherapy on d 10, 14, and 17. (B) Survival curve of aPD1 monotherapy. C-F) Survival curves of E0771 tumors according to administration route with 10, 30, or 100 μg aPD1+aCTLA4 (clone: 9H10) therapy starting when tumors reached 100 mm^3 (d 10 or 12) and continued on d 14 and 20 or 16 and 22 pending start date: (**C**) i.p. administration, (**D**) c.l. administration, (**E**) i.l. administration, (**F**) i.t. administration. (**G**) Size of LNs at endpoint for tumor bearing mice and d 80 for surviving mice. (**H**) Size of LNs at endpoint for tumor bearing mice and d 80 for surviving mice. (**I**) Growth curve of 4T1 tumors using 50 μg aPD1+aCTLA4 (9H10) on d 7 and 10. (**J**) Survival curve of 4T1 mice. Data represent one experiment (total n=4-5, mean ± SEM). Statistical analyses were done using ANOVA with Tukey's test. Log-rank (Mantel-Cox) test for survival curves. *p < 0.05, **p < 0.01, n.s., not significant.

3.2.7 Locoregional administration reduces toxicities of ICB

ICB is associated with immune related adverse events that can lead to discontinuation of treatment, especially when aPD1 and aCTLA4 are combined *(7)*. Following completion of treatment in each therapeutic regimen, blood was collected 2-3 d following the last mAb administration and serum analyzed. When treated with ICB alone, i.p. administration led to elevated alanine transaminase serum levels compared to no treatment and cutaneous injections in both the B16F10 and E0771 tumor models (Fig. 20A). When mice were vaccinated, similar trends were observed as measured on d 16 post tumor implantation (Fig. 20B). Furthermore, mAb concentration in the liver, kidneys, and lungs was proportional to the administered dose of ICB

mAb (Fig. 20C, S21). Overall, these results suggest that locoregional administration of ICB mAb, which can elicit robust immunity and anti-tumor efficacy, results in reduced toxicity associated with systemic and high dose ICB therapy.

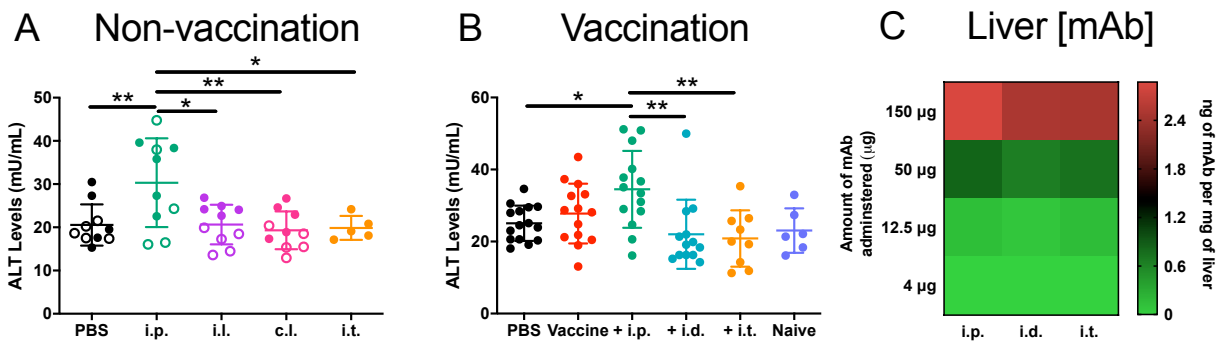

Figure 20: Locoregional administration reduces ICB-associated toxicities. ALT levels from serum of animals (**A**) d 12 post B16F10 implantation or d 22 post E0771 implantation and (**B**) d 16 post tumor implantation in B16F10-OVA bearing animals following vaccination. (**C**) Concentration of mAb in liver 24 hr post i.p. administration at various total doses. Naïve: tumor-free mouse. PBS was administered i.t. In A; closed circles represent B16F10 experiments while open circles represent E0771 experiments. A) represents one experiment in each tumor model (total n=10, mean ± SD), B) represents at least two independent experiments (total n=6-16, mean ± SD), C) represents one experiment in B16F10 bearing mouse (n=2). Statistical analyses were done using ANOVA with Tukey's test. *p < 0.05, **p < 0.01.

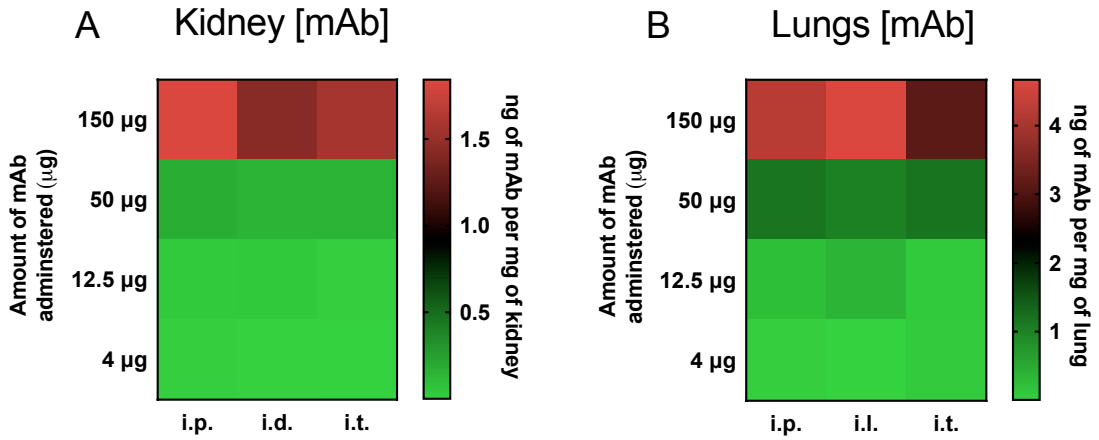

Figure 21: mAb accumulation in systemic tissues proportional to administered dose. 24 hr post administration using aPD1, mice were sacrificed and tissues harvested to measure concentrations of accumulated mAb. (**A**) Kidneys. (**B**) Lungs. Data represent one experiment (total n=2).

3.3 Discussion

ICB has emerged as a promising new class of anti-cancer therapy, but these treatments are associated with low response rates and substantial toxicities, which may be related to systemic administration of these drugs. Targeting the TME versus LNs and spleen using different administration routes and doses was explored in order to increase mAb accumulation within these tissues and therefore modulate these pathways at the effector and priming phases, respectively. In three tumor models, varying from poorly to highly responsive to ICB, administration routes that result in pronounced levels of mAb accumulation in (Td)LNs led to superior therapeutic effects on tumor control compared to those achieved by systemic administration.

A profound abscopal effect was observed with tumor-localized ICB using i.t. administration, demonstrating the generation of an anti-tumor immune response that is systemically functional. It also suggests that tumor localized therapy is capable of expanding endogenous anti-tumor immunity, given observations of elevated TIL frequencies. Many studies suggest that increasing levels of CD8 TILs improve response to immunotherapy and patient survival *(169, 173, 190)*. Whether they originate from the TME or elsewhere prior to migrating into the TME remains unclear, however, tumor specific T cells have been found in the blood post-ICB treatment suggesting the latter *(172, 191, 192)*. Here, we observed elevated frequencies of proliferating CD8 T cells in the TME, but also in the TdLN and spleen following i.t. treatment, suggesting that TILs may originate from multiple tissue sites. We observed stem-like CD8 TILs; however, the predominate phenotype of activated CD8 TILs was effector-like, which may be due to proliferation and differentiation of tumor resident stem-like CD8 T cells *(163, 164)*. In line with this, stem-like CD8 TILs reside in APC-enriched niches that support their function, and loss or absence of these niches is associated with disease progression *(193)*. In addition to the TME, we observed stem-like CD8 T cells in secondary lymphoid tissues, consistent with previous reports

(10, 164) including human LNs *(181)*. Thus, secondary lymphoid tissues are a potential source of tumor killing effector-like CD8 T cells. Consistent with this, accumulation of mAb within the spleen and LNs is associated with expansion of the effector-like cell pool within these tissues. Poorly immunogenic TMEs lacking APC niches or TILs may therefore not respond to systemic ICB therapy and may instead benefit from targeted delivery of ICB mAbs into lymphoid tissues where these stem-like CD8 T cells reside. Notably, T cell phenotyping performed here was not restricted to known antigen-specific T cell clones. Overall, our results support the conclusions that ICB therapy increases TIL frequencies and that, as TILs may originate outside the TME, lymphoid tissues represent potential tissue targets for ICB modulation.

The effect of LN-directed mAb delivery was found to be beneficial in multiple therapeutic settings. In the B16F10 melanoma model, systemic i.p. administration led to minimal therapeutic efficacy that may be due to poor delivery and accumulation of ICB mAbs in the TME and TdLNs. ICB therapy directed towards TdLNs via i.l. forelimb administration greatly improved response rates regardless of aCTLA4 clone used, which we hypothesize is due to improved T cell activation and subsequent infiltration into the TME. Interestingly, dose de-escalation experiments revealed that ICB mAb directed to the TdLNs alone versus in combination with the TME via i.l. forelimb or i.t. administration, respectively, result in similar anti-tumor therapeutic effects. This is suggestive of the therapeutic benefits of ICB being conferred, at least partially, by activity within LNs, presumably at the APC:T cell synapse during the T cell priming phase. It may also be explained by the immune exclusion and poorly immunogenic hallmarks of the B16F10 model. In other words, drugging the TME does not afford therapeutic effects when anti-tumor TILs are locally absent. This concept is in line with previous observations in melanoma models where knockout of T cell PD1 expression does not improve tumor responses *(167)*. This is further supported by our vaccination studies in the B16F10-OVA model where ICB injected i.t. in

combination with a tumor vaccine resulted in longer survival. Vaccination alone resulted in dramatic expansion and infiltration of anti-tumor T cells, thus providing local TILs for potential ICB modulation. Therefore, addition of ICB directly into the tumor, along with a reduction of proliferating trTregs, resulted in an improved survival of i.t. treated mice. In line with neoadjuvant phenotyping results, addition of ICB therapy increased frequencies of TILs, which may be due to the elevated levels of proliferating T cells in lymphoid tissues. This suggests that modulation of ICB in the spleen or TdLN may promote and sustain tumor TIL infiltration.

In breast tumor models, targeting mAb to (Td)LNs alone or in combination with the TME improved therapeutic benefits compared to systemic therapy. Drastic differences were observed in the E0771 model when using a trTreg depleting clone of aCTLA4 (9H10) versus a non-depleting clone (4F10), suggesting these tumors are highly infiltrated with suppressive Tregs and/or that Tregs play a dominant role in immune-regulated disease progression in these models. A LN drugging approach, which appears effective in eliciting robust T cell immunity, may thus need to be combined with other therapies to modulate such suppressive cell types to successfully combat breast cancer. Another consideration is tumor physiology that can vary greatly in tumor types and consequently affect mAb transport (*34)*. Breast cancer models may have improved mAb access to the TME from the blood relative to melanoma models which may explain the i.p. efficacy observed. In the 4T1 model, c.l. administration improved treatment efficacy compared to systemic i.p. administration. This could be explained by the metastatic propensity and subsequent presence of tumor associated antigen in tissues beyond the TME and TdLN including nTdLNs, thereby explaining the beneficial effects of nTdLN targeting.

When toxicity was explored, systemic i.p. administration led to elevated levels of ALT whereas locoregional delivery did not. This data may be explained by a slower, more sustained delivery of ICB mAb into the blood following a cutaneous injection by virtue of lymphatic

transport compared to a bolus delivery post i.p. administration *(194)*. Accumulation of mAb in systemic tissues was proportional to administered dose. This indicates that administration routes that afford dose sparing, e.g. injection into locoregional tissues, have the potential to minimize off target toxicities.

There is interest in locoregional delivery of mAbs as systemic administration has several disadvantages, including cost and compliance *(195)*. Local immune therapy via i.t. administration using aCTLA4 and s.c. administration using aPD1 has been reported for a variety of cancers including melanoma *(8, 130)*. However, locoregional injections hold approximately 1/10 the volume of systemic infusions, thus mAb solutions must be concentrated, which can lead to protein aggregation, and therefore compromised efficacy, increased immunogenicity, and concerns for pharmacokinetic profiles *(194)*. Here, we show the LN is a tissue of interest and using route administration to direct ICB mAbs to TdLNs allows for efficient ICB drugging and reduced dosing relative to systemic administration, helping to overcome the aforementioned concerns. Considering i.t. injections are not always feasible due to tumor size and internal location *(129)*, locoregional administration targeting the LNs and not TME directly may be advantageous as TIL frequencies are often low, exhausted T cells undergo epigenetic reprogramming *(196)* that can limit TIL rejuvenation potential *(197, 198)*, and, as noted above, tumor physiology is highly variable which can negatively influence intratumoral mAb diffusion and lymphatic transport *(89)*. TdLNs may be challenging to identify and in some cases absent due to removal during LN biopsy/dissection, which make this approach limited to certain indications or in neoadjuvant settings. Nevertheless, locoregional injection in a distant site from the tumor that drains to the same TdLNs may be of interest as an alternative to i.t. administration in order to broaden the number of patients whom might benefit from a locoregional treatment approach as well as reduce treatment invasiveness.

In conclusion, directing ICB mAbs to (Td)LNs by locoregional administration enhanced anti-tumor efficacy compared to systemically administered mAb and reduced associated toxicities in both melanoma and breast cancers. This simple approach requires no chemical modifications to the ICB mAbs, only reformulation that may hold potential for clinical translation due to current FDA approval, interest in patient compliant administrations, and need to improve safety and response rates.

3.5 Materials and Methods

3.5.1 Experimental Design

This study was designed to explore the mechanism and test the antitumor efficacy of ICB by targeting mAbs to LN tissues compared to the TME and the spleen in mouse melanoma and breast cancer models. We explored in what tissues immune checkpoint pathways were active and whether tumor localized immunotherapy led to systemic immunity by effects measured in a distant, untreated tumor site. We explored how ICB delivery to LNs differed from systemic delivery therapy in an antigen expressing cell line in combination with vaccination and endogenous cell lines with only ICB therapy. The goal of these experiments was to explore ways to improve checkpoint therapy from traditional systemic dosing. Sample sizes were chosen based on previously published results. For animal studies, mice were randomized prior to treatment with each cage having one mouse in each treatment group. Tumor growth was determined by direct measurement using calipers and endpoint was reached when tumor sizes reached 1.5 cm in any dimension. Experiments were not performed in a blinded fashion. Statistical methods are described in the “Statistical analysis” section.

3.5.2 Mice and cell lines

Cell lines were cultured in Dulbecco’s Modified Eagle Medium supplemented with 10% fetal bovine serum and 1% penicillin/streptomycin/amphotericin B and periodically checked for

mycoplasma contamination. C57Bl/6 and BalbC mice were purchased from Jackson Laboratories. All protocols were approved by the Institutional Animal Case and Use Committee. Tumors were implanted intradermally in 6-12 wk old mice and were monitored in anesthetized mice by caliper measurements by width, length, and depth. Mice were sacrificed when tumors led to ulceration or maximum tumor size of 1.5 cm in any dimension.

3.5.3 Treatment of B16F10 melanoma bearing mice

The backs of C57Bl6 were shaved and B16F10 cells (10^5) were implanted in the right dorsal area on day 0. After 5 (when all tumors were visible), 7, and 9 d, mice were injected with 150, 50, or 12.5 μg of anti-mouse CTLA4 (clone: 9H10 or UC10-4F10-11, BioXCell) and/or rat anti-mouse PD1 (clone RMP1-14, BioXCell) intradermally into the tumor, intradermally into the forearm, or intraperitoneally in 30 μL saline. For distant tumor experiments, 10^5 B16F10 cells were injected intradermally on the right side of the mouse on day 0 and on the left side on day 2. On days, 5, 7, and 9, mice were injected with 150 μg of aCTLA4 (clone: 9H10) and aPD1 (intratumorally or intraperitoneally) in saline. For immune cell phenotyping, mice were sacrificed on d 12 where tumors, spleens, and LNs were harvested.

3.5.4 Treatment of B16F10-OVA melanoma bearing mice

The backs of C57Bl6 were shaved and B16F10-OVA cells (10^5) were implanted in the right dorsal area on day 0. After 4 and 10 d, CpG (3 μg) and OVA (10 μg) were administered in each limb using 30 μL of PBS. On day 5, 8, 11, and 14, mice received 150 μg of aCTLA4 and aPD1 i.d. into the tumor, i.d. into the forelimb, or i.p. in 30 μL. In mice responding to therapy, if no tumor was observed at day 60, mice were rechallenged with B16F10-OVA cells (10^5) and if no tumor was observed after another 60 d, mice were challenged with B16F10 cells (10^5).

3.5.5 In vivo biodistribution of mAbs

The lateral dorsal skin of C57Bl6 mice was shaved and implanted with 10^5 B16F10 cells on day 0. Fluorescent labeling of aCTLA4 (9H10), aPD1 (RMP1-14), or aCD3 (KT3) was performed using AlexaFluor647-NHS-Ester for one hr and purified using a CL-6B sepharose column. mAb fractions were pooled and concentrated using a 10 kDa (Millipore) spin filter. Concentration was determined using a BCA assay. On day 5, mice were administered with specified dose (μg) of indicated aCTLA4 or aPD1 at the indicated site. For aCD3 experiments, naïve mice were used and injected with 6.25 μg mAb and sacrificed after 1, 5, or 24 hr when LNs were either collagenase treated for 30 min followed by single cell preparations (subsequently described) or immediately cut up and generated as a single cell suspension to prevent *ex vivo* T cell labeling. Fluorescent imaging was performed with an IVIS® Spectrum instrument (Perkin Elmer) at the injection site over 24 hr and of tissues following sacrifice. Following 24 hr from Ab injection, mice were euthanized, and tissues collected for imaging and homogenization. Concentration in tissues was determined following homogenization using the injected Ab solution as a standard curve from naïve tissues.

3.5.6 Tissue and single cell preparations

Following tissue collection, tissues were processed by cutting up tissues to prevent cell surface receptor degradation. Single cell suspensions were generated by disrupting the organs through a 70-mm cell strainer followed by wash steps in PBS buffer. Red blood cells were lysed with lysing buffer hybrid-max (Sigma) for 7 min at room temperature followed by quenching in PBS buffer. Cells were plated in 96-well U bottom plates where 30% of LN cells, 2 x 10^6 splenocytes, or 5 x 10^6 tumor cells were plated for *ex vivo* T cell restimulation in Iscove's modified Dulbecco's medium supplemented with 10% FBS and 1% penicillin/streptomycin (complete media). 70% of

LN cells, 2 x 10^6 splenocytes, or 5 x 10^6 tumor cells were plated for surface/intracellular staining in PBS buffer.

3.5.7 Flow cytometry and antibodies

Single cell suspensions from tumors, LNs, and spleens were prepared as described above. After washing steps, live/dead staining was performed using Zombie Aqua fixable viability kit (Biolegend), followed by wash steps and surface staining of molecules all from BioLegend: CD45 (clone: 30-F11), CD3 (clone: 17A2), CD4 (GK1.5.), CD8 (clone: 53-6.7), PD1 (clone: 29F.1A12), FoxP3 (clone: MF-14), Tcf1 (clone: S33-966), Tim3 (clone: RMT3-23), Ki-67 (clone: 16A8) Granzyme B (clone: GB11). Surface staining was carried out on ice for 30 min, with tetramer staining done for 15 min. Intracellular staining was performed using the FoxP3 staining kit (eBioscience) according to the manufacturer's instructions. All flow cytometric analyses were performed using a Fortessa flow cytometer (BD Biosciences) and analyzed using Flowjo software (Tree star).

3.5.8 ALT assay

For non-vaccination experiments, mice were treated with aCTLA4 and aPD1 (150 μg each) on d 5,7, and 9 for B16F10 experiments, serum was collected on d 12. For E0771 experiments, mice were treated with aCTLA4 and aPD1 (100 μg each) on d 10, 14, 20 and serum collected on d 22. For B16F10-OVA vaccination experiments, serum was collected on d 16. ALT activity was measured according to manufacturer's protocol (BioVision).

3.5.9 Treatment of E0771 and 4T1 breast cancer bearing mice

5 x 10^5 E0771 cells or 3.5 x 10^5 4T1 cells resuspended in 30 μL of PBS were implanted intradermally in the left mammary fatpad (4^{th}) in C57Bl6 or BalbC mice respectively. For E0771 experiments, 100 μg of aPD1 and aCTLA4 (clone:9H10) were administered intradermally in the

specified area one time when tumors were ~100 mm^3 or 30 μg of both aPD1 and aCTLA4 (clone: 4F10) on d 10, 14, and 17. For 4T1 experiments, 50 μg of aPD1 and aCTLA4 (clone: 4F10) were administered in the specified area on d 7.

3.5.10 PD1 staining with multiple clones

Single-cell suspensions from tissues were prepared as described in the article. Complete media was spiked with PMA and ionomyocin and cells were cultured in this media for 6 hr. Following activation, staining was performed with a surface stain of BV785 labeled aPD1 (Biolegend, clone: 29F.1A12) or incubated with non-fluorescent aPD1 (BioXCell, clone: RMP1-14, same clone used in therapeutic experiments) for 20 min on ice, followed by wash step and incubation with BV785-aPD1 (Biolegend, clone: 29F.1A12) stain.

3.5.11 Ex vivo T cell stimulation

Single-cell suspensions from tissues were prepared as described in the article. Complete media was spiked with either ovalbumin (10 μg/mL) for CD4 T cells or SIINFEKL (1 μg/mL) for CD8 T cells. Cells were cultured for 3 hr at 37°C followed by the addition of brefeldin A (1X: BioLegend) for 3 hr. Cells were harvested, stained, and analyzed by flow cytometry as described in the article.

3.5.12 Treatment of E0771 and 4T1 breast cancer bearing mice

5 x 10^5 E0771 cells or 3.5 x 10^5 4T1 cells resuspended in 30 μL of PBS were implanted intradermally in the left mammary fatpad (4^{th}) in C57Bl6 or BalbC mice respectively. For E0771 experiments, 100 μg of aPD1 or both aPD1 and aCTLA4 (clone:9H10) were administered intradermally in the specified area one time when tumors were ~100 mm^3 (d 10 or 12) and again 4 and 10 d later. For 4T1 experiments, 50 μg of aPD1 and aCTLA4 (clone: 9H10) were administered

in the specified area on d 7 and 10. When tumors reached endpoint, mice were sacrificed with LNs and the spleen harvested for metastasis investigation using Image J.

3.5.13 Treatment of B16F10 melanoma bearing mice

The backs of C57Bl6 were shaved and B16F10 cells (5 x 10^5) were implanted in the right dorsal skin on day 0. After 5, 7, and 9 d, mice were injected with 150 μg of rat anti-mouse PD1 (clone RMP1-14, BioXCell) intradermally into the tumor or intraperitoneally in 30 μL saline and monitored for survival.

3.5.14 Analysis of non-fluorescent aCTLA4 accumulation in dLNs

Following 24 hours of administrations of 150 μg of aCTLA4 using i.p., c.l., and i.l. administrations, mice were sacrificed and draining LNs were harvested (axial and brachial). LNs were placed in optimal cutting temperature (OCT) compound and frozen in 2-methylbutane solutions using liquid nitrogen. OCT frozen LNs were sliced using a CryoStar NX70 instrument to 8-10 micrometers. LN sections were prepped and blocked with donkey serum, followed by an anti-hamster secondary staining antibody (IgG). LNs sections were then read on a Laser Scanning Confocal microscope (Zeiss 700) and analyzed using Zeiss Blue software.

3.5.15 Flow cytometry antibodies

Staining was performed as described in the article. In addition to the aforementioned antibodies, CXCR5 (clone: L138D7), CD39 (clone: Duha59), IFN-γ (clone: XMG1.2), and TNF-α (clone: MP6-XT22) were used.

3.5.16 Statistical analysis

Statistical significance of differences between experimental groups was calculated with Prism software (GraphPad). All data is expressed as mean ± standard error mean except for tumor growth. ****$p<0.0001$, ***$p<0.001$, **$p<0.01$, and *$p<0.05$ by unpaired two-tailed t-tests or one-

or two-way ANOVA followed by Tukey post-hoc test for multiple comparisons. For survival curves, log-rank (Mantel-Cox) test was performed.

CHAPTER 4. ENGINEERING A DRUG ELUTING CHECKPOINT ANTIBODY-NANOPARTICLE CONJUGATE PLATFORM TO ENHANCE CANCER IMMUNOTHERAPY

4.1 Introduction

Cancer immunotherapy utilizes the body's own immune system, rather than cytotoxic agents like chemotherapeutics, to recognize and eradicate cancers.*(199)* One way this is achieved is through activation and invigoration of T cells via immune checkpoint blockade (ICB) using monoclonal antibody (mAb) immunotherapies, such as anti-programmed cell death 1 (aPD1) and anti-cytotoxic T-lymphocyte associated protein 4 (aCTLA4).*(156, 200)* While ICB therapies have generated tremendous improvements in the survival of responsive patients, response rates of ICB therapies remain low and are thus combinations with other small molecule immune modulators that block non-redundant suppressive pathways are actively being explored to overcome ICB resistance.*(7, 201)* However, the ability to deliver small molecule therapeutics to cells of interest at bioactive doses to completely harness the potential of immunotherapy remains challenging as these drugs distribute in a non-affinity based manner and have short circulation times.*(202)* We therefore engineered an antibody-nanoparticle conjugate (ANC) platform to achieve targeted delivery of small molecule immune modulating drugs with ICB mAbs to immune checkpoint expressing cells to generate a more robust anti-tumor immune response.

While many nanoparticle (NP) platforms have been described elsewhere, they primarily rely on passive accumulation within the tumor microenvironment (TME).*(203)* However, accumulation within the TME can vary dramatically and primarily relies on the enhanced permeability and retention effect (EPR) which has not improved anti-tumor efficacy as much as

initially proposed.*(99)* Furthermore, the development of targeted platforms have been engineering including ANCs and antibody drug conjugates (ADCs) yet have primarily focused on tumor targeting strategies to deliver toxic chemotherapeutic agents to eliminate cancer cells.*(204, 205)* While promising, these do require large doses to fully target and saturate tumor cells and may require a stimuli to release the delivered drug via pH or enzyme presence within tumor cells or tissue.*(206)* Instead, we leveraged ANCs to target T lymphocytes which release encapsulated drug in a sustained paracrine fashion requiring no stimuli. The NP utilized herein are composed of a hydrophobic poly(propylene) sulfide core with a hydrophilic polyethylene glycol (PEG) corona which allows for efficient encapsulation of hydrophobic small molecule drugs into the core*(207)* and surface functionalization with proteins.*(208)* Using this approach thus allows for improved drug potency as it is localized to the cell surface and requires no chemical modifications to the drug structure. Furthermore, rather than needing to deliver ANCs directly to the TME, ANCs may bind to T cells within systemic tissues trafficking into the TME which provides an additional route to achieve bioactive doses in the TME.

The transforming growth factor-beta (TGFβ) has garnered attention recently as it is commonly upregulated in tumor microenvironments and lymphoid tissues where it can promote suppressive milieus, in part by suppression of T cell cytotoxic function.*(3, 63)* Furthermore, heightened TGFβ signaling can reduce T cell infiltration into the TME leading to immune excluded tumors of which have been shown to respond poorly to ICB therapies.*(209, 210)* We hypothesized that codelivery of SB-431542, a TGFβ kinase inhibitor, and ICB to tumor resident checkpoint expressing cells using ANCs could combat immune-excluded tumors thereby improving anti-tumor efficacy. In addition to ANCs enabling codelivery of TGFβ inhibition and ICB, ANCs improve drug retention at the injection site thereby increasing likelihood of interaction

with target cells as immune infiltration into the TME happens continuously during tumor progression.

Adenosine signaling pathways have also emerged drug candidates to combine with ICB as adenosine concentrations are greatly increased within tumor tissues as cancer cells rapidly turnover and release intracellular adenosine triphosphate which is broken down to free adenosine by CD39 and CD73, surface ectonucleotidases.*(76, 211)* Free adenosine acts to suppress effective CD8 T cell priming within lymph nodes (LNs) and helps protect tumor cells via suppressed CD8 T cell cytotoxic function.*(80, 212)* This has spurred the development of various adenosine modulation strategies including mAbs targeting CD39 and CD73 to prevent adenosine formation*(71)* along with several small molecule adenosine receptor antagonists*(4)* including those for the adenosine 2A receptor which has a high adenosine affinity.*(72)* We hypothesized that codelivery of SCH-58261 to PD1 expressing T cells would improve anti-tumor responses as these pathways, while non-redundant, have been shown to upregulate each other's expression upon modulation of either pathway.*(81, 82)*

We hypothesized that sustained delivery of small molecule immune modulators using ANCs directed towards checkpoint expressing immune cells would improve anti-tumor responses compared to non-targeted delivery. We show successful engineering of ANCs using a gentle but robust synthesis and conjugation schema that retains conjugated mAb binding functions that is versatile and applicable to multiple mAbs. Using this platform, we show ANCs can target checkpoint expressing cells and sustain delivery of a small molecule agent. ANCs also have a unique biodistribution profile that improves both mAb retention at the site of injection and accumulation within draining LNs. ANCs targeting results in improved colocalization with both circulating and LN resident T cells over short time scales that correspond to improved therapeutic effects. Specifically, targeted delivery of a TGFβ kinase inhibitor and adenosine receptor

antagonist to immune checkpoints expressed by immune cells compared to non-targeted formulations is substantially improved in two animal tumor models using both systemic and local administrations. These so-called drug eluting ICB-ANC thus demonstrate the unique benefits of co-delivery formulations for improving combination therapy of ICB mAb with small molecule immunomodulators.

4.2 Results and Discussions

4.2.1 Antibody-Nanoparticles Conjugates (ANCs) retain Fab binding.

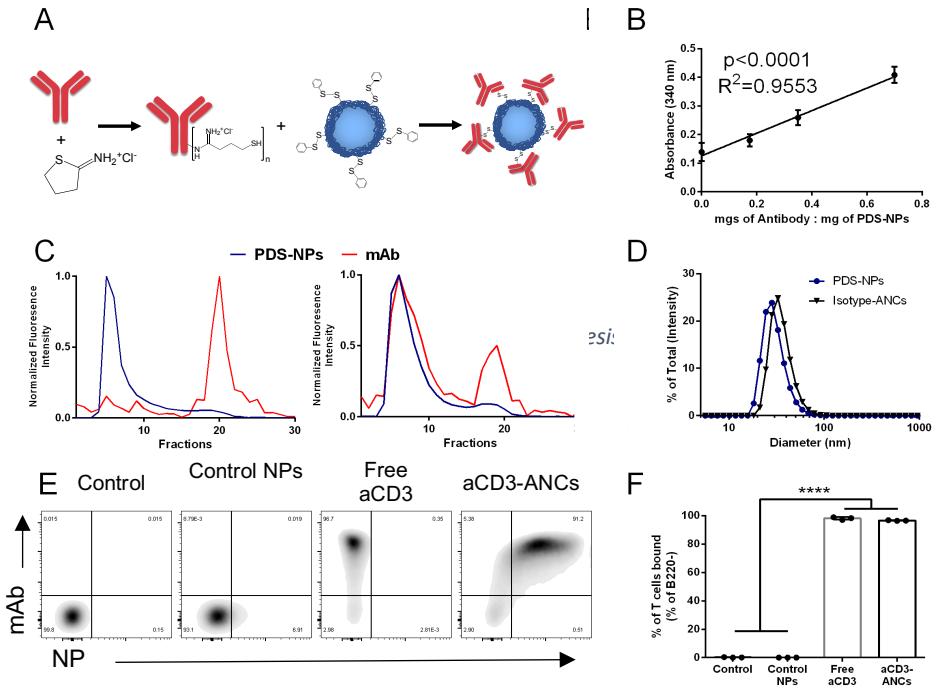

Figure 22: Antibody conjugated nanoparticle (ANC) synthesis. A) Synthesis scheme B) Ratio of thiolated Ab to NP determine disulfide bonds as measured by released pyridyl absorbance (340 nm). C) Size exclusion chromatography is used to purify away non-conjugated Ab. Only when Abs are modified with Traut's reagent are ACNs generated. D) Dynamic light scattering plots of NPs and ANCs post purification. E) Representative flow cytometry plots of T cell binding using different formulations after incubation *ex vivo* with mouse splenocytes. F) Quantification of F. Statistical analyses were done using ANOVA with Tukey's test. ****$p < 0.0001$.

As Abs rely on their tertiary structure for their recognition functions, we utilized a previously described NP platform functionalized and bioconjugation scheme based on reacting thiol containing species with pyridyl disulfide (PDS) groups on the corona of polymeric NP*(208)*

(referred to as PDS-NPs) to form ANCs (Fig. 22A). The advantage of this method is the use of gentle, aqueous solvents and rapid reaction times to minimize loss of mAb functions. Thiols were amended onto commercially purchased mAbs by treatment with 2-iminothiolane (Traut's reagent). The resulting extent of thiolation was proportional to molar excess used (Fig. 23A). After cleaning, thiolated mAb were incubated overnight with poly(propylene sulfide) NP synthesized by emulsion polymerization and derivatized post synthesis with PDS (referred to as PDS-NPs). Through a disulfide displacement reaction monitored by absorbance at 340 nm of the displaced pyridyl group, the generation of ANCs could be monitored, which occurred in a manner proportional to both the mAb thiolation (Fig. 23B) and ratio of thiolated mAb to PDS-NP (Fig. 22B). ANC were purified from unreacted mAb by size exclusion chromatography (Fig. 22C) and ANC-containing fractions were collected and concentrated, processes that did not influence ANC hydrodynamic size (Fig. 22D), prior to further investigations. Rhodamine labeled anti-CD3 (aCD3) to Alexa-Fluor 647 labeled PDS-NPs yielding aCD3-ANCs that were incubated with lymphocytes engaged with T cells ($CD3^+$) within murine splenocyte suspensions to similar extents (as quantified in the double positive gate) compared to free (non-NP conjugated, rhodamine labelled) aCD3 mAb (single positive for mAb) as control (Fig. 22E-F). These results demonstrate mAb functionality is sustained upon ANC formation.

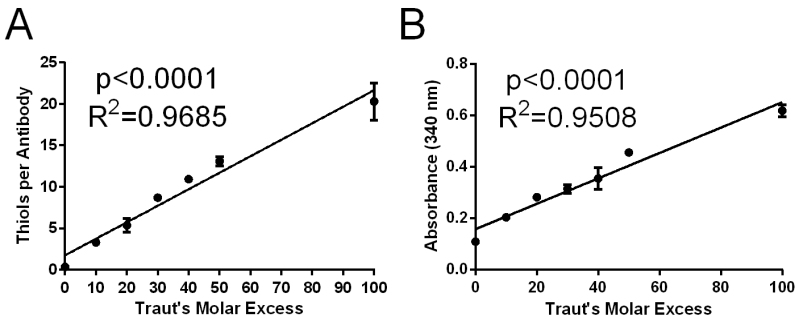

Figure 23: Antibody conjugated nanoparticle (ANC) synthesis measured by absorbance. A) Excess traut's reagent controls number of thiols on Ab surface. B) Thiol concentration on Ab surface determines disulfide bonds as measured by released pyridyl absorbance (340 nm).

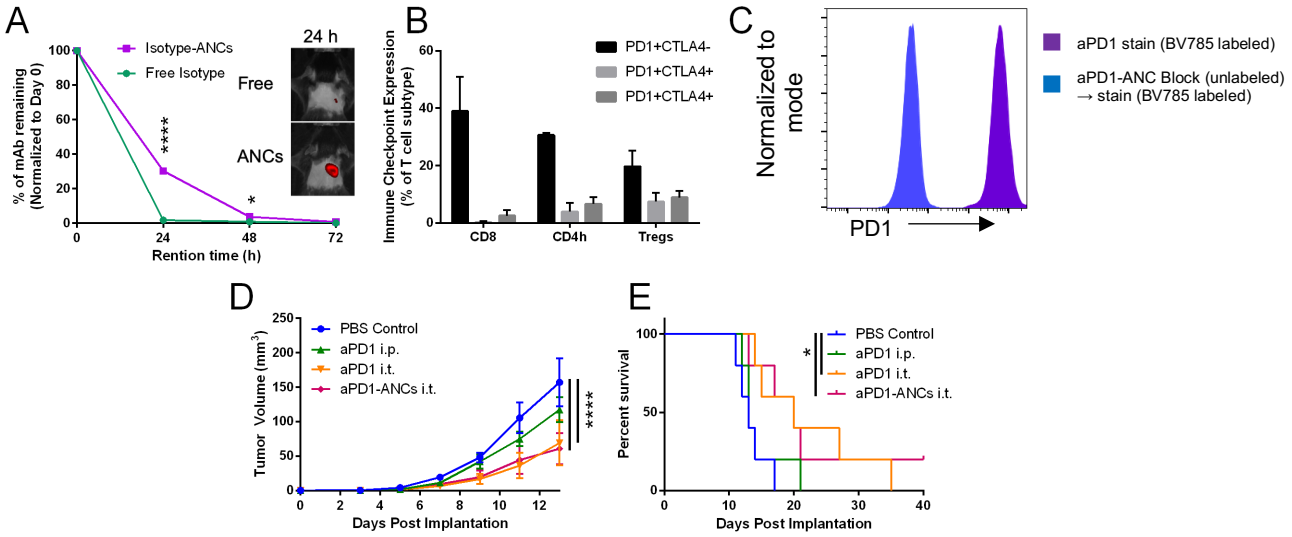

Figure 24: aPD1-ANCs have similar anti-tumor efficacy compared to free aPD1. A) Antibody retention using ANC or free formulation at injection site. B) Immune checkpoint expression of tumor resident T cells. C) aPD1-ANCs bind to EL4 cells, purple line – EL4 expression of PD1, blue line – aPD1-ANCs bind and prevent labeled aPD1 from labeling EL4 cells. D) B16F10 tumor growth using aPD1 monotherapy (non-drug loaded). E) Survival curves of D. Statistical analyses were done using ANOVA with Tukey's test. Log-rank (Mantel-Cox) test for survival curves. *$p < 0.05$, ****$p < 0.0001$.

4.2.2 Anti-tumor efficacy of ANC-mediated ICB

The ability of NP conjugation to improve mAb retention after injection, biodistribution analysis via IVIS imaging was performed. After i.t. injection, ANC were found to prolong mAb retention at the injection site over 48 h (Fig. 24A). The potential of this feature of the ANC to potentiate the therapeutic effects of ICB, which targets immune checkpoint molecules expressed by T cells (Fig. 24B) was explored. aPD1-ANCs were found to engage PD1-expression EL4 thymoma cells (Fig. 24C). When administered i.t., aPD1-ANCs were as efficacious as free mAb, which both exhibited improved effects and survival benefit over systemic intraperitoneal (i.p.) injection free aPD1 (Fig. 24D-E). These results demonstrate that ANCs maintain the beneficial therapeutic effects of ICB.

4.2.3 Targeting of drug eluting ANCs to immune checkpoints improves anti-tumor effects

ANC offer multiple unique advantages to combination immunotherapies, including mAb multivalency, tailorable biodistribution profiles, and the capacity to co-formulate agents with synergistic or orthogonal bioactivities to potentiate drug effects. The potential for ANC formed from therapeutic mAb with amphiphilic NP to encapsulate drug to facilitate its release and effects in a targeted manner was explored (Fig. 25A). As proof-of-concept, amphiphilic chemotherapeutic paclitaxel (PTX) well established for its cytostatic activities and poorly soluble in aqueous solutions was encapsulated into the NP,*(207)* which enabled sustained release over days (Fig. 25B). Its dose-dependent effects on EL4 cultures when incorporated into the NP were only modestly reduced (Fig. 25C). As aPD1-ANCs result in targeting-dependent association of NPs with PD1-expressing EL4 cells *in vitro* (Fig. 25D-E), PXL-loaded ANCs were found to induce concentration-dependent EL4 cell death that was enhanced by aPD1 targeting (Fig. 25F). These results highlight the ability of ANCs to deliver small molecule cargo in a targeted manner.

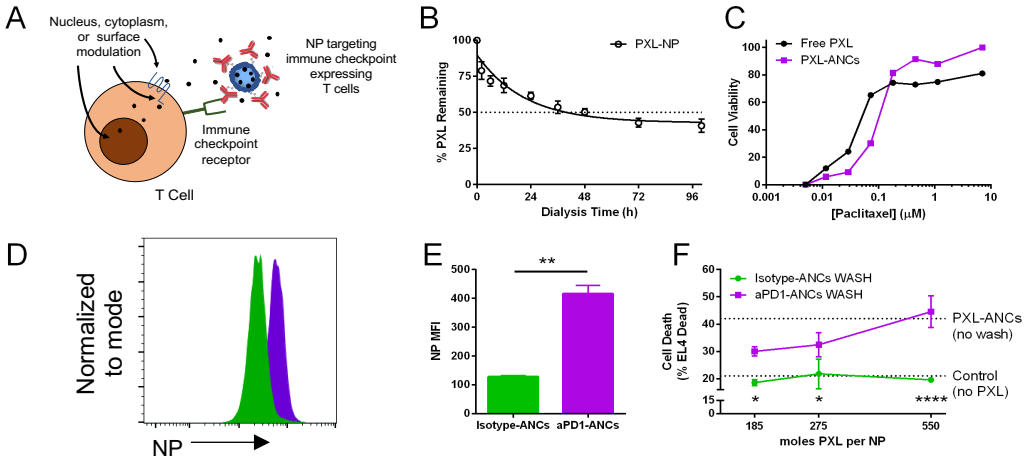

Figure 25: ANC mediated delivery of PXL sustains drug effects to PD1 expressing target cells. A) Schematic demonstrating co-delivery of ICB and small molecule drug to T cells of interest. B) Paclitaxel release from NPs. C) Toxicity curves using paclitaxel with EL4 cells in vitro. D) aPD1-ANCs (fluorescently labeled NPs) facilitate NPs to bind to EL4 cells. E) MFI quantified from D. F) Paclitaxel loaded aPD1-ANCs selectively kill PD1 expressing cells. Statistical analyses were done using ANOVA with Tukey's test. *$p < 0.05$, **$p < 0.01$, ****$p < 0.0001$.

To assess the therapeutic potential of immunotherapeutic codelivery via drug eluting ANC, delivery of TGFβ kinase inhibitor SB-431542 to immune checkpoint expressing T cells was investigated as the TGFβ pathway has been previously reported to promote immune exclusion*(209, 210)* and its inhibition may help overcome the immune-excluded B16F10 tumors observed (Fig. 26A) following treatment with non-drug loaded aPD1-ANCs described earlier (Fig. 24D-E). Like PXL, encapsulated SB-431542 was released from NP over 24 hours (Fig. 26B). When PXL-a administered i.t., targeting of SB-431542-encapsulating NP via aPD1 and aCTLA4 (6 μg each) dramatically improved the therapeutic effects of combination therapy compared to non-targeted SB-431542-encapsulating NP functionalized isotype mAb when co-administered with aPD1 and aCTLA4-ANCs with respect to reduced tumor growth (Fig. 26C-D), resulting in

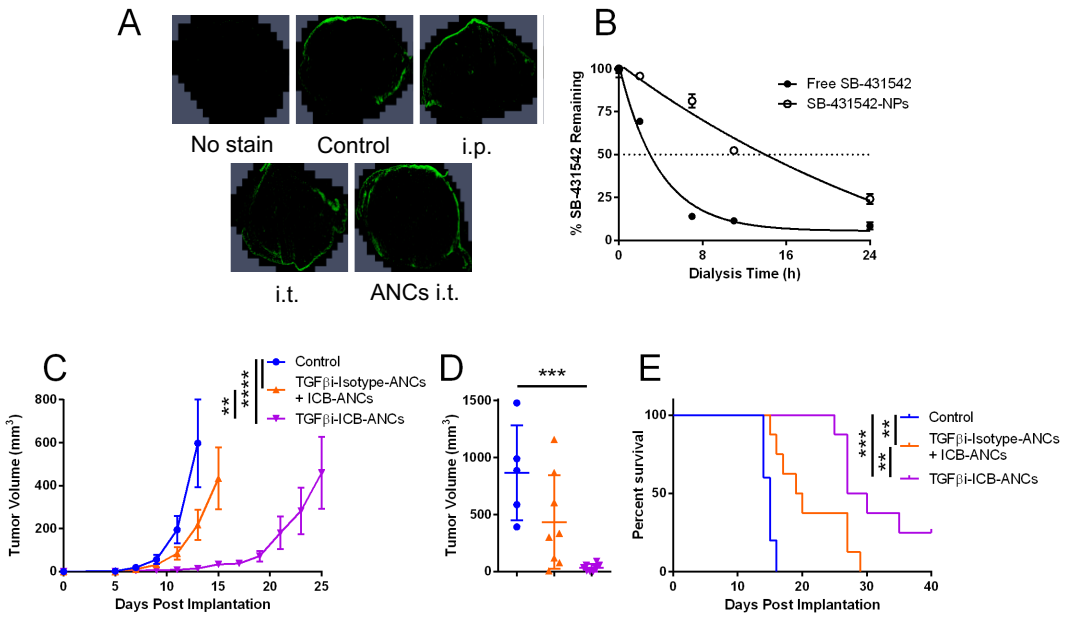

Figure 26: Targeted TGFβ inhibition locally improves anti-tumor response. A) T cell infiltration in B16F10 tumors from 2D. B) SB-431542 release from NPs. C) B16F10 tumor growth using aPD1, aCTLA4, and TGFb inhibitor using various formulations. D) Tumor volume at day 15. E) Survival curves of C. Statistical analyses were done using ANOVA with Tukey's test. Log-rank (Mantel-Cox) test for survival curves. **p < 0.01, ***p < 0.001, ****p < 0.0001.

prolonged animal survival (Fig. 26E). Targeting of SB-431542 via ICB thus improves the combination therapeutic effects.

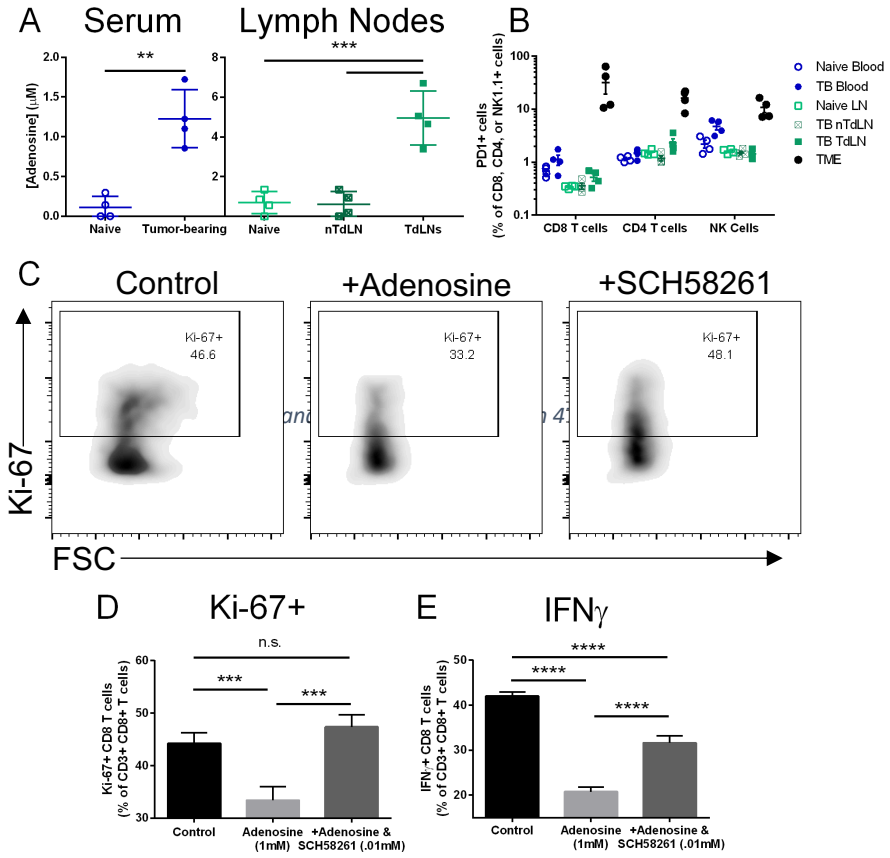

Figure 27: Adenosine and PD1 are upregulated in 4T1 tumor model. A) Adenosine concentrations in serum and LNs from 4T1 tumor bearing mice. B) PD1 expression in CD8, CD4, and NK cell populations in various tissues from 4T1 bearing mice. C) Flow cytometry plots for Ki-67 in *ex vivo* stimulated CD8 T cells using adenosine and SCH-58261. D) Quantified flow cytometry data of Ki-67 expression in CD8 T cells. E) Quantified flow cytometry data of IFNγ expression in CD8 T cells. Statistical analyses were done using ANOVA with Tukey's test. **p < 0.01, ***p < 0.001, ****p < 0.0001. n.s. not significant.

4.2.4 Adenosine suppression is active in TNBC and antagonism restores T cell function

Adenosine is commonly upregulated in cancers and contributes to immune suppression, including TNBC which currently is lacking targeted therapies.*(213)* We thus explored the levels of adenosine and PD1 in the 4T1 tumor model of TNBC. Adenosine concentrations in the serum

and TdLNs of tumor bearing mice were found to be significantly increased (Fig. 27A), which we hypothesize is due to the high metastatic propensity of this model to infiltrate systemic tissues and TdLNs.*(214)* Within these same tissues, frequencies of PD1+ cells were also found to be high within CD8 and CD4 T cells and NK cells (Fig. 27B). Based off these active pathways, along with reports showing upregulation of A2A receptor expression in PD1 expressing T cells, we explored whether adenosine receptor antagonism could restore T cell activity. In line with this, CD8 T cells incubated with aCD3/aCD28 dynabeads in the presence of adenosine resulted in suppressed IFNγ production and Ki-67 expression, effects reversed by co-treatment with SCH-58261 (Fig. 27C-E). These results highlight the adenosine and PD1 mediated suppression in the 4T1 TNBC model and the ability for adenosine receptor antagonism to rescue immune suppression.

4.2.5 Targeting of ANCs to IC enables targeting of circulating and lymph node resident T cells

While ANCs are able to successfully bind to T cells *in vitro* (Fig. 22) and sustain mAb retention at the site of injection (Fig. 24A), we explored whether ANCs could successfully target and interact with circulating and peripheral T cells *in vivo*. aCD3-ANC administered i.v. resulted in 90% of T cells within the blood and spleen being NP-associated 1 h post treatment, in contrast to isotype-ANCs (<10%, Fig. 28A-B). aCD3 targeted also improved delivery to LN-, but not tumor-, localized T cells but to substantially lower extents (Fig. 28B). Off target uptake by B cells was higher for aCD3- relative to isotype-ANC (Fig. 28C).

Unsurprising given the requirement of interstitial retention to facilitate lymphatic uptake,*(112)* accumulation of isotype mAb within the dLN was also increased with NP conjugation at 24 h post injection (Fig. 29A-B). Furthermore, isotype-ANC appeared to not be solely restricted to the LN periphery (and presumably not restricted from the LN parenchyma, Fig. 29C), the capacity of lymph-draining ANC to access LN T cells was next assessed. aCD3 in its free and

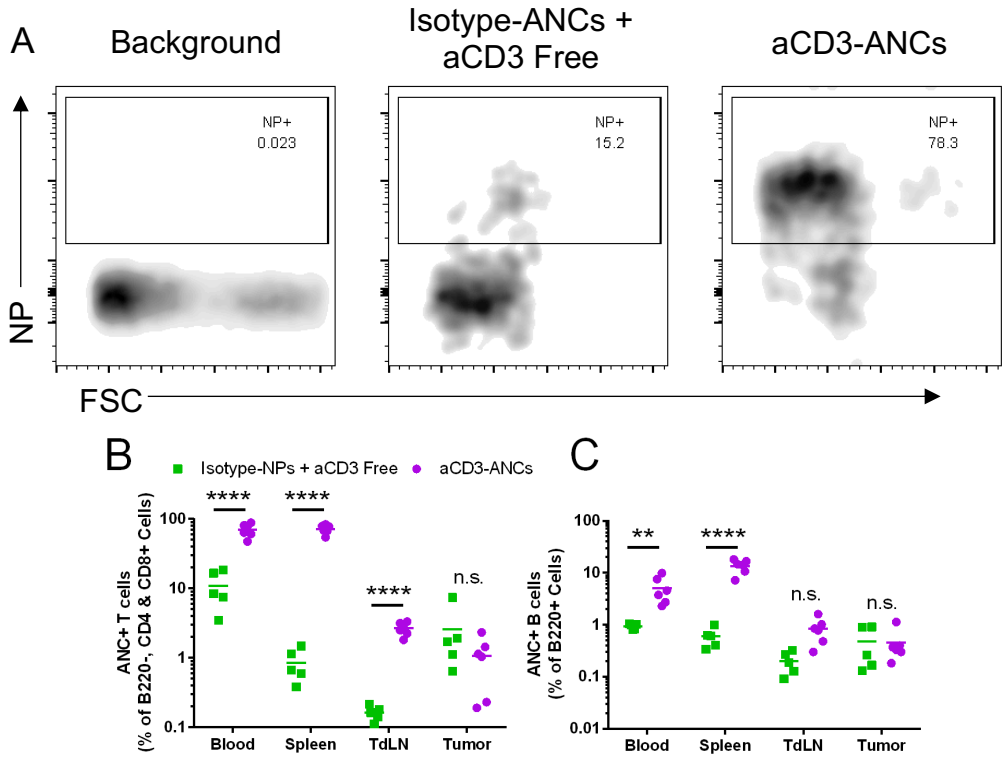

Figure 28: aCD3-ANCs bind to T cells *in vivo* after i.v. administration. AlexaFluor 647 ANCs (isotype or aPD1) were administered intravenously in 4T1 bearing mice. One hour after administration, mice were euthanized and tissues processed for flow cytometry. A) Flow cytometry plots of NP binding to CD4/CD8 T cells. B) NP binding from A quantified. C) NP binding to B cells. Statistical analyses were done using ANOVA with Tukey's test. **p < 0.01, ****p < 0.0001. n.s. not significant.

ANC forms was administered i.d. and labeling of CD4 and CD8+ cells within dLN assessed 24 h post injection (Fig. 29D-E). Strikingly, approximately 40% of T cells labeled with aCD3-ANCs, levels comparable to labeling achieved using free aCD3. Correspondingly, ~40% of T cells were also NP+ (AlexaFluor647+), in sharp contrast to the <1% of T cells were labeled with control, non-targeted NPs (Fig. 29D-E), results in line with previous literature.*(144)* Very little association with off-target cells was noted, including B cells (Fig. 29F). ANC thus improves delivery to dLN of mAb and mAb targeting improves NP delivery to localized immune cells.

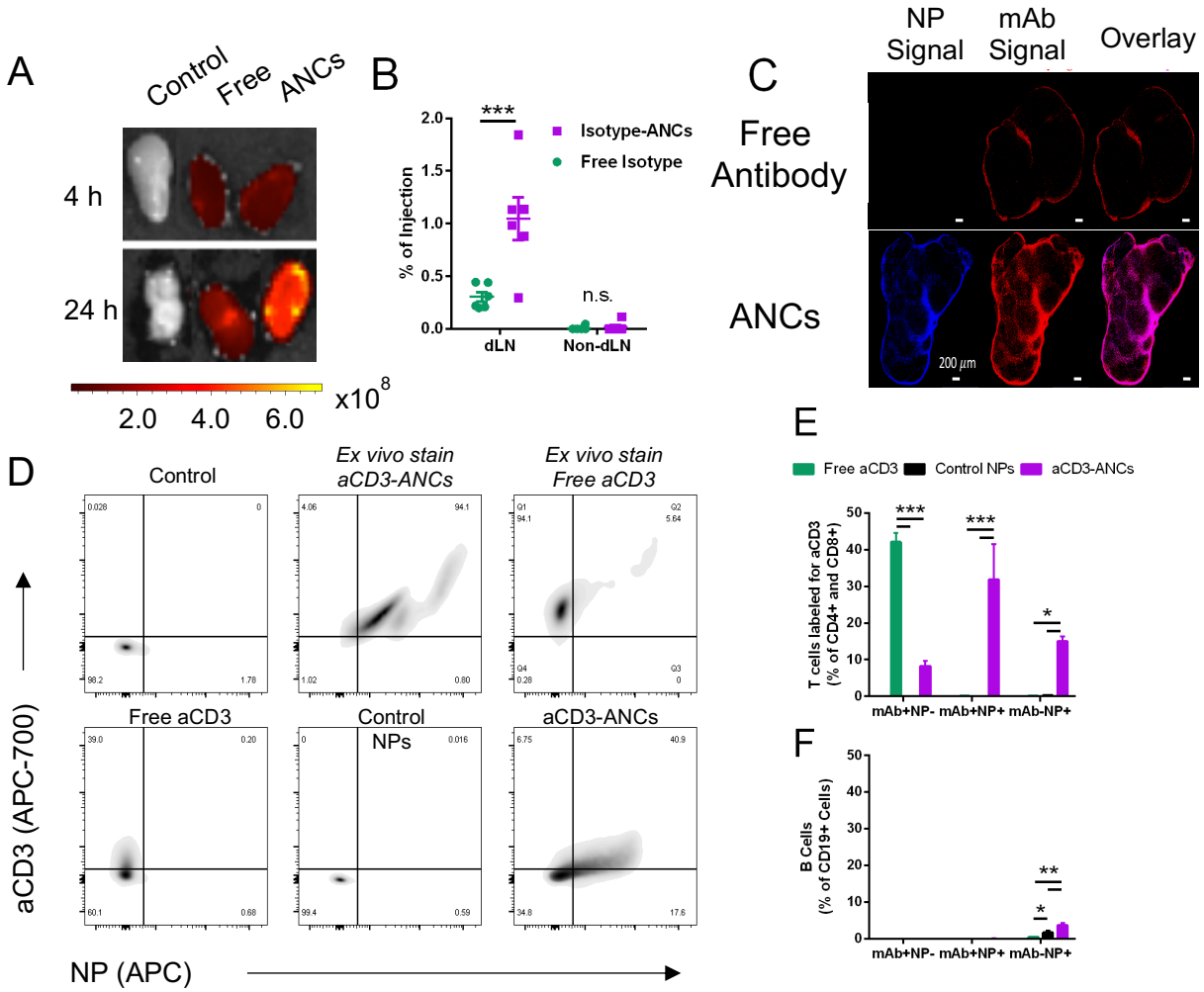

Figure 29: i.d. administration of ANCs improves mAb LN accumulation and access. A) Isotype Ab accumulation in dLNs using various formulations. B) Quantification of isotype Ab accumulation in LNs via homogenization. C) Confocal microscopy of whole LNs using isotype Ab. D) Flow cytometry plots of aCD3 and NP accumulation in LNs of CD4+ & CD8+ T cells. E) Quantified flow cytometry data of D. F) Flow cytometry of aCD3 and NPs in B cell compartment. Statistical analyses were done using ANOVA with Tukey's test. *p < 0.05, **p < 0.01, ***p < 0.001. n.s. not significant

4.2.6 IC targeted antagonism of adenosine reduces breast cancer growth and metastasis

The potential for aPD1 targeting of ANCs co-delivering SCH-58261 to PD1 expressing cells to augment anti-tumor immune response compared to non-targeted therapy was next explored. NP encapsulation that improved SCH-58261 solubility (Fig. 30A) resulted in 50% of drug to be released within 9 h (Fig. 30B). When systemically administered, i.v. administration of

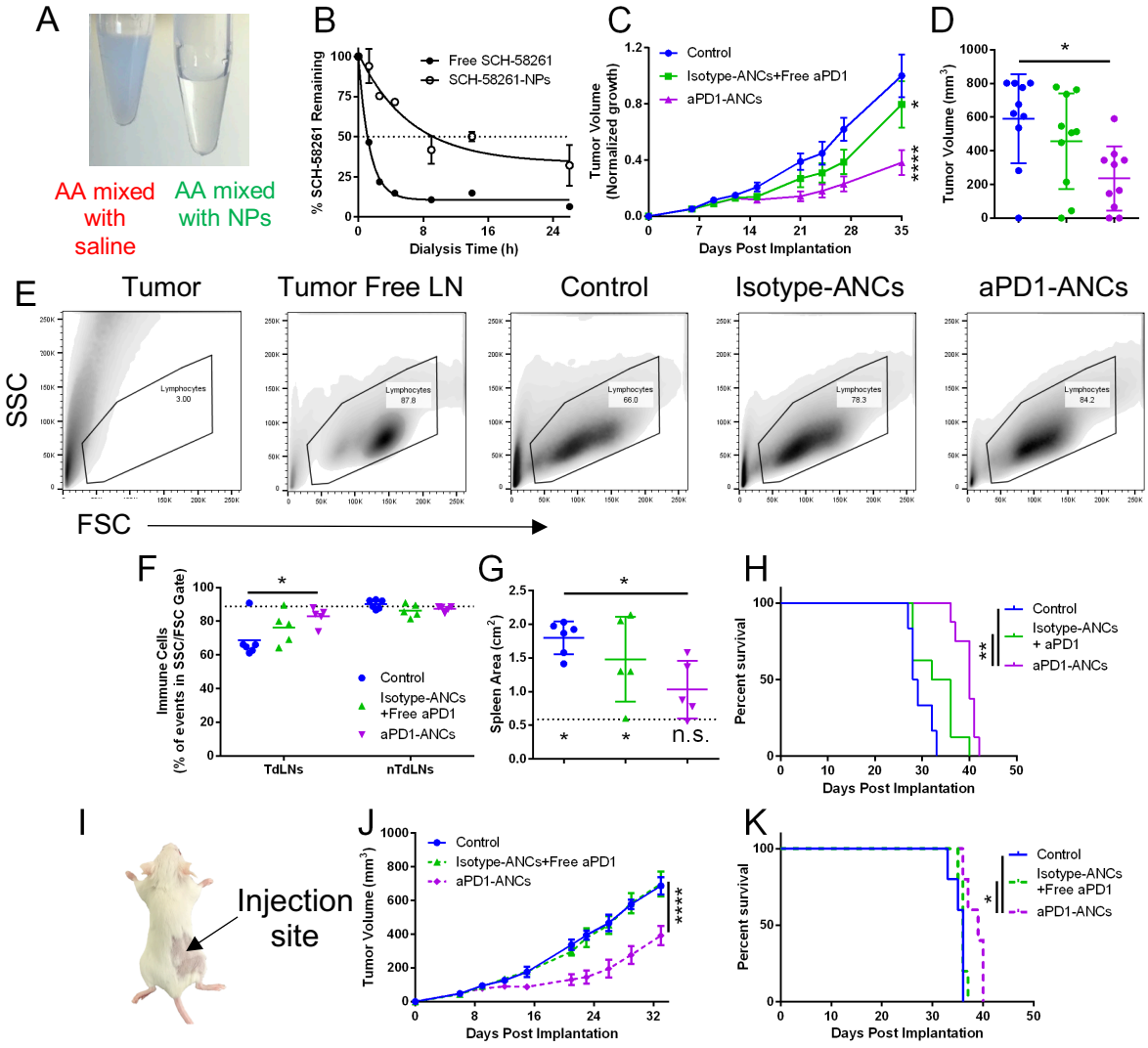

Figure 30: Adenosine antagonist loaded aPD1-ANCs improve anti-tumor therapy compared to non-targeted ANCs. A) AA is soluble in aqueous solvents when encapsulated in NPs. B) AA release profile from NPs using dialysis filters. C-H) Systemic administration of drug formulations. C) 4T1 tumor growth using Isotype- and aPD1-ANCs loaded with AA over first 35 days. D) Tumor volume at day 35. E) Flow cytometry plots of LNs. F) Quantified levels of lymphocytes cells in LNs on day 35. Dotted line represents % lymphocytes in non-tumor bearing mice LN. G) Spleen area size of 4T1 treated mice. Dotted line represents spleen area in non-tumor bearing mice, statistics below dotted line compared to non-tumor bearing mouse spleen size. H) Survival of 4T1 animals. I-K) i.d. administration of drug formulations. I) Injection location for i.d. administration. H) Tumor growth curves. I) Survival curves H. Statistical analyses were done using ANOVA with Tukey's test. Log-rank (Mantel-Cox) test for survival curves. *$p < 0.05$, **$p < 0.01$, ****$p < 0.0001$. n.s. not significant.

60 μg of aPD1, either in the free or ANC formulation along with 2 μg of encapsulated SCH-58261

in isotype- or aPD1-ANCs resulted in reduced 4T1 tumor growth, that was improved by drug-

eluting ANC targeting (Fig. 30C). As with primary tumors 20 d after the last treatment on day 35 post tumor implantation that demonstrated reduced growth resulting from aPD1-ANC encapsulating SCH-58261 (Fig. 30D), metastatic tumor burden in LNs was reduced, as indicated by reduced immune cell frequencies relative to non-TdLNs and LNs from non-tumor bearing mice (Fig. 30E-F). Furthermore, spleen size, which has previously been correlated with metastatic disease burden*(214)*, was found to be reduced in animals treated with aPD1-ANC encapsulating SCH-58261 and comparable to the sizes of non-tumor bearing mice (Fig. 30G). Survival of a separate mouse cohort treated using the same schedule demonstrated improved animal survival by aPD1 targeting of NP-encapsulated SCH-58261 (Fig. 30H). Similarly, when administered i.d. into the forelimb ipsilateral to the tumor (thus resulting in drainage to LNs co-draining the tumor, Fig. 8I) and with the same treatment schedule described above, SCH58261 loaded aPD1-ANCs reduced tumor growth and prolonged mouse survival compared to non-targeted SCH-58261 loaded isotype-ANCs (Fig. 30J-K). These results highlight the ability of drug eluting targeted ANC to improve combination immunotherapy for TNBC.

4.3 Conclusions

An ANC platform capable of delivering small molecule therapeutics in a targeted fashion to immune checkpoint expressing cells was developed as a versatile system to augment targeted delivery and sustain drug synergies to improve combination cancer immunotherapies. Using this platform, delivery of three unique small molecule compounds was improved; model chemotherapeutic drug PXL, a TGFβ kinase inhibitor, and an adenosine receptor antagonist. Interestingly each of these three drugs works in different cellular locations; the nucleus, cytoplasm, and extracellular surface, respectively, suggesting the capacity of NP-released small molecule to drug cells within multiple intracellular compartments. To this end, we show released drug retains its drug activity which is of interest as this carrier requires no chemical modifications to deliver

the cargo, a major barrier that can affect drug activity in other platforms. Furthermore, the mAb conjugation synthesis can be applied to multiple mAb while retaining binding activity as the reaction conditions are mild (require no heating, organic solvents, etc). Due to their low levels of phagocytosis and pinocytosis, T cells represent a challenging target to drug via passive targeting, yet are immensely important for generating robust anti-cancer immune responses.*(215)* Our results demonstrate the ability to target T cells both *in vitro* and *in vivo* using targeting mAbs is not impaired by incorporation into ANCs and dramatically improves co-association of ANCs with T cells relative to isotype-ANCs. Furthermore, ANC formulation did not diminish effects of ICB. When leveraging the NP as a drug reservoir, anti-tumor responses induced by the synergies of ICB with immune modulators were substantial. As immune suppression and exclusion has emerged as a multi-pathway process, thus requiring multiple modes of modulation to fully restore cytotoxic function, the potential of enabling codelivery of multiple immunotherapies and immune synergies is enormous.*(216)* Conventional combination therapies consists of co-administered agents but is unlikely to lead to concurrent delivery to and thus modulation to the same cell target, thereby diminishing effects. Considering the emerging interest in combining ICB therapies with other small molecule modulators including those targeting the TGFβ and adenosine pathways, these results highlight the potential for co-delivery approaches, such as the drug eluting immune checkpoint inhibitor ANC approach described herein, to substantially improve therapeutic efficacy.

4.4 Materials and Methods

4.4.1 Synthesis of PDS-NPs. Poly(propylene sulfide) NPs are synthesized according to previous literature. Briefly, 500 mg of –COOH Pluronic F127 is dissolved in 10 mL of DI water for 30 min under argon, followed by addition of 400 μL of propylene sulfide for 15 min. Initiator*(143)* is activated using sodium methoxide for 15 min after which time is added to the reaction for another

15 min. 1,8-Diazabicyclo[5.4.0]undec-7-ene is subsequently added and stirred overnight followed by reaction exposure to oxygen (uncapping) for 2 h to mediate crosslinking of the NP core. NPs are then dialyzed against DI water using a 100,000 Da MW cutoff cellulose membrane dialysis tubing (SpectrumLabs). Following dialysis, core thiols are capped using either N-ethylmaleimide or Alexa Fluor 647-maleimide, followed by N-ethylmaleimide in 1X PBS overnight. NPs are functionalized with pyridyl disulfide (PDS) on the carboxy Pluronic using EDC/NHS crosslinking for 24 h followed by dialysis against DI water for 3 d, yielding PDS-NPs.

4.4.2 Antibody thiolation. mAb were thiolated by reacting with 2-iminothiolane (Traut's reagent) in 1X PBS at room temperature for 60 min with stirring. Thiolated mAb was subsequently purified using a 7 kDa MW cutoff zeba filter according to manufacturer's instructions. The number of thiols per IgG molecule was determined by Ellman's assay using a thiomalic acid standard curve. Thiolated mAb was immediately used for NP conjugation and characterization.

4.4.3 ANC synthesis and purification. Thiolated-mAb was mixed with PDS-NPs and reacted overnight at RT while stirring. Following reaction, ANCs were purified from unreacted mAb using size exclusion chromatography using a Sepharose 4B resin. ANC-containing fractions identified using fluorescamine and concentrated using a 4 mL 30 kDa MW cutoff spin filters and stored until use at 4° C. Final mAb concentrations in ANC suspensions were determined using the bicinchoninic acid protein assay kit (ThermoFisher). Following initial synthesis parameters, we synthesized subsequent ANCs using a 40 fold molar excess of trauts which equated to a 6-8 molar thiol concentration per antibody and 0.2-0.6 mgs of antibody to mgs of NP pending the application.

4.4.4 ANC binding to target ligand. Anti-CD3 (clone:KT3, BioXcell) or aPD1 (clone:29F.1A12, BioXcell) mAb were conjugated to AlexaFluor 647 labelled PDS-NPs. ANCs were incubated with the lymphocytes or EL4 cell suspensions in 96 well plates for 15 min on ice and then stained for surface markers flow cytometry as described below. For aPD1 mAb blocking experiments, EL4

cells were incubated with stock, non-fluorescent aPD1 mAb for 15 min on ice, followed by washing step in phosphate buffered saline (PBS), followed by 15 min incubation with aPD1 mAb or aPD1-ANCs, followed by processing for conventional surface staining (described below) for flow cytometry analysis.

4.4.5 Tissue and single cell preparations. Following tissue collection, tissues were processed by cutting rather than enzymatic digestion to prevent cell surface receptor degradation. Single cell suspensions were generated by disrupting organs through a 70-mm cell strainer followed by wash steps in PBS. Red blood cells were lysed with lysing buffer hybrid-max (Sigma) for 7 min at room temperature followed by quenching in PBS. Cells were plated in 96-well U bottom plates for surface/intracellular staining in PBS.

4.4.6 Flow cytometry and antibodies. Single cell suspensions from tumors, LNs, and spleens were prepared as described above. After washing, live/dead staining was performed using Zombie Aqua fixable viability kit (Biolegend), followed by wash steps and surface staining using mAb (all from Biolegend): CD45 (clone: 30-F11), CD3 (clone: 17A2), CD4 (GK1.5.), CD8 (clone: 53-6.7), NK1.1 (PK136), B220 (RA3-6B2), CD19 (6D5), IFN-γ (clone: XMG1.2), PD1 (clone: 29F.1A12 or RMP1-14). Surface staining was carried out on ice for 30 min. All flow cytometric analyses were performed using a Fortessa flow cytometer (BD Biosciences) and analyzed using Flowjo software (Tree star).

4.4.7 Small molecule encapsulation and drug release profiles. To encapsulate small molecule drugs, lyophilized drug was reconstituted at 10 mg/ml in DMSO. Stock drug was subsequently dispersed into 30 μL ANC suspension or PBS by simple pipette mixing. Drug loaded ANCs suspensions or drug solutions were then loaded into dialysis cups (100 kDa MWCO, ThermoFisher) and dialyzed against PBS with constant stirring. Dialysate were periodically removed over 26-96 h and drug absorbance measured by plate reader (Synergy H4 BioTek).

4.4.8 Animals and cell lines. Cell lines were cultured in Dulbecco's Modified Eagle Medium (DMEM) supplemented with 10% fetal bovine serum and 1% penicillin/streptomycin/amphotericin B referred to as complete media and periodically checked for mycoplasma contamination. C57Bl/6 and BalbC mice were purchased from Jackson Laboratories. All protocols were approved by the Institutional Animal Case and Use Committee. Tumors were implanted intradermally in 6-12 wk old mice and were monitored in anesthetized mice by caliper measurements by width, length, and depth. Mice were sacrificed when tumors led to ulceration or maximum tumor size of 1.5 cm in any dimension.

4.4.9 In vitro cytotoxic effects of PTX. EL4 cells were cultured and plated in 96-well plates at a density of 10^5 cells per well in 198 μL of complete media. 2 μL of sample (vehicle, PTX, ANC formulation) was added to each well and allowed to incubate for 4 d. Cells were then stained for flow cytometry with LiveDead marker to determine IC50 curves. To investigate targeted ANC potential, cells were plated, and sample added as mentioned, but following a 25 min incubation of sample with cells on ice in 1% BSA in PBS, cells were then pelleted and washed twice with complete media before incubating for 2 d followed by flow cytometry staining.

4.4.10 In vivo mAb biodistribution. Fluorescent labeling of isotype or aCD3 (KT3, BioXCell) mAb was done using AlexaFluor700-NHS-Ester for 1 h following by purification using a Sepharose CL-6B column with fluorescent mAb fractions pooled and concentrated using a 10 kDa (Millipore) spin filter. mAb concentrations were determined using a BCA assay. Fluorescent NPs (AlexaFluor 647) were synthesized as previously mentioned. The lateral dorsal skin of C57Bl6 mice was shaved and mAb or ANCs were administered using the specified administration route at the indicated site. For retention studies, fluorescent imaging was performed with an IVIS® Spectrum instrument (Perkin Elmer) at the injection site over 3 d and of tissues following sacrifice. Following 24 h from injection, mice were euthanized, and tissues collected for imaging and homogenization.

Concentration in tissues were determined following homogenization using the injected mAb or ANC solutions as a standard curve from naïve tissues. For aCD3 experiments, naïve mice were used and injected with either 40 or 6.25 μg of mAb for i.v. and i.d. administration respectively. For i.v. biodistribution, mice were euthanized after 1 h with tissues collected and processed for flow cytometry. For aCD3 labeling of T cells within LNs following i.d. administration, mice were euthanized after 24 h after injection and resected LNs were either collagenase treated for 30 min or immediately digested with scissors to prevent *ex vivo* T cell labeling followed by processing into single cell suspensions (previously described).

4.4.11 B16F10 melanoma bearing mice treatments. The dorsal skin of C57Bl6 mice was shaved and B16F10 cells (10^5) implanted in the right lateral dorsal skin on day 0. After 5 (when all tumors were visible), 7, and 9 d, mice were injected i.d. with 10 μg of anti-mouse CTLA4- (clone:UC10-4F10-11, BioXCell) and rat anti-mouse PD1-ANCs (clone: 29F.1A12, BioXCell) or Armenian hamster IgG- (BioXcell) and rat isotype control-ANCs (clone: 2A3) in 30 μL saline. 5 μg of SB431542 (Sigma) was encapsulated in aforementioned ANCs prior to injection. Mice were monitored every other day for survival studies. For immunofluorescence studies, mice were euthanized at endpoint and tumors were harvested. Tumors were placed in optimal cutting temperature (OCT) compound and frozen in 2-methylbutane solutions using liquid nitrogen. OCT frozen tumors were sliced using a CryoStar NX70 instrument to 8-10 um. Tumor sections were blocked with donkey serum, followed by an anti-CD3 (FITC) primary staining antibody (IgG). Tumors sections were then read on a Laser Scanning Confocal microscope (Zeiss 700) and analyzed using Zeiss Blue software.

4.4.12 Quantification of adenosine and PD1 expression in 4T1 model. 3.5 x 10^5 4T1 cells resuspended in 30 μL of PBS were implanted i.d. in the left mammary fatpad (4^{th}) in BalbC mice. On d 15, mice were euthanized for serum collection or LNs were collected and mechanically

disrupted in a 96 well round bottom plate for ELISA assays. Following disruption, debris was pelleted, and supernatants collected, and adenosine levels measured by ELISA (Abcam) according to the on manufacturer's protocol. To determine PD1 expression, on day 15 post tumor implantation, tissues were collected and processed for flow cytometry.

4.4.13 4T1 breast tumor bearing mouse treatments. 3.5 x 10^5 4T1 cells resuspended in 30 μL of PBS were implanted i.d. in the left mammary fatpad (4^{th}) in BalbC mice and 60 μg of aPD1 mAb with 2 μg of SCH58261 (Sigma) was administered in the aforementioned areas on days 6, 9, 12, and 15. Tumors were monitored every 2-3 d until endpoint for survival analysis. Analysis of metastatic disease, mice were sacrificed day 35 mice and the spleen and LNs collected. TdLNs and nTdLNs were harvested and prepared for flow cytometry analysis as described above and the spleen areas were analyzed by ImageJ.

4.4.14 Statistical analysis. Statistical significance of differences between experimental groups was calculated with Prism software (GraphPad). All data is expressed as mean ± standard error mean except for tumor growth. ****$p<0.0001$, ***$p<0.001$, **$p<0.01$, and *$p<0.05$ by unpaired two-tailed t-tests or one- or two-way ANOVA followed by Tukey post-hoc test for multiple comparisons. For survival curves, log-rank (Mantel-Cox) test was performed.

CHAPTER 5. CONCLUDING REMARKS AND FUTURE DIRECTIONS

5.1 Conclusions

ICB immunotherapy has rapidly emerged as the most promising form of cancer therapy as it offers robust responses and complete cures in some patients. However, these therapies are far from ideal with three main challenges remaining; 1) low response rates, 10-50% *(6)*, 2) high rates of iRAEs *(7)*, and 3) partial responses, but high levels of relapse over time *(6)*. While current research has made great strides of overcoming these barriers through better understandings of how ICB therapies work and by combination with multiple therapies, the aspect of drug delivery is a critical barrier that may help overcome these challenges. First, mAb therapies are primarily administered systemically (i.v./i.p.) which results in poor TME accumulation (~1% of administered dose), or the canonical site of interest, thus requiring high doses to obtain a concentration above the therapeutic threshold in these tissues which contribute to iRAEs. Second, many immunotherapies are now combined with one another (e.g. aCTLA4+ aPD1) including combination therapies consisting of mAbs and small molecule inhibitors to simultaneously block independent pathways to prevent relapse. While this has improved efficacy in some patients, the responses are still variable and require further research *(1, 3, 4, 71)*.

Given the unique characteristics of mAb therapies including large molecular size compared to tradition small molecule drugs (150 vs 1 kDa) as well as their affinity towards cognate ligand, we have harnessed these salient features to drug an alternative tissue from the TME, specifically the TdLNs, and have designed a biomaterial to codeliver both mAbs and small molecule drugs over a sustained period to T cells. In the first aim, we explored how drugging LNs which are home to high concentrations of T cells affects anti-tumor efficacy utilizing different administration routes. By harnessing the lymphatic clearance mechanisms of larger compounds including mAbs,

we show that mAbs efficiently drain to dLNs and can access T cells within these LNs. This led to improved anti-tumor responses compared to traditional systemic administrations and allowed for reduced dosing while maintaining anti-tumor responses. In the second aim, we engineered an ANC to improve codelivery of multiple therapeutics to the same cell of interest to block non-redundant suppressive pathways, specifically immune checkpoints and TGFβ or adenosine. Using the mAb as both a drug and targeting agent, we demonstrate both improved delivery and sustained delivery of small molecule drugs to cells of interest. We applied this delivery system to a variety of therapeutics including aPD1, aCTLA4, a TGFβ inhibitor, and an adenosine receptor antagonist highlighting the versatility of this platform and showed improved anti-tumor responses against melanoma and breast cancers.

5.2 Contributions to the field

The overall impact of this work was to explore new ways to improve cancer immunotherapies, specifically by focusing on drug delivery to T cells, the cells of interest for many drugs. While research in the immunotherapy field has advanced tremendously in the last two decades, it has primarily focused on discovering new druggable pathways and/or modulating multiple therapies concurrently via combination therapy. However, drug efficacy is partially due to drug reaching its target site of interest at the bioactive dose where it can then mediate its effect. The main contributions of this work are 1) we have identified the TdLN as a critical tissue in mediating the efficacy of ICB therapies and it is efficiently druggable by cutaneous administration, and 2) using an ANC platform, we can achieve sustained codelivery of multiple therapies to the same cell of interest which is required with certain combination therapies to generate an anti-tumor response.

5.2.1 ICB mAb delivery to TdLNs augments anti-tumor efficacy

Chapter 3 of this work described an approach to drug LNs and thus block immune checkpoint pathways by simply modifying the route of administration leading to improved anti-tumor efficacy. This work helps advance the understandings of mAb biodistribution as well as the immunological roles of checkpoint pathways in lymphoid tissues or the priming phase. By drugging LNs using cutaneous administration routes, we show mAb has access to deeper areas of the LN, a process thought to not occur due to the size restrictions and cell barriers protecting the deeper T cell zones of the LN. Using various administration routes, we then demonstrate that TdLNs, which are bathed in tumor associated antigen *(207)*, are critical tissues to augment ICB efficacy as LNs are sites of high concentrations and robust T cell proliferation *(178)*. Additionally, we show that the high LN accumulation of mAb in dLNs allows for significant reductions in administered dose which may help reduce iRAEs. Due to the simplicity of this approach, combined with extensive research into mAb formulations for subcutaneous administration, this work provides valuable information to clinicians for local administration sites and alternatives to conventional i.v. administration in patients not responding to ICB therapies.

5.2.2 ICB-ANCs for targeted and sustained small molecule drug delivery to IC expressing cells

Chapter 4 of this work explored the design of an ANC platform to augment delivery of small molecule drugs to PD1 and CTLA4 expressing cells. Our system is unique as it is polymer based thus 1) allowing small molecule drug to be encapsulated, rather than chemically conjugated thereby retaining the small molecule structure and thus function and 2) allowing drug to release over time with no stimuli required like many other ANC or ADC platforms. This is particularly attractive for drugging T cells as they reside in many different microenvironments where stimuli including pH and enzymes vary thus complicating a stimuli release mechanism. While other ANC platforms have been engineered, they have primarily been focused on improving small molecule or nucleic acid delivery to tumor cells rather than immune cells *(217)*. Furthermore, this work, to

the best of our knowledge, is the first ANC platform to drug a T cell surface receptor with a small molecule immune modulator. Of the ANC platforms tailored for immune cell targeting, they have focused on drugging intracellular pathways as these drug carriers must be degraded in order to release encapsulated cargo generally intracellularly thereby preventing modulation of surface. In addition, this work demonstrates that codelivery of immunotherapies to the same cell of interest can generate or improve existing anti-cancer immune responses thus elucidating a necessary criterion for emerging drug delivery systems.

5.3 Future Directions

The future directions of my work should seek to further the applicability and translatability made in this thesis on modifying route of administration and co-delivery of immune modulators to immune cells. Regarding the aim 1 on route of administration, I would like to see this approach applied to other mAb therapies as the biologics field is rapidly emerging as the most popular and efficacious treatment approach in a plethora of disease indications not limited to oncology or ICB therapeutics. These mAb therapies could be applied to other ICB mAbs as many immune checkpoint pathways work at the priming phase within LNs or they could be applied to tumor targeting mAbs used to recognize and eliminate LN-resident tumors. Furthermore, non-therapeutic applications using this approach could be used to explore basic science questions regarding the adaptive or innate immune response in LNs as various mAbs can be used as ligand traps to reduce cytokine or other protein concentrations in LNs or can be used as depleting clones to probe questions about each cell compartments role in immunity. Furthermore, considering this approach is using FDA approved targets, developing clinically translatable formulations is a great interest I have as local administrations of mAbs can be challenging due to injection volume constraints and repeated injections in the same location. The development of a sustained mAb formulation (e.g. hydrogel) holds promise for overcoming the need of multiple injections which is a major barrier

for patient compliance. In respect to aim 2, I would like to see future projects aimed at expanding both the immunotherapies delivered and tissues targeted with ANCs. The ANC platform can be applied to virtually any mAb due to the mild reaction conditions and amine/thiol conjugation chemistry. Furthermore, the hydrophobic NP core allows for a diversity of small molecule modulators to be encapsulated and delivered with this platform enabling a plethora of different combination strategies. By using existing and novel combinations of mAbs and small molecule drugs for codelivery to cells of interest, new insights on immunotherapies and improvements in anti-tumor responses may result that were not observed in the past lacking codelivery approaches. Furthermore, drugging LNs with this ANC platform has the potential to create a drug depot in dLNs allowing for new therapeutic interventions with less injections. Projects such as these could provide insight and further our understandings of mAb therapies, the role of LNs in immunological pathways, and help contribute towards therapeutic interventions in the cancer immunotherapy field.

5.3.1 Extending LN drugging to other mAb therapies and sustained release formulations

Future work for this approach should aim at exploring the administration of other ICB mAbs such as those targeting PD-L1, T cell immunoreceptor with Ig and ITIM domains (TIGIT), T-cell immunoglobulin and mucin-domain containing-3 (Tim3), and others involved in T cell activation. All of these mAbs are currently FDA approved or are in clinical trials and have expression on APCs/T cells which can be found in LNs, yet these therapies have variable response rates motivating alternative strategies to improve efficacies. From my work and others showing LN accumulation of mAbs is based on molecular size, therapeutic experiments should be designed, and anti-tumor responses measured. In addition to the LN being home to immune cells, certain cancers metastasize leading to LN resident tumors. Thus, these diseased tissues are prime targets for drug modulation. mAb therapies (applicable to ADCs and ANCs as well) targeting tumor

antigens such as HER2 could be viable options using cutaneous administration to drug LN resident tumors and eradicate them circumventing the need for LN resections.

Drugging LNs with mAbs outside of ligand blocking is also a potential direction, specifically ligand traps. Inhibiting TGFβ within T cells is one way to block the suppressive functions, however, mAbs have been developed to sequester and prevent TGFβ from exerting its function. Literature suggests TGFβ is upregulated in TdLNs which can lead to immune suppression and metastatic invasion therefore reducing the concentration of TGFβ here represents an interesting approach. Related to this, LN drugging with mAbs could be used to explore basic science questions as sequestering various cytokines or chemokines with ligand traps or depleting certain cells types in dLNs may help determine the role of these proteins/cells in different contexts helping to further our understandings of immunological mechanisms.

In addition to expanding the mAb therapies, the development of a sustained release formulation at the injection site to prolong mAb lymphatic drainage has promising upsides. One of the main reasons local administrations have been developed is due to patient compliance as it is a much quicker administration compared to i.v. administration in terms of injection time. To advance this convenience, developing a system that requires one injection in the skin vs multiple injections may further improve patient compliance. We have done preliminary work showing continually drugging the dLN over several days using a hydrogel system improves anti-tumor immunity. This work needs to be further developed in larger animal studies and multiple tumor models but holds potential for translation into the clinic.

5.3.2 Determining ANC biodistribution further and expanding applications

Future work for the ANC system should aim at expanding the biodistribution characterization as this has important implications for toxicity, efficacy, and sustained drugging applications. Following systemic and local administrations using fluorescent tagged ANCs,

exploring the circulation time along with tissue accumulation within the TME and LNs would be of great interest to determine whether affinity based ANCs show differences in these tissue targets. Additionally, using checkpoint targeted ANCs and exploring whether ANCs interact preferentially with different cell types would be of interest, i.e. would ANCs primarily accumulate with Tregs as they express higher levels of checkpoint receptors comparted to CD8 or Natural Killer cells. As eluded to earlier, T cells exert low levels of phagocytosis and pinocytosis suggesting ANCs would stay bound to the surface of these cells. However, directly exploring this and determining how long ANCs stay bound to their target T cells would be intriguing and important for sustained drugging applications.

Additionally, future work for the ANC system should aim at expanding the codelivery of various immunotherapeutics. Due to the ease of conjugation, multiple mAbs could be conjugated to the same NP to block different proteins simultaneously while encapsulation of multiple small molecule modulators within the same NP will allow for codelivery of two classes of drugs (mAbs and small molecules), but also modulation of two plus pathways. We have previously shown that the NPs can encapsulate a diversity of small molecules separately which should be extended to the same NP. By expanding on the original ANC platform to deliver multiple small molecule drugs, a feature challenging to achieve with ADCs due to the drug loading constraint per mAb, dozens of pathways could theoretically by modulated within a single cell. Alternatively, using this system to drug LNs is another area of interest where mAbs with affinities to LN ECM proteins could be conjugated to ANCs to prolong retention in the LNs compared to non-targeted ANCs. Combined with the unique ability of ANCs to enable sustained small molecule drugging due to the hydrophobic NP core, ANCs could selectively drug dLNs with modulators over days.

REFERENCES

1. M. K. Callahan, J. D. Wolchok, f BASIC-TRANSLATIONAL REVIEW At the Bedside : CTLA-4- and PD-1-blocking antibodies in cancer immunotherapy, **94**, 41–53 (2017).

2. S. C. Wei, C. R. Duffy, J. P. Allison, fundamental Mechanisms of Immune Checkpoint Blockade Therapy, (2018), doi:10.1158/2159-8290.CD-18-0367.

3. E. C. Connolly, J. Freimuth, R. J. Akhurst, Complexities of TGF-β targeted cancer therapy, *Int. J. Biol. Sci.* **8** (2012), doi:10.7150/ijbs.4564.

4. R. D. Leone, Y. C. Lo, J. D. Powell, A2aR antagonists: Next generation checkpoint blockade for cancer immunotherapy, *Comput. Struct. Biotechnol. J.* **13**, 265–272 (2015).

5. J. Duraiswamy, K. M. Kaluza, G. J. Freeman, G. Coukos, Dual blockade of PD-1 and CTLA-4 combined with tumor vaccine effectively restores T-cell rejection function in tumors, *Cancer Res.* **73**, 3591–3603 (2013).

6. P. S. Hegde, D. S. Chen, Top 10 Challenges in Cancer Immunotherapy, *Immunity* **52**, 17–35 (2020).

7. J. Larkin, V. Chiarion-Sileni, R. Gonzalez, J. J. Grob, C. L. Cowey, C. D. Lao, D. Schadendorf, R. Dummer, M. Smylie, P. Rutkowski, P. F. Ferrucci, A. Hill, J. Wagstaff, M. S. Carlino, J. B. Haanen, M. Maio, I. Marquez-Rodas, G. A. McArthur, P. A. Ascierto, G. V. Long, M. K. Callahan, M. A. Postow, K. Grossmann, M. Sznol, B. Dreno, L. Bastholt, A. Yang, L. M. Rollin, C. Horak, F. S. Hodi, J. D. Wolchok, Combined Nivolumab and Ipilimumab or Monotherapy in Untreated Melanoma, *N. Engl. J. Med.* **373**, 23–34 (2015).

8. M. L. Johnson, F. Braiteh, J. E. Grilley-Olson, J. Chou, J. Davda, A. Forgie, R. Li, I. Jacobs, F. Kazazi, S. Hu-Lieskovan, Assessment of Subcutaneous vs Intravenous Administration of Anti-PD-1 Antibody PF-06801591 in Patients with Advanced Solid Tumors: A Phase 1 Dose-Escalation Trial, *JAMA Oncol.* **5**, 999–1007 (2019).

9. R. He, S. Hou, C. Liu, A. Zhang, Q. Bai, M. Han, Y. Yang, G. Wei, T. Shen, X. Yang, L. Xu, X. Chen, Y. Hao, P. Wang, C. Zhu, J. Ou, H. Liang, T. Ni, X. Zhang, X. Zhou, K. Deng, Y. Chen, Y. Luo, J. Xu, H. Qi, Y. Wu, L. Ye, Follicular CXCR5-expressing CD8+ T cells curtail chronic viral infection, *Nat.*

Publ. Gr. **537**, 412–428 (2016).

10. S. J. Im, M. Hashimoto, M. Y. Gerner, J. Lee, H. T. Kissick, M. C. Burger, Q. Shan, J. S. Hale, J. Lee, T. H. Nasti, A. H. Sharpe, G. J. Freeman, R. N. Germain, H. I. Nakaya, H. H. Xue, R. Ahmed, Defining CD8+ T cells that provide the proliferative burst after PD-1 therapy, *Nature* **537**, 417–421 (2016).

11. N. Dan, S. Setua, V. K. Kashyap, S. Khan, M. Jaggi, M. M. Yallapu, S. C. Chauhan, Antibody-Drug Conjugates for Cancer Therapy : Chemistry to Clinical Implications, (2018), doi:10.3390/ph11020032.

12. D. S. Chen, I. Mellman, Oncology Meets Immunology: The Cancer-Immunity Cycle, *Immunity* **39**, 1–10 (2013).

13. J. F. Brunet, F. Denizot, M. F. Luciani, M. Roux-Dosseto, M. Suzan, M. G. Mattei, P. Golstein, A new member of the immunoglobulin superfamily--CTLA-4., *Nature* **328**, 267–270 (1987).

14. R. J. Greenwald, V. A. Boussiotis, R. B. Lorsbach, A. K. Abbas, A. H. Sharpe, CTLA-4 regulates induction of anergy in vivo., *Immunity* **14**, 145–155 (2001).

15. P. Waterhouse, J. M. Penninger, E. Timms, A. Wakeham, A. Shahinian, K. P. Lee, C. B. Thompson, H. Griesser, T. W. Mak, Lymphoproliferative disorders with early lethality in mice deficient in Ctla-4., *Science* **270**, 985–988 (1995).

16. T. Lindsten, K. P. Lee, E. S. Harris, B. Petryniak, N. Craighead, P. J. Reynolds, D. B. Lombard, G. J. Freeman, L. M. Nadler, G. S. Gray, Characterization of CTLA-4 structure and expression on human T cells., *J. Immunol.* **151**, 3489–3499 (1993).

17. M. L. Alegre, P. J. Noel, B. J. Eisfelder, E. Chuang, M. R. Clark, S. L. Reiner, C. B. Thompson, Regulation of surface and intracellular expression of CTLA4 on mouse T cells., *J. Immunol.* **157**, 4762–4770 (1996).

18. P. S. Linsley, J. Bradshaw, J. Greene, R. Peach, K. L. Bennett, R. S. Mittler, Intracellular trafficking of CTLA-4 and focal localization towards sites of TCR engagement., *Immunity* **4**, 535–543 (1996).

19. D. Perkins, Z. Wang, C. Donovan, H. He, D. Mark, G. Guan, Y. Wang, T. Walunas, J. Bluestone, J. Listman, P. W. Finn, Regulation of CTLA-4 expression during T cell activation., *J. Immunol.* **156**, 4154–4159 (1996).

20. K. Wing, Y. Onishi, P. Prieto-Martin, T. Yamaguchi, M. Miyara, Z. Fehervari, T. Nomura, S.

Sakaguchi, CTLA-4 control over Foxp3+ regulatory T cell function, *Science (80-.).* **322**, 271–275 (2008).

21. A. V Collins, D. W. Brodie, R. J. C. Gilbert, A. Iaboni, R. Manso-Sancho, B. Walse, D. I. Stuart, P. A. van der Merwe, S. J. Davis, The interaction properties of costimulatory molecules revisited., *Immunity* **17**, 201–210 (2002).

22. O. S. Qureshi, Y. Zheng, K. Nakamura, K. Attridge, C. Manzotti, E. M. Schmidt, J. Baker, L. E. Jeffery, S. Kaur, Z. Briggs, T. Z. Hou, C. E. Futter, G. Anderson, L. S. K. Walker, D. M. Sansom, Trans-endocytosis of CD80 and CD86: a molecular basis for the cell-extrinsic function of CTLA-4., *Science* **332**, 600–603 (2011).

23. Y. Ishida, Y. Agata, K. Shibahara, T. Honjo, Induced expression of PD-1, a novel member of the immunoglobulin gene superfamily, upon programmed cell death., *EMBO J.* **11**, 3887–3895 (1992).

24. M. E. Keir, M. J. Butte, G. J. Freeman, A. H. Sharpe, PD-1 and its ligands in tolerance and immunity, *Annu Rev Immunol* **26**, 677–704 (2008).

25. H. Nishimura, M. Nose, H. Hiai, N. Minato, T. Honjo, Development of lupus-like autoimmune diseases by disruption of the PD-1 gene encoding an ITIM motif-carrying immunoreceptor., *Immunity* **11**, 141–151 (1999).

26. D. L. Barber, E. J. Wherry, D. Masopust, B. Zhu, J. P. Allison, A. H. Sharpe, G. J. Freeman, R. Ahmed, Restoring function in exhausted CD8 T cells during chronic viral infection., *Nature* **439**, 682–687 (2006).

27. C. L. Day, D. E. Kaufmann, P. Kiepiela, J. A. Brown, E. S. Moodley, S. Reddy, E. W. Mackey, J. D. Miller, A. J. Leslie, C. DePierres, Z. Mncube, J. Duraiswamy, B. Zhu, Q. Eichbaum, M. Altfeld, E. J. Wherry, H. M. Coovadia, P. J. R. Goulder, P. Klenerman, R. Ahmed, G. J. Freeman, B. D. Walker, PD-1 expression on HIV-specific T cells is associated with T-cell exhaustion and disease progression., *Nature* **443**, 350–354 (2006).

28. S. C. Liang, Y. E. Latchman, J. E. Buhlmann, M. F. Tomczak, B. H. Horwitz, G. J. Freeman, A. H. Sharpe, Regulation of PD-1, PD-L1, and PD-L2 expression during normal and autoimmune responses., *Eur. J. Immunol.* **33**, 2706–2716 (2003).

29. L. M. Francisco, V. H. Salinas, K. E. Brown, V. K. Vanguri, G. J. Freeman, V. K. Kuchroo, A. H. Sharpe, PD-L1 regulates the development, maintenance, and function of induced regulatory T cells, *J. Exp. Med.* **206**, 3015–3029 (2009).

30. D. R. Leach, M. F. Krummel, J. P. Allison, Enhancement of antitumor immunity by CTLA-4 blockade., *Science* **271**, 1734–1736 (1996).

31. K. S. Peggs, S. A. Quezada, J. P. Allison, Cell intrinsic mechanisms of T-cell inhibition and application to cancer therapy., *Immunol. Rev.* **224**, 141–165 (2008).

32. W. J. Lesterhuis, J. Salmons, A. K. Nowak, E. N. Rozali, A. Khong, I. M. Dick, J. A. Harken, B. W. Robinson, R. A. Lake, Synergistic Effect of CTLA-4 Blockade and Cancer Chemotherapy in the Induction of Anti-Tumor Immunity, *PLoS One* **8**, 1–8 (2013).

33. S. Demaria, N. Kawashima, A. M. Yang, M. L. Devitt, J. S. Babb, J. P. Allison, S. C. Formenti, Immune-mediated inhibition of metastases after treatment with local radiation and CTLA-4 blockade in a mouse model of breast cancer, *Clin. Cancer Res.* **11**, 728–734 (2005).

34. C. T.-S. Victor, A. J. Rech, A. Maity, R. Rengan, K. E. Pauken, E. Stelekati, J. L. Benci, B. Xu, H. Dada, P. M. Odorizzi, R. S. Herati, K. D. Mansfield, D. Patsch, R. K. Amaravadi, L. M. Schuchter, H. Ishwaran, R. Mick, D. A. Pryma, X. Xu, M. D. Feldman, T. C. Gangadhar, S. M. Hahn, E. J. Wherry, R. H. Vonderheide, A. J. Minn, Radiation and dual checkpoint blockade activate non-redundant immune mechanisms in cancer, *Nature* **520**, 373–377 (2015).

35. A. van Elsas, A. A. Hurwitz, J. P. Allison, Combination Immunotherapy of B16 Melanoma Using Anti–Cytotoxic T Lymphocyte–Associated Antigen 4 (Ctla-4) and Granulocyte/Macrophage Colony-Stimulating Factor (Gm-Csf)-Producing Vaccines Induces Rejection of Subcutaneous and Metastatic Tumors Accompanied , *J. Exp. Med.* **190**, 355 LP-366 (1999).

36. K. S. Peggs, S. A. Quezada, C. A. Chambers, A. J. Korman, J. P. Allison, Blockade of CTLA-4 on both effector and regulatory T cell compartments contributes to the antitumor activity of anti-CTLA-4 antibodies, *J Exp Med* **206**, 1717–1725 (2009).

37. Y. Bulliard, R. Jolicoeur, M. Windman, S. M. Rue, S. Ettenberg, D. A. Knee, N. S. Wilson, G. Dranoff, J. L. Brogdon, Activating Fc γ receptors contribute to the antitumor activities of

immunoregulatory receptor-targeting antibodies., *J. Exp. Med.* **210**, 1685–93 (2013).

38. M. J. Selby, J. J. Engelhardt, M. Quigley, K. A. Henning, T. Chen, M. Srinivasan, A. J. Korman, Anti-CTLA-4 antibodies of IgG2a isotype enhance antitumor activity through reduction of intratumoral regulatory T cells., *Cancer Immunol. Res.* **1**, 32–42 (2013).

39. T. R. Simpson, F. Li, W. Montalvo-Ortiz, M. A. Sepulveda, K. Bergerhoff, F. Arce, C. Roddie, J. Y. Henry, H. Yagita, J. D. Wolchok, K. S. Peggs, J. V Ravetch, J. P. Allison, S. A. Quezada, Fc-dependent depletion of tumor-infiltrating regulatory T cells co-defines the efficacy of anti-CTLA-4 therapy against melanoma., *J. Exp. Med.* **210**, 1695–710 (2013).

40. P. Kvistborg, D. Philips, S. Kelderman, L. Hageman, C. Ottensmeier, D. Joseph-Pietras, M. J. Welters, S. van der Burg, E. Kapiteijn, O. Michielin, E. Romano, C. Linnemann, D. Speiser, C. Blank, J. B. Haanen, T. N. Schumacher, Anti-CTLA-4 therapy broadens the melanoma-reactive CD8+ T cell response, *Sci Transl Med* **6**, 254ra128 (2014).

41. Y. Iwai, M. Ishida, Y. Tanaka, T. Okazaki, T. Honjo, N. Minato, Involvement of PD-L1 on tumor cells in the escape from host immune system and tumor immunotherapy by PD-L1 blockade., *Proc. Natl. Acad. Sci. U. S. A.* **99**, 12293–12297 (2002).

42. W. Zou, L. Chen, Inhibitory B7-family molecules in the tumour microenvironment., *Nat. Rev. Immunol.* **8**, 467–477 (2008).

43. M. Ahmadzadeh, L. a Johnson, B. Heemskerk, J. R. Wunderlich, M. E. Dudley, D. E. White, S. a Rosenberg, W. Dc, Tumor antigen − specific CD8 T cells infiltrating the tumor express high levels of PD-1 and are functionally impaired Tumor antigen – specific CD8 T cells infiltrating the tumor express high levels of PD-1 and are functionally impaired, *Blood* **114**, 1537–1544 (2009).

44. F. Hirano, K. Kaneko, H. Tamura, H. Dong, S. Wang, M. Ichikawa, C. Rietz, D. B. Flies, J. S. Lau, G. Zhu, K. Tamada, L. Chen, Blockade of B7-H1 and PD-1 by monoclonal antibodies potentiates cancer therapeutic immunity., *Cancer Res.* **65**, 1089–1096 (2005).

45. H. Dong, S. E. Strome, D. R. Salomao, H. Tamura, F. Hirano, D. B. Flies, P. C. Roche, J. Lu, G. Zhu, K. Tamada, V. A. Lennon, E. Celis, L. Chen, Tumor-associated B7-H1 promotes T-cell apoptosis: a potential mechanism of immune evasion, *Nat Med* **8**, 793–800 (2002).

46. J. Lee, E. Ahn, H. T. Kissick, R. Ahmed, Reinvigorating Exhausted T Cells by Blockade of the PD-1 Pathway, *For. Immunopathol. Dis. Therap.* **6**, 7–17 (2015).

47. C. Stecher, C. Battin, J. Leitner, M. Zettl, K. Grabmeier-Pfistershammer, C. Höller, G. J. Zlabinger, P. Steinberger, PD-1 blockade promotes emerging checkpoint inhibitors in enhancing T Cell responses to allogeneic dendritic cells, *Front. Immunol.* **8**, 1–13 (2017).

48. E. Ahn, K. Araki, M. Hashimoto, W. Li, J. L. Riley, J. Cheung, A. H. Sharpe, Role of PD-1 during effector CD8 T cell differentiation, **115**, 4749–4754 (2018).

49. S. J. Im, M. Hashimoto, M. Y. Gerner, J. Lee, H. T. Kissick, M. C. Burger, Q. Shan, J. S. Hale, J. Lee, T. H. Nasti, A. H. Sharpe, G. J. Freeman, R. N. Germain, H. I. Nakaya, H. H. Xue, R. Ahmed, Defining CD8+T cells that provide the proliferative burst after PD-1 therapy, *Nature* **537**, 417–421 (2016).

50. R. Dahan, E. Sega, J. Engelhardt, M. Selby, A. J. Korman, J. V. Ravetch, FcγRs Modulate the Anti-tumor Activity of Antibodies Targeting the PD-1/PD-L1 Axis, *Cancer Cell* **28**, 285–295 (2015).

51. S. P. Arlauckas, C. S. Garris, R. H. Kohler, M. Kitaoka, M. F. Cuccarese, K. S. Yang, M. A. Miller, J. C. Carlson, G. J. Freeman, R. M. Anthony, R. Weissleder, M. J. Pittet, In vivo imaging reveals a tumor-associated macrophage–mediated resistance pathway in anti–PD-1 therapy, *Sci. Transl. Med.* **9**, eaal3604 (2017).

52. J. D. Wolchok, B. Neyns, G. Linette, S. Negrier, J. Lutzky, L. Thomas, W. Waterfield, D. Schadendorf, M. Smylie, T. Guthrie, J. J. Grob, J. Chesney, K. Chin, K. Chen, A. Hoos, S. J. O'Day, C. Lebbé, Ipilimumab monotherapy in patients with pretreated advanced melanoma: a randomised, double-blind, multicentre, phase 2, dose-ranging study, *Lancet Oncol.* **11**, 155–164 (2010).

53. S. A. Quezada, K. S. Peggs, M. A. Curran, J. P. Allison, CTLA4 blockade and GM-CSF combination immunotherapy alters the intratumor balance of effector and regulatory T cells, *J. Clin. Invest.* **116**, 1935–1945 (2006).

54. B. Kavanagh, S. O. Brien, D. Lee, Y. Hou, V. Weinberg, B. Rini, J. P. Allison, E. J. Small, L. Fong, CTLA4 blockade expands FoxP3 + regulatory and activated effector CD4 + T cells in a dose-dependant fashion CTLA4 blockade expands FoxP3 + regulatory and activated effector CD4 + T cells in a dose-dependant fashion, *Online* **112**, 1175–1184 (2008).

55. J. R. Brahmer, C. G. Drake, I. Wollner, J. D. Powderly, J. Picus, W. H. Sharfman, E. Stankevich, A. Pons, T. M. Salay, T. L. McMiller, M. M. Gilson, C. Wang, M. Selby, J. M. Taube, R. Anders, L. Chen, A. J. Korman, D. M. Pardoll, I. Lowy, S. L. Topalian, Phase I study of single-agent anti-programmed death-1 (MDX-1106) in refractory solid tumors: Safety, clinical activity, pharmacodynamics, and immunologic correlates, *J. Clin. Oncol.* **28**, 3167–3175 (2010).

56. S. L. Topalian, M. Sznol, D. F. McDermott, H. M. Kluger, R. D. Carvajal, W. H. Sharfman, J. R. Brahmer, D. P. Lawrence, M. B. Atkins, J. D. Powderly, P. D. Leming, E. J. Lipson, I. Puzanov, D. C. Smith, J. M. Taube, J. M. Wigginton, G. D. Kollia, A. Gupta, D. M. Pardoll, J. A. Sosman, F. S. Hodi, Survival, durable tumor remission, and long-term safety in patients with advanced melanoma receiving nivolumab, *J. Clin. Oncol.* **32**, 1020–1030 (2014).

57. O. Hamid, C. Robert, A. Daud, F. S. Hodi, W.-J. Hwu, R. Kefford, J. D. Wolchok, P. Hersey, R. W. Joseph, J. S. Weber, R. Dronca, T. C. Gangadhar, A. Patnaik, H. Zarour, A. M. Joshua, K. Gergich, J. Elassaiss-Schaap, A. Algazi, C. Mateus, P. Boasberg, P. C. Tumeh, B. Chmielowski, S. W. Ebbinghaus, X. N. Li, S. P. Kang, A. Ribas, Supplementary - Safety and tumor responses with lambrolizumab (anti-PD-1) in melanoma., *N. Engl. J. Med.* **369**, 134–44 (2013).

58. Y. Li, M. Fang, J. Zhang, J. Wang, Y. Song, J. Shi, W. Li, G. Wu, J. Ren, Z. Wang, W. Zou, L. Wang, Hydrogel dual delivered celecoxib and anti-PD-1 synergistically improve antitumor immunity, *Oncoimmunology* **5**, e1074374 (2016).

59. J. R. Brahmer, S. S. Tykodi, L. Q. M. Chow, W.-J. Hwu, S. L. Topalian, P. Hwu, C. G. Drake, L. H. Camacho, J. Kauh, K. Odunsi, H. C. Pitot, O. Hamid, S. Bhatia, R. Martins, K. Eaton, S. Chen, T. M. Salay, S. Alaparthy, J. F. Grosso, A. J. Korman, S. M. Parker, S. Agrawal, S. M. Goldberg, D. M. Pardoll, A. Gupta, J. M. Wigginton, Safety and activity of anti-PD-L1 antibody in patients with advanced cancer., *N. Engl. J. Med.* **366**, 2455–65 (2012).

60. R. Stewart, M. Morrow, S. A. Hammond, K. Mulgrew, D. Marcus, E. Poon, A. Watkins, S. Mullins, M. Chodorge, J. Andrews, D. Bannister, E. Dick, N. Crawford, J. Parmentier, M. Alimzhanov, J. S. Babcook, I. N. Foltz, A. Buchanan, V. Bedian, R. W. Wilkinson, M. McCourt, Identification and Pre-clinical Characterization of MEDI4736, an Antagonistic anti-PD-L1 Monoclonal Antibody, *Cancer*

Immunol Res **3**, 1052–1063 (2015).

61. J. D. Wolchok, H. Kluger, M. K. Callahan, M. a Postow, N. a Rizvi, A. M. Lesokhin, N. H. Segal, C. E. Ariyan, R.-A. Gordon, K. Reed, M. M. Burke, A. Caldwell, S. a Kronenberg, B. U. Agunwamba, X. Zhang, I. Lowy, H. D. Inzunza, W. Feely, C. E. Horak, Q. Hong, A. J. Korman, J. M. Wigginton, A. Gupta, M. Sznol, Nivolumab plus ipilimumab in advanced melanoma., *N. Engl. J. Med.* **369**, 122–33 (2013).

62. Y. Q. Xiao, C. G. Freire-de-Lima, W. P. Schiemann, D. L. Bratton, R. W. Vandivier, P. M. Henson, Transcriptional and Translational Regulation of TGF- Production in Response to Apoptotic Cells, *J. Immunol.* **181**, 3575–3585 (2008).

63. J. Massagué, TGFβ in Cancer, *Cell* **134**, 215–230 (2008).

64. E. C. Connolly, R. J. Akhurst, The complexities of TGF-beta action during mammary and squamous cell carcinogenesis., *Curr. Pharm. Biotechnol.* **12**, 2138–2149 (2011).

65. J. S. Nam, M. Terabe, M. J. Kang, H. Chae, N. Voong, Y. A. Yang, A. Laurence, A. Michalowska, M. Mamura, S. Lonning, J. A. Berzofsky, L. M. Wakefield, Transforming growth factor β subverts the immune system into directly promoting tumor growth through interleukin-17, *Cancer Res.* **68**, 3915–3923 (2008).

66. Z. G. Fridlender, J. Sun, S. Kim, V. Kapoor, G. Cheng, L. Ling, G. S. Worthen, S. M. Albelda, Polarization of tumor-associated neutrophil phenotype by TGF-beta: “N1” versus “N2” TAN., *Cancer Cell* **16**, 183–194 (2009).

67. T. Fujita, K. Teramoto, Y. Ozaki, J. Hanaoka, N. Tezuka, Y. Itoh, T. Asai, S. Fujino, K. Kontani, K. Ogasawara, Inhibition of transforming growth factor-beta-mediated immunosuppression in tumor-draining lymph nodes augments antitumor responses by various immunologic cell types, *Cancer Res* **69**, 5142–5150 (2009).

68. B. I. Dalal, P. A. Keown, A. H. Greenberg, Immunocytochemical localization of secreted transforming growth factor-beta 1 to the advancing edges of primary tumors and to lymph node metastases of human mammary carcinoma, *Am. J. Pathol.* **143**, 381–389 (1993).

69. J. Stagg, M. J. Smyth, Extracellular adenosine triphosphate and adenosine in cancer, *Oncogene* **29**,

5346–5358 (2010).

70. G. Kroemer, L. Galluzzi, O. Kepp, L. Zitvogel, Immunogenic cell death in cancer therapy., *Annu. Rev. Immunol.* **31**, 51–72 (2013).

71. B. Allard, M. S. Longhi, S. C. Robson, J. Stagg, The ectonucleotidases CD39 and CD73: Novel checkpoint inhibitor targets., *Immunol. Rev.* **276**, 121–144 (2017).

72. R. D. Leone, L. A. Emens, Targeting adenosine for cancer immunotherapy, *J. Immunother. Cancer* **6**, 57 (2018).

73. A. S. Robeva, R. L. Woodard, X. Jin, Z. Gao, S. Bhattacharya, H. E. Taylor, D. L. Rosin, J. Linden, Molecular characterization of recombinant human adenosine receptors, *Drug Dev. Res.* **39**, 243–252 (1996).

74. A. Ohta, M. Sitkovsky, Role of G-protein-coupled adenosine receptors in downregulation of inflammation and protection from tissue damage., *Nature* **414**, 916–920 (2001).

75. J. J. Butler, J. S. Mader, C. L. Watson, H. Zhang, J. Blay, D. W. Hoskin, Adenosine inhibits activation-induced T cell expression of CD2 and CD28 co-stimulatory molecules: role of interleukin-2 and cyclic AMP signaling pathways., *J. Cell. Biochem.* **89**, 975–991 (2003).

76. A. Ohta, A Metabolic Immune Checkpoint: Adenosine in Tumor Microenvironment., *Front. Immunol.* **7**, 109 (2016).

77. M. Terabe, F. C. Robertson, K. Clark, E. De Ravin, A. Bloom, D. J. Venzon, S. Kato, A. Mirza, J. A. Berzofsky, Blockade of only TGF-β 1 and 2 is sufficient to enhance the efficacy of vaccine and PD-1 checkpoint blockade immunotherapy, *Oncoimmunology* **6**, e1308616 (2017).

78. R. B. Holmgaard, D. A. Schaer, Y. Li, S. P. Castaneda, M. Y. Murphy, X. Xu, I. Inigo, J. Dobkin, J. R. Manro, P. W. Iversen, D. Surguladze, G. E. Hall, R. D. Novosiadly, K. A. Benhadji, G. D. Plowman, M. Kalos, K. E. Driscoll, Targeting the TGFβ pathway with galunisertib, a TGFβRI small molecule inhibitor, promotes anti-tumor immunity leading to durable, complete responses, as monotherapy and in combination with checkpoint blockade, *J. Immunother. Cancer* **6**, 1–15 (2018).

79. R. Ravi, K. A. Noonan, V. Pham, R. Bedi, A. Zhavoronkov, I. V Ozerov, E. Makarev, A. V Artemov, P. T. Wysocki, R. Mehra, S. Nimmagadda, L. Marchionni, D. Sidransky, I. M. Borrello, E. Izumchenko,

A. Bedi, enhance the ef fi cacy of cancer immunotherapy, *Nat. Commun.* (2018), doi:10.1038/s41467-017-02696-6.

80. A. Ohta, E. Gorelik, S. J. Prasad, F. Ronchese, D. Lukashev, M. K. K. Wong, X. Huang, S. Caldwell, K. Liu, P. Smith, J.-F. Chen, E. K. Jackson, S. Apasov, S. Abrams, M. Sitkovsky, A2A adenosine receptor protects tumors from antitumor T cells, *Proc. Natl. Acad. Sci.* **103**, 13132–13137 (2006).

81. P. A. Beavis, N. Milenkovski, M. A. Henderson, L. B. John, B. Allard, S. Loi, M. H. Kershaw, J. Stagg, P. K. Darcy, Adenosine Receptor 2A Blockade Increases the Efficacy of Anti-PD-1 through Enhanced Antitumor T-cell Responses, *Cancer Immunol. Res.* **3**, 506–517 (2015).

82. B. Allard, S. Pommey, M. J. Smyth, J. Stagg, Targeting CD73 enhances the antitumor activity of anti-PD-1 and anti-CTLA-4 mAbs, *Clin. Cancer Res.* **19**, 5626–5635 (2013).

83. G. M. Thurber, M. M. Schmidt, K. D. Wittrup, Antibody tumor penetration: Transport opposed by systemic and antigen-mediated clearance, *Adv. Drug Deliv. Rev.* **60**, 1421–1434 (2008).

84. G. M. Thurber, M. M. Schmidt, K. D. Wittrup, Factors determining antibody distribution in tumors, *Trends Pharmacol. Sci.* **29**, 57–61 (2008).

85. M. Pitorre, G. Bastiat, E. M. Dit Chatel, J. P. Benoit, Passive and specific targeting of lymph nodes: The influence of the administration route, *Eur. J. Nanomedicine* **7**, 121–128 (2015).

86. R. Deng, D. Bumbaca, C. V. Pastuskovas, C. A. Boswell, D. West, K. J. Cowan, H. Chiu, J. McBride, C. Johnson, Y. Xin, H. Koeppen, M. Leabman, S. Iyer, Preclinical pharmacokinetics, pharmacodynamics, tissue distribution, and tumor penetration of anti-PD-L1 monoclonal antibody, an immune checkpoint inhibitor, *MAbs* **8**, 593–603 (2016).

87. J. T. Ryman, B. Meibohm, Pharmacokinetics of monoclonal antibodies, *CPT Pharmacometrics Syst. Pharmacol.* **6**, 576–588 (2017).

88. L. E. van Vlerken, Z. Duan, S. R. Little, M. V. Seiden, M. M. Amiji, Biodistribution and pharmacokinetic analysis of paclitaxel and ceramide administered in multifunctional polymer-blend nanoparticles in drug resistant breast cancer model, *Mol. Pharm.* **5**, 516–526 (2008).

89. N. A. Rohner, S. N. Thomas, Melanoma growth effects on molecular clearance from tumors and biodistribution into systemic tissues versus draining lymph nodes, *J Control Release* **223**, 99–108 (2016).

90. R. H. Kelly, Functional anatomy of lymph nodes. I. The paracortical cords., *Int. Arch. Allergy Appl. Immunol.* **48**, 836–849 (1975).

91. P. G. Forkert, J. A. Thliveris, F. D. Bertalanffy, Structure of sinuses in the human lymph node., *Cell Tissue Res.* **183**, 115–130 (1977).

92. J. E. Gretz, E. P. Kaldjian, A. O. Anderson, S. Shaw, Sophisticated strategies for information encounter in the lymph node: the reticular network as a conduit of soluble information and a highway for cell traffic., *J. Immunol.* **157**, 495–499 (1996).

93. J. E. Gretz, A. O. Anderson, S. Shaw, Cords, channels, corridors and conduits: critical architectural elements facilitating cell interactions in the lymph node cortex., *Immunol. Rev.* **156**, 11–24.

94. I. C. MacLennan, Germinal centers., *Annu. Rev. Immunol.* **12**, 117–139 (1994).

95. N. Romani, G. Ratzinger, K. Pfaller, W. Salvenmoser, H. Stossel, F. Koch, P. Stoitzner, Migration of dendritic cells into lymphatics-the Langerhans cell example: routes, regulation, and relevance., *Int. Rev. Cytol.* **207**, 237–270 (2001).

96. J. P. Girard, C. Moussion, R. Forster, HEVs, lymphatics and homeostatic immune cell trafficking in lymph nodes, *Nat Rev Immunol* **12**, 762–773 (2012).

97. G. J. Randolph, S. Ivanov, B. H. Zinselmeyer, J. P. Scallan, The Lymphatic System: Integral Roles in Immunity, *Annu. Rev. Immunol.* **35**, 31–52 (2017).

98. S. H. Jang, M. G. Wientjes, D. Lu, J. L. S. Au, Drug delivery and transport to solid tumors, *Pharm. Res.* **20**, 1337–1350 (2003).

99. R. K. Jain, T. Stylianopoulos, Delivering nanomedicine to solid tumors., *Nat. Rev. Clin. Oncol.* **7**, 653–64 (2010).

100. T. P. Padera, B. R. Stoll, J. B. Tooredman, D. Capen, E. di Tomaso, R. K. Jain, Pathology: cancer cells compress intratumour vessels., *Nature* **427**, 695 (2004).

101. K. Greish, in *Cancer Nanotechnology: Methods and Protocols*, S. R. Grobmyer, B. M. Moudgil, Eds. (Humana Press, Totowa, NJ, 2010), pp. 25–37.

102. E. P. Kaldjian, J. E. Gretz, A. O. Anderson, Y. Shi, S. Shaw, Spatial and molecular organization of lymph node T cell cortex: a labyrinthine cavity bounded by an epithelium-like monolayer of fibroblastic

reticular cells anchored to basement membrane-like extracellular matrix, *Int. Immunol.* **13**, 1243–1253 (2001).

103. M. F. Cesta, Normal Structure, Function, and Histology of Mucosa-Associated Lymphoid Tissue, *Toxicol. Pathol.* **34**, 599–608 (2006).

104. P. Baluk, J. Fuxe, H. Hashizume, T. Romano, E. Lashnits, S. Butz, D. Vestweber, M. Corada, C. Molendini, E. Dejana, D. M. McDonald, Functionally specialized junctions between endothelial cells of lymphatic vessels, *J. Exp. Med.* **204**, 2349–2362 (2007).

105. M. A. Swartz, The physiology of the lymphatic system, *Adv. Drug Deliv. Rev.* **50**, 3–20 (2001).

106. G. W. Schmid-Schonbein, Microlymphatics and lymph flow, *Physiol. Rev.* **70**, 987–1028 (1990).

107. W. Kastenmu, P. Torabi-parizi, N. Subramanian, T. La, R. N. Germain, A Spatially-Organized Multicellular Innate Immune Response in Lymph Nodes Limits Systemic Pathogen Spread, , 1235–1248 (2012).

108. P. Rantakari, K. Auvinen, N. Jäppinen, M. Kapraali, J. Valtonen, M. Karikoski, H. Gerke, I. Iftakhar-E-Khuda, J. Keuschnigg, E. Umemoto, K. Tohya, M. Miyasaka, K. Elima, S. Jalkanen, M. Salmi, The endothelial protein PLVAP in lymphatics controls the entry of lymphocytes and antigens into lymph nodes, *Nat. Immunol.* **16**, 386–396 (2015).

109. R. Roozendaal, T. R. Mempel, L. A. Pitcher, S. F. Gonzalez, A. Verschoor, R. E. Mebius, U. H. von Andrian, M. C. Carroll, Conduits Mediate Transport of Low-Molecular-Weight Antigen to Lymph Node Follicles, *Immunity* **30**, 264–276 (2009).

110. J. E. Gretz, C. C. Norbury, A. O. Anderson, A. E. I. Proudfoot, S. Shaw, Lymph-Borne Chemokines and Other Low Molecular Weight Molecules Reach High Endothelial Venules via Specialized Conduits While a Functional Barrier Limits Access to the Lymphocyte Microenvironments in Lymph Node Cortex, *J. Exp. Med.* **192**, 1425–1440 (2000).

111. M. Sixt, N. Kanazawa, M. Selg, T. Samson, G. Roos, D. P. Reinhardt, R. Pabst, M. B. Lutz, L. Sorokin, The conduit system transports soluble antigens from the afferent lymph to resident dendritic cells in the T cell area of the lymph node, *Immunity* **22**, 19–29 (2005).

112. S. N. Thomas, A. Schudel, Overcoming transport barriers for interstitial-, lymphatic-, and lymph

node-targeted drug delivery, *Curr. Opin. Chem. Eng.* **7**, 65–74 (2015).

113. J. Azzi, Q. Yin, M. Uehara, S. Ohori, L. Tang, K. Cai, T. Ichimura, M. McGrath, O. Maarouf, E. Kefaloyianni, S. Loughhead, J. Petr, Q. Sun, M. Kwon, S. Tullius, U. H. von Andrian, J. Cheng, R. Abdi, Targeted Delivery of Immunomodulators to Lymph Nodes, *Cell Rep.* **15**, 1202–1213 (2016).

114. K. Murphy, P. Travers, M. Walport, C. Janeway, *Janeway's immunobiology. LK - https://gatech.on.worldcat.org/oclc/212399882* (Garland Science, New York SE - xxi, 887 pages : illustrations (chiefly color) ; 28 cm + 1 CD-ROM (4 3/4 in.), 7th ed. /., 2008; http://catdir.loc.gov/catdir/toc/ecip079/2007002499.html).

115. A. Ager, High endothelial venules and other blood vessels: Critical regulators of lymphoid organ development and function, *Front. Immunol.* **8**, 1–16 (2017).

116. A. O. Anderson, S. Shaw, T cell adhesion to endothelium: the FRC conduit system and other anatomic and molecular features which facilitate the adhesion cascade in lymph node., *Semin. Immunol.* **5**, 271–282.

117. A. Takeda, N. Sasaki, M. Miyasaka, The molecular cues regulating immune cell trafficking, *Proc. Japan Acad. Ser. B Phys. Biol. Sci.* **93**, 183–195 (2017).

118. H. Liu, D. J. Irvine, Guiding principles in the design of molecular bioconjugates for vaccine applications, *Bioconjug Chem* **26**, 791–801 (2015).

119. B. Huang, W. D. Abraham, Y. Zheng, S. C. Bustamante López, S. S. Luo, D. J. Irvine, Active targeting of chemotherapy to disseminated tumors using nanoparticle-carrying T cells, *Sci. Transl. Med.* **7** (2015), doi:10.1126/scitranslmed.aaa5447.

120. P. J. Tanis, O. E. Nieweg, R. A. Valdés Olmos, E. J. T. Rutgers, B. B. R. Kroon, History of sentinel node and validation of the technique, *Breast Cancer Res.* **3**, 109–112 (2001).

121. C. M. Jewell, S. C. Lopez, D. J. Irvine, In situ engineering of the lymph node microenvironment via intranodal injection of adjuvant-releasing polymer particles, *Proc Natl Acad Sci U S A* **108**, 15745–15750 (2011).

122. L. H. Tostanoski, Y. C. Chiu, J. M. Gammon, T. Simon, J. I. Andorko, J. S. Bromberg, C. M. Jewell, Reprogramming the Local Lymph Node Microenvironment Promotes Tolerance that Is Systemic and

Antigen Specific, *Cell Rep.* **16**, 2940–2952 (2016).

123. G. Senti, P. Johansen, T. M. Kündig, in *Vaccines against Allergies*, R. Valenta, R. L. Coffman, Eds. (Springer Berlin Heidelberg, Berlin, Heidelberg, 2011), pp. 71–84.

124. M. Binnewies, E. W. Roberts, K. Kersten, V. Chan, D. F. Fearon, M. Merad, L. M. Coussens, D. I. Gabrilovich, S. Ostrand-Rosenberg, C. C. Hedrick, R. H. Vonderheide, M. J. Pittet, R. K. Jain, W. Zou, T. K. Howcroft, E. C. Woodhouse, R. A. Weinberg, M. F. Krummel, Understanding the tumor immune microenvironment (TIME) for effective therapy, *Nat. Med.* **24**, 541–550 (2018).

125. T. T. Goodman, P. L. Olive, S. H. Pun, Increased nanoparticle penetration in collagenase-treated multicellular spheroids., *Int. J. Nanomedicine* **2**, 265–274 (2007).

126. M. Magzoub, S. Jin, A. S. Verkman, Enhanced macromolecule diffusion deep in tumors after enzymatic digestion of extracellular matrix collagen and its associated proteoglycan decorin., *FASEB J.* **22**, 276–84 (2008).

127. B. Diop-Frimpong, V. P. Chauhan, S. Krane, Y. Boucher, R. K. Jain, Losartan inhibits collagen I synthesis and improves the distribution and efficacy of nanotherapeutics in tumors, *Pnas* **108**, 2909–2914 (2011).

128. R. T. Tong, Y. Boucher, S. V. Kozin, F. Winkler, D. J. Hicklin, R. K. Jain, Vascular normalization by vascular endothelial growth factor receptor 2 blockade induces a pressure gradient across the vasculature and improves drug penetration in tumors, *Cancer Res.* **64**, 3731–3736 (2004).

129. A. Marabelle, L. Tselikas, T. de Baere, R. Houot, Intratumoral immunotherapy: Using the tumor as the remedy, *Ann. Oncol.* **28**, xii33-xii43 (2017).

130. A. Marabelle, H. Kohrt, C. Caux, R. Levy, Intratumoral immunization: A new paradigm for cancer therapy, *Clin. Cancer Res.* **20**, 1747–1756 (2014).

131. A. Marabelle, H. Kohrt, R. Levy, Intratumoral anti-CTLA-4 therapy: Enhancing efficacy while avoiding toxicity, *Clin. Cancer Res.* **19**, 5261–5263 (2013).

132. D. A. Knorr, R. Dahan, J. V. Ravetch, Toxicity of an Fc-engineered anti-CD40 antibody is abrogated by intratumoral injection and results in durable antitumor immunity, *Proc. Natl. Acad. Sci. U. S. A.* **115**, 11048–11053 (2018).

133. S. Wang, J. Campos, M. Gallotta, M. Gong, C. Crain, E. Naik, R. L. Coffman, C. Guiducci, Intratumoral injection of a CpG oligonucleotide reverts resistance to PD-1 blockade by expanding multifunctional CD8+ T cells., *Proc. Natl. Acad. Sci. U. S. A.* **113**, E7240–E7249 (2016).

134. L. M. Kaminskas, J. Kota, V. M. McLeod, B. D. Kelly, P. Karellas, C. J. Porter, PEGylation of polylysine dendrimers improves absorption and lymphatic targeting following SC administration in rats, *J. Control. Release* **140**, 108–116 (2009).

135. L. Mei, J. Rao, Y. Liu, M. Li, Z. Zhang, Q. He, Effective treatment of the primary tumor and lymph node metastasis by polymeric micelles with variable particle sizes, *J. Control. Release* , #pagerange# (2018).

136. R. Kuai, L. J. Ochyl, K. S. Bahjat, A. Schwendeman, J. J. Moon, Designer vaccine nanodiscs for personalized cancer immunotherapy, *Nat. Mater.* **16**, 489–496 (2016).

137. T. R. Fadel, F. A. Sharp, N. Vudattu, R. Ragheb, J. Garyu, D. Kim, E. Hong, N. Li, G. L. Haller, L. D. Pfefferle, A carbon nanotube–polymer composite for T-cell therapy, *Nat. Nanotechnol.* **9**, 639–647 (2014).

138. H. Liu, K. D. Moynihan, Y. Zheng, G. L. Szeto, A. V Li, B. Huang, D. S. Van Egeren, C. Park, D. J. Irvine, Structure-based programming of lymph-node targeting in molecular vaccines, *Nature* **507**, 519–522 (2014).

139. W. Jiang, B. Y. S. Kim, J. T. Rutka, W. C. W. Chan, Nanoparticle-mediated cellular response is size-dependent., *Nat. Nanotechnol.* **3**, 145–50 (2008).

140. Y. Zhang, H. F. Chan, K. W. Leong, Advanced materials and processing for drug delivery: the past and the future, *Adv Drug Deliv Rev* **65**, 104–120 (2013).

141. S. T. Reddy, A. Rehor, H. G. Schmoekel, J. A. Hubbell, M. A. Swartz, In vivo targeting of dendritic cells in lymph nodes with poly(propylene sulfide) nanoparticles, *J. Control. Release* **112**, 26–34 (2006).

142. S. N. Thomas, E. Vokali, A. W. Lund, J. A. Hubbell, M. A. Swartz, Biomaterials Targeting the tumor-draining lymph node with adjuvanted nanoparticles reshapes the anti-tumor immune response, *Biomaterials* **35**, 814–824 (2014).

143. A. J. Van Der Vlies, C. P. Oneil, U. Hasegawa, N. Hammond, J. A. Hubbell, Synthesis of pyridyl

disulfide-functionalized nanoparticles for conjugating thiol-containing small molecules, peptides, and proteins, *Bioconjug. Chem.* **21**, 653–662 (2010).

144. I. C. Kourtis, S. Hirosue, A. de Titta, S. Kontos, T. Stegmann, J. A. Hubbell, M. A. Swartz, Peripherally Administered Nanoparticles Target Monocytic Myeloid Cells, Secondary Lymphoid Organs and Tumors in Mice, *PLoS One* **8** (2013), doi:10.1371/journal.pone.0061646.

145. L. Tang, Y. Zheng, M. B. Melo, L. Mabardi, A. P. Castaño, Y.-Q. Xie, N. Li, S. B. Kudchodkar, H. C. Wong, E. K. Jeng, M. V Maus, D. J. Irvine, Enhancing T cell therapy through TCR-signaling-responsive nanoparticle drug delivery, *Nat. Biotechnol.* (2018), doi:10.1038/nbt.4181.

146. Y. Zheng, M. T. Stephan, S. A. Gai, W. Abraham, A. Shearer, D. J. Irvine, In vivo targeting of adoptively transferred T-cells with antibody- and cytokine-conjugated liposomes, *J Control Release* **172**, 426–435 (2013).

147. D. Schmid, C. G. Park, C. A. Hartl, N. Subedi, A. N. Cartwright, R. B. Puerto, Y. Zheng, J. Maiarana, G. J. Freeman, K. W. Wucherpfennig, D. J. Irvine, M. S. Goldberg, T cell-targeting nanoparticles focus delivery of immunotherapy to improve antitumor immunity, *Nat. Commun.* **8**, 1747 (2017).

148. N. A. Rohner, S. N. Thomas, Flexible Macromolecule versus Rigid Particle Retention in the Injected Skin and Accumulation in Draining Lymph Nodes Are Differentially Influenced by Hydrodynamic Size, *ACS Biomater. Sci. Eng.* **3**, 153–159 (2017).

149. S. Rahimian, M. F. Fransen, J. W. Kleinovink, M. Amidi, F. Ossendorp, W. E. Hennink, Polymeric microparticles for sustained and local delivery of antiCD40 and antiCTLA-4 in immunotherapy of cancer, *Biomaterials* **61**, 33–40 (2015).

150. Y. Ye, J. Wang, Q. Hu, G. M. Hochu, H. Xin, C. Wang, Z. Gu, Synergistic Transcutaneous Immunotherapy Enhances Antitumor Immune Responses through Delivery of Checkpoint Inhibitors, *ACS Nano* **10**, 8956–8963 (2016).

151. C. Wang, Y. Ye, G. M. Hochu, H. Sadeghifar, Z. Gu, Enhanced Cancer Immunotherapy by Microneedle Patch-Assisted Delivery of Anti-PD1 Antibody, *Nano Lett* **16**, 2334–2340 (2016).

152. A. Manuscript, NIH Public Access, *Acta Crystallogr. Sect. D Biol. Crystallogr.* **18**, 281–287 (2009).

153. G. F. Nash, L. F. Turner, M. F. Scully, A. K. Kakkar, Platelets and cancer, *Lancet Oncol.* **3**, 425–430 (2002).

154. A. T. Nurden, P. Nurden, M. Sanchez, I. Andia, E. Anitua, Platelets and wound healing., *Front. Biosci.* **13**, 3532–3548 (2008).

155. C. Wang, W. Sun, Y. Ye, Q. Hu, H. N. Bomba, Z. Gu, D. Baker, T. Masterson, R. Pace, W. Constable, H. Wanebo, E. Y. Lukianova-Hleb, S. B. Stephan, R. Demicheli, M. Retsky, W. Hrushesky, M. Baum, I. Gukas, W. Ceelen, P. Pattyn, M. Mareel, L. E. Klevorn, R. M. Teague, D. O'Sullivan, E. L. Pearce, C. Robert, M. A. Postow, P. Sharma, J. P. Allison, C. Wang, Y. Ye, G. M. Hochu, H. Sadeghifar, Z. Gu, W. Zou, J. D. Wolchok, L. Chen, E. I. Buchbinder, F. S. Hodi, E. C. Smyth, D. Cunningham, J. E. Rosenberg, J. Naidoo, M. Mellati, C. Boutros, J. Larkin, L. Chen, X. Han, J. S. Weber, K. C. Kahler, A. Hauschild, S. R. Woo, L. Corrales, T. F. Gajewski, P. S. Hegde, V. Karanikas, S. Evers, S. Spranger, T. F. Gajewski, H. Schreiber, Y. X. Fu, A. D. Fesnak, C. H. June, B. L. Levine, J. W. Yoo, D. J. Irvine, D. E. Discher, S. Mitragotri, R. Tamagawa-Mineoka, A. T. Franco, A. Corken, J. Ware, C. M. Hu, L. A. Harker, A. T. Nurden, P. Nurden, M. Sanchez, I. Andia, E. Anitua, L. J. Gay, B. Felding-Habermann, G. F. Nash, L. F. Turner, M. F. Scully, A. K. Kakkar, Q. Hu, O. Garraud, C. N. Morrell, A. A. Aggrey, L. M. Chapman, K. L. Modjeski, J. W. Semple, J. E. Italiano, J. Freedman, B. D. Elzey, L. Seifert, S. L. Topalian, C. G. Drake, D. M. Pardoll, P. R. M. Siljander, J. Li, C. C. Sharkey, B. Wun, J. L. Liesveld, M. R. King, Z. M. Ruggeri, G. L. Mendolicchio, S. F. Mause, P. von Hundelshausen, A. Zernecke, R. R. Koenen, C. Weber, S. Tripathi, I. Guleria, M. B. Headley, R. Flaumenhaft, M. L. Rand, H. Wang, K. W. Bang, M. A. Packham, J. Freedman, Y. Lu, A. A. Aimetti, R. Langer, Z. Gu, A. Janowska-Wieczorek, N. F. Cheville, J. Stasko, M. Zimmerman, X. Hu, K. Liu, A. H. Fischer, C. Wang, In situ activation of platelets with checkpoint inhibitors for post-surgical cancer immunotherapy, *Nat. Biomed. Eng.* **1**, 0011 (2017).

156. D. M. Pardoll, The blockade of immune checkpoints in cancer immunotherapy., *Nat. Rev. Cancer* **12**, 252–64 (2012).

157. S. L. Topalian, C. G. Drake, D. M. Pardoll, Immune checkpoint blockade: A common denominator approach to cancer therapy, *Cancer Cell* **27**, 451–461 (2015).

158. K. M. Hargadon, C. E. Johnson, C. J. Williams, Immune checkpoint blockade therapy for cancer: An overview of FDA-approved immune checkpoint inhibitors, *Int. Immunopharmacol.* **62**, 29–39 (2018).

159. J. Tang, J. X. Yu, V. M. Hubbard-Lucey, S. T. Neftelinov, J. P. Hodge, Y. Lin, The clinical trial landscape for PD1/PDl1 immune checkpoint inhibitors, *Nat. Rev. Drug Discov.* **17**, 854–855 (2018).

160. J. F. Grosso, M. N. Jure-Kunkel, CTLA-4 blockade in tumor models: an overview of preclinical and translational research., *Cancer Immun.* **13**, 5 (2013).

161. A. M. Intlekofer, C. B. Thompson, f BASIC-TRANSLATIONAL REVIEW At the Bench : Preclinical rationale for CTLA-4 and PD-1 blockade as cancer immunotherapy, **94**, 25–39 (2017).

162. A. O. Kamphorst, A. O. Kamphorst, A. Wieland, T. Nasti, S. Yang, R. Zhang, D. L. Barber, B. T. Konieczny, Z. Candace, L. Koenig, K. Yu, G. L. Sica, A. H. Sharpe, G. J. Freeman, B. R. Blazar, L. A. Turka, K. Owonikoko, R. Pillai, S. S. Ramalingam, K. Araki, R. Ahmed, Rescue of exhausted CD8 T cells by PD-1 – targeted therapies is CD28-dependent, **0683** (2017), doi:10.1126/science.aaf0683.

163. I. Siddiqui, K. Schaeuble, V. Chennupati, S. A. Fuertes Marraco, S. Calderon-Copete, D. Pais Ferreira, S. J. Carmona, L. Scarpellino, D. Gfeller, S. Pradervand, S. A. Luther, D. E. Speiser, W. Held, Intratumoral Tcf1 + PD-1 + CD8 + T Cells with Stem-like Properties Promote Tumor Control in Response to Vaccination and Checkpoint Blockade Immunotherapy, *Immunity* **50**, 195–211.e10 (2019).

164. B. C. Miller, D. R. Sen, R. Al Abosy, K. Bi, Y. V. Virkud, M. W. LaFleur, K. B. Yates, A. Lako, K. Felt, G. S. Naik, M. Manos, E. Gjini, J. R. Kuchroo, J. J. Ishizuka, J. L. Collier, G. K. Griffin, S. Maleri, D. E. Comstock, S. A. Weiss, F. D. Brown, A. Panda, M. D. Zimmer, R. T. Manguso, F. S. Hodi, S. J. Rodig, A. H. Sharpe, W. N. Haining, Subsets of exhausted CD8 + T cells differentially mediate tumor control and respond to checkpoint blockade, *Nat. Immunol.* **20**, 326–336 (2019).

165. J. Brummelman, E. M. C. Mazza, G. Alvisi, F. S. Colombo, A. Grilli, J. Mikulak, D. Mavilio, M. Alloisio, F. Ferrari, E. Lopci, P. Novellis, G. Veronesi, E. Lugli, High-dimensional single cell analysis identifies stem-like cytotoxic CD8 $^{+}$ T cells infiltrating human tumors, *J. Exp. Med.* **215**, 2520–2535 (2018).

166. M. Sade-Feldman, K. Yizhak, S. L. Bjorgaard, J. P. Ray, C. G. de Boer, R. W. Jenkins, D. J. Lieb, J. H. Chen, D. T. Frederick, M. Barzily-Rokni, S. S. Freeman, A. Reuben, P. J. Hoover, A.-C. Villani, E.

Ivanova, A. Portell, P. H. Lizotte, A. R. Aref, J.-P. Eliane, M. R. Hammond, H. Vitzthum, S. M. Blackmon, B. Li, V. Gopalakrishnan, S. M. Reddy, Z. A. Cooper, C. P. Paweletz, D. A. Barbie, A. Stemmer-Rachamimov, K. T. Flaherty, J. A. Wargo, G. M. Boland, R. J. Sullivan, G. Getz, N. Hacohen, Defining T Cell States Associated with Response to Checkpoint Immunotherapy in Melanoma, *Cell* **175**, 998–1013.e20 (2018).

167. V. R. Juneja, K. A. Mcguire, R. T. Manguso, M. W. Lafleur, N. Collins, W. N. Haining, G. J. Freeman, A. H. Sharpe, PD-L1 on tumor cells is sufficient for immune evasion in immunogenic tumors and inhibits CD8 T cell cytotoxicity, , 895–904 (2017).

168. J. Willem, K. A. Marijt, M. J. A. Schoonderwoerd, T. Van Hall, M. F. Fransen, PD-L1 expression on malignant cells is no prerequisite for checkpoint therapy, *Oncoimmunology* **6**, 1–7 (2017).

169. C. Kümpers, M. Jokic, O. Haase, A. Offermann, W. Vogel, V. Grätz, E. A. Langan, S. Perner, P. Terheyden, Immune Cell Infiltration of the Primary Tumor, Not PD-L1 Status, Is Associated With Improved Response to Checkpoint Inhibition in Metastatic Melanoma, *Front. Med.* **6**, 1–11 (2019).

170. E. J. Crosby, J. Wei, X. Y. Yang, G. Lei, T. Wang, C. X. Liu, P. Agarwal, A. J. Korman, M. A. Morse, K. Gouin, S. R. V. Knott, H. K. Lyerly, Z. C. Hartman, Complimentary mechanisms of dual checkpoint blockade expand unique T-cell repertoires and activate adaptive anti-tumor immunity in triple-negative breast tumors, *Oncoimmunology* **7** (2018), doi:10.1080/2162402X.2017.1421891.

171. L. Robert, J. Tsoi, X. Wang, R. Emerson, B. Homet, T. Chodon, S. Mok, R. R. Huang, A. J. Cochran, B. Comin-Anduix, R. C. Koya, T. G. Graeber, H. Robins, A. Ribas, CTLA4 blockade broadens the peripheral T-cell receptor repertoire, *Clin. Cancer Res.* **20**, 2424–2432 (2014).

172. K. E. Yost, A. T. Satpathy, D. K. Wells, Y. Qi, C. Wang, R. Kageyama, K. L. McNamara, J. M. Granja, K. Y. Sarin, R. A. Brown, R. K. Gupta, C. Curtis, S. L. Bucktrout, M. M. Davis, A. L. S. Chang, H. Y. Chang, Clonal replacement of tumor-specific T cells following PD-1 blockade, *Nat. Med.* **25**, 1251–1259 (2019).

173. P. C. Tumeh, C. L. Harview, J. H. Yearley, I. P. Shintaku, E. J. M. Taylor, L. Robert, B. Chmielowski, M. Spasic, G. Henry, V. Ciobanu, A. N. West, M. Carmona, C. Kivork, E. Seja, G. Cherry, A. J. Gutierrez, T. R. Grogan, C. Mateus, G. Tomasic, J. A. Glaspy, R. O. Emerson, H. Robins, R. H.

Pierce, D. A. Elashoff, C. Robert, A. Ribas, PD-1 blockade induces responses by inhibiting adaptive immune resistance., *Nature* **515**, 568–71 (2014).

174. E. Cha, M. Klinger, Y. Hou, C. Cummings, A. Ribas, M. Faham, L. Fong, Improved survival with T cell clonotype stability after anti-CTLA-4 treatment in cancer patients, *Sci. Transl. Med.* **6**, 1–10 (2014).

175. M. H. Spitzer, Y. Carmi, N. E. Reticker-Flynn, S. S. Kwek, D. Madhireddy, M. M. Martins, P. F. Gherardini, T. R. Prestwood, J. Chabon, S. C. Bendall, L. Fong, G. P. Nolan, E. G. Engleman, Systemic Immunity Is Required for Effective Cancer Immunotherapy, *Cell* **168**, 487–502.e15 (2017).

176. M. Poggio, T. Hu, C.-C. Pai, B. Chu, C. D. Belair, A. Chang, E. Montabana, U. E. Lang, Q. Fu, L. Fong, R. Blelloch, Suppression of Exosomal PD-L1 Induces Systemic Anti-tumor Immunity and Memory, *Cell* **177**, 414–427.e13 (2019).

177. H. Salmon, J. Idoyaga, A. Rahman, M. Leboeuf, R. Remark, S. Jordan, M. Casanova-Acebes, M. Khudoynazarova, J. Agudo, N. Tung, S. Chakarov, C. Rivera, B. Hogstad, M. Bosenberg, D. Hashimoto, S. Gnjatic, N. Bhardwaj, A. K. Palucka, B. D. Brown, J. Brody, F. Ginhoux, M. Merad, Expansion and Activation of CD103+ Dendritic Cell Progenitors at the Tumor Site Enhances Tumor Responses to Therapeutic PD-L1 and BRAF Inhibition, *Immunity* **44**, 924–938 (2016).

178. E. W. Roberts, M. L. Broz, M. Binnewies, M. B. Headley, A. E. Nelson, D. M. Wolf, T. Kaisho, D. Bogunovic, N. Bhardwaj, M. F. Krummel, Critical Role for CD103+/CD141+ Dendritic Cells Bearing CCR7 for Tumor Antigen Trafficking and Priming of T Cell Immunity in Melanoma, *Cancer Cell* **30**, 324–336 (2016).

179. M. F. Fransen, T. C. Van Der Sluis, F. Ossendorp, R. Arens, C. J. M. Melief, Controlled local delivery of CTLA-4 blocking antibody induces CD8 + T-cell-dependent tumor eradication and decreases risk of toxic side effects, *Clin. Cancer Res.* **19**, 5381–5389 (2013).

180. M. F. Fransen, T. Van Hall, F. Ossendorp, M. F. Fransen, M. Schoonderwoerd, P. Knopf, M. G. M. Camps, Tumor-draining lymph nodes are pivotal in PD- 1 / PD-L1 checkpoint therapy Find the latest version : Tumor-draining lymph nodes are pivotal in PD-1 / PD-L1 checkpoint therapy, **3**, 1–7 (2018).

181. M. Miron, B. V. Kumar, W. Meng, T. Granot, D. J. Carpenter, T. Senda, D. Chen, A. M. Rosenfeld, B. Zhang, H. Lerner, A. L. Friedman, U. Hershberg, Y. Shen, A. Rahman, E. T. Luning Prak, D. L.

Farber, Human Lymph Nodes Maintain TCF-1 hi Memory T Cells with High Functional Potential and Clonal Diversity throughout Life , *J. Immunol.* **201**, 2132–2140 (2018).

182. D. M. Francis, S. N. Thomas, Progress and opportunities for enhancing the delivery and ef fi cacy of checkpoint inhibitors for cancer immunotherapy ☆ , ☆☆, *Adv. Drug Deliv. Rev.* (2017), doi:10.1016/j.addr.2017.04.011.

183. A. Schudel, D. M. Francis, S. N. Thomas, Material design for lymph node drug delivery, *Nat. Rev. Mater.* **4** (2019), doi:10.1038/s41578-019-0110-7.

184. I. Sagiv-Barfi, D. K. Czerwinski, S. Levy, I. S. Alam, A. T. Mayer, S. S. Gambhir, R. Levy, Eradication of spontaneous malignancy by local immunotherapy, *Sci. Transl. Med* **10** (2018), doi:10.1126/scitranslmed.aan4488.

185. J. R. Ingram, O. S. Blomberg, J. T. Sockolosky, L. Ali, F. I. Schmidt, N. Pishesha, C. Espinosa, S. K. Dougan, K. C. Garcia, H. L. Ploegh, M. Dougan, Localized CD47 blockade enhances immunotherapy for murine melanoma, *Proc. Natl. Acad. Sci. U. S. A.* **114**, 10184–10189 (2017).

186. L. van Hooren, L. C. Sandin, I. Moskalev, P. Ellmark, A. Dimberg, P. Black, T. H. Tötterman, S. M. Mangsbo, Local checkpoint inhibition of CTLA-4 as a monotherapy or in combination with anti-PD1 prevents the growth of murine bladder cancer., *Eur. J. Immunol.* **46**, 1–9 (2016).

187. L. Kähäri, R. Fair-Mäkelä, K. Auvinen, P. Rantakari, S. Jalkanen, J. Ivaska, M. Salmi, Transcytosis route mediates rapid delivery of intact antibodies to draining lymph nodes, *J. Clin. Invest.* **130** (2019), doi:10.1172/JCI125740.

188. S. Khan, D. J. Burt, C. Ralph, F. C. Thistlethwaite, R. E. Hawkins, E. Elkord, Tremelimumab (anti-CTLA4) mediates immune responses mainly by direct activation of T effector cells rather than by affecting T regulatory cells, *Clin. Immunol.* **138**, 85–96 (2011).

189. A. Sharma, S. K. Subudhi, J. Blando, J. Scutti, L. Vence, J. Wargo, J. P. Allison, A. Ribas, P. Sharma, Anti-CTLA-4 immunotherapy does not deplete Foxp3 þ regulatory T cells (Tregs) in human cancers, *Clin. Cancer Res.* **25**, 1233–1238 (2019).

190. R. S. Herbst, J. C. Soria, M. Kowanetz, G. D. Fine, O. Hamid, M. S. Gordon, J. A. Sosman, D. F.

McDermott, J. D. Powderly, S. N. Gettinger, H. E. K. Kohrt, L. Horn, D. P. Lawrence, S. Rost, M. Leabman, Y. Xiao, A. Mokatrin, H. Koeppen, P. S. Hegde, I. Mellman, D. S. Chen, F. S. Hodi, Predictive correlates of response to the anti-PD-L1 antibody MPDL3280A in cancer patients, *Nature* **515**, 563–567 (2014).

191. A. Gros, M. R. Parkhurst, E. Tran, A. Pasetto, P. F. Robbins, S. Ilyas, T. D. Prickett, J. J. Gartner, J. S. Crystal, I. M. Roberts, K. Trebska-Mcgowan, J. R. Wunderlich, J. C. Yang, S. A. Rosenberg, Prospective identification of neoantigen-specific lymphocytes in the peripheral blood of melanoma patients, *Nat. Med.* **22**, 433–438 (2016).

192. A. O. Kamphorst, R. N. Pillai, S. Yang, T. H. Nasti, R. S. Akondy, A. Wieland, G. L. Sica, K. Yu, L. Koenig, N. T. Patel, M. Behera, H. Wu, M. McCausland, Z. Chen, C. Zhang, F. R. Khuri, T. K. Owonikoko, R. Ahmed, S. S. Ramalingam, Proliferation of PD-1+ CD8 T cells in peripheral blood after PD-1–targeted therapy in lung cancer patients, *Proc. Natl. Acad. Sci.* **114**, 4993–4998 (2017).

193. C. S. Jansen, N. Prokhnevska, V. A. Master, M. G. Sanda, J. W. Carlisle, M. A. Bilen, M. Cardenas, S. Wilkinson, R. Lake, A. G. Sowalsky, R. M. Valanparambil, W. H. Hudson, D. Mcguire, K. Melnick, A. I. Khan, K. Kim, Y. M. Chang, A. Kim, C. P. Filson, M. Alemozaffar, A. O. Osunkoya, P. Mullane, C. Ellis, R. Akondy, An intra-tumoral niche maintains and differentiates stem-like CD8 T cells, *Nature* (2019), doi:10.1038/s41586-019-1836-5.

194. L. Kagan, M. R. Turner, S. V. Balu-Iyer, D. E. Mager, Subcutaneous absorption of monoclonal antibodies: Role of dose, site of injection, and injection volume on rituximab pharmacokinetics in rats, *Pharm. Res.* **29**, 490–499 (2012).

195. M. Viola, J. Sequeira, R. Seiça, F. Veiga, J. Serra, Subcutaneous delivery of monoclonal antibodies : How do we get there ?, **286**, 301–314 (2018).

196. D. R. Sen, J. Kaminski, R. A. Barnitz, M. Kurachi, U. Gerdemann, K. B. Yates, H. Tsao, J. Godec, M. W. Lafleur, F. D. Brown, P. Tonnerre, R. T. Chung, D. C. Tully, T. M. Allen, N. Frahm, G. M. Lauer, E. J. Wherry, N. Yosef, W. N. Haining, Supplementary Materials for The epigenetic landscape of T cell exhaustion, **354** (2016), doi:10.1126/science.aae0491.

197. E. J. Wherry, J. Godec, W. N. Haining, S. L. Berger, C. Bartman, D. R. Sen, B. Bengsch, J. M.

Schenkel, G. Vahedi, P. M. Odorizzi, K. E. Pauken, A. M. Drake, S. Manne, A. C. Huang, M. Kurachi, R. A. Barnitz, M. A. Sammons, Z. Chen, O. Khan, Epigenetic stability of exhausted T cells limits durability of reinvigoration by PD-1 blockade, *Science (80-.).* **354**, 1160–1165 (2016).

198. H. E. Ghoneim, Y. Fan, A. Moustaki, H. A. Abdelsamed, P. Dash, P. Dogra, R. Carter, W. Awad, G. Neale, P. G. Thomas, B. Youngblood, De Novo Epigenetic Programs Inhibit PD-1 Blockade-Mediated T Cell Rejuvenation, *Cell* **170**, 142–157.e19 (2017).

199. D. S. Chen, I. Mellman, Oncology meets immunology: The cancer-immunity cycle, *Immunity* **39**, 1–10 (2013).

200. S. L. Topalian, C. G. Drake, D. M. Pardoll, Immune checkpoint blockade: a common denominator approach to cancer therapy, *Cancer Cell* **27**, 450–461 (2015).

201. C. M. Fares, E. M. Van Allen, C. G. Drake, J. P. Allison, S. Hu-Lieskovan, Mechanisms of Resistance to Immune Checkpoint Blockade: Why Does Checkpoint Inhibitor Immunotherapy Not Work for All Patients?, *Am. Soc. Clin. Oncol. Educ. B.* , 147–164 (2019).

202. Z. G. Chen, Small-molecule delivery by nanoparticles for anticancer therapy, *Trends Mol. Med.* **16**, 594–602 (2010).

203. E. Blanco, H. Shen, M. Ferrari, Principles of nanoparticle design for overcoming biological barriers to drug delivery, *Nat. Biotechnol.* **33**, 941 (2015).

204. L. Ducry, B. Stump, Antibody-drug conjugates: Linking cytotoxic payloads to monoclonal antibodies, *Bioconjug. Chem.* **21**, 5–13 (2010).

205. T. Carter, P. Mulholland, K. Chester, Antibody-targeted nanoparticles for cancer treatment, *Immunotherapy* **8**, 941–958 (2016).

206. L. Zhu, V. P. Torchilin, Stimulus-responsive nanopreparations for tumor targeting, *Integr. Biol. (United Kingdom)* **5**, 96–107 (2013).

207. S. N. Thomas, E. Vokali, A. W. Lund, J. A. Hubbell, M. A. Swartz, Targeting the tumor-draining lymph node with adjuvanted nanoparticles reshapes the anti-tumor immune response, *Biomaterials* (2013), doi:10.1016/j.biomaterials.2013.10.003.

208. A. J. van der Vlies, C. P. O'Neil, U. Hasegawa, N. Hammond, J. A. Hubbell, Synthesis of Pyridyl

Disulfide-Functionalized Nanoparticles for Conjugating Thiol -Containing Small Molecules, Peptides and Proteins.pdf, *Bioconjug. Chem.* **21**, 653–662 (2010).

209. D. V. F. Tauriello, S. Palomo-Ponce, D. Stork, A. Berenguer-Llergo, J. Badia-Ramentol, M. Iglesias, M. Sevillano, S. Ibiza, A. Cañellas, X. Hernando-Momblona, D. Byrom, J. A. Matarin, A. Calon, E. I. Rivas, A. R. Nebreda, A. Riera, C. S. O. Attolini, E. Batlle, TGFβ drives immune evasion in genetically reconstituted colon cancer metastasis, *Nature* **554**, 538–543 (2018).

210. S. Mariathasan, S. J. Turley, D. Nickles, A. Castiglioni, K. Yuen, Y. Wang, E. E. Kadel, H. Koeppen, J. L. Astarita, R. Cubas, S. Jhunjhunwala, R. Banchereau, Y. Yang, Y. Guan, C. Chalouni, J. Ziai, Y. Şenbabaoğlu, S. Santoro, D. Sheinson, J. Hung, J. M. Giltnane, A. A. Pierce, K. Mesh, S. Lianoglou, J. Riegler, R. A. D. Carano, P. Eriksson, M. Höglund, L. Somarriba, D. L. Halligan, M. S. Van Der Heijden, Y. Loriot, J. E. Rosenberg, L. Fong, I. Mellman, D. S. Chen, M. Green, C. Derleth, G. D. Fine, P. S. Hegde, R. Bourgon, T. Powles, TGFβ attenuates tumour response to PD-L1 blockade by contributing to exclusion of T cells, *Nature* **554**, 544–548 (2018).

211. D. Vijayan, A. Young, M. W. L. Teng, M. J. Smyth, Targeting immunosuppressive adenosine in cancer, *Nat. Publ. Gr.* **17**, 709–724 (2017).

212. A. Ohta, A. Ohta, M. Madasu, R. Kini, M. Subramanian, N. Goel, M. Sitkovsky, A2A Adenosine Receptor May Allow Expansion of T Cells Lacking Effector Functions in Extracellular Adenosine-Rich Microenvironments, *J. Immunol.* **183**, 5487–5493 (2009).

213. S. Loi, S. Pommey, B. Haibe-Kains, P. A. Beavis, P. K. Darcy, M. J. Smyth, J. Stagg, CD73 promotes anthracycline resistance and poor prognosis in triple negative breast cancer, *Proc. Natl. Acad. Sci. U. S. A.* **110**, 11091–11096 (2013).

214. B. A. Pulaski, S. Ostrand-Rosenberg, Mouse 4T1 Breast Tumor Model, *Curr. Protoc. Immunol.* **39**, 20.2.1-20.2.16 (2000).

215. A. Xia, Y. Zhang, J. Xu, T. Yin, X.-J. Lu, T Cell Dysfunction in Cancer Immunity and Immunotherapy, *Front. Immunol.* **10**, 1719 (2019).

216. B. S. Guerrouahen, C. Maccalli, C. Cugno, S. Rutella, E. T. Akporiaye, Reverting Immune Suppression to Enhance Cancer Immunotherapy, *Front. Oncol.* **9** (2020), doi:10.3389/fonc.2019.01554.

217. M. Arruebo, M. Valladares, Á. González-Fernández, Antibody-conjugated nanoparticles for biomedical applications, *J. Nanomater.* **2009** (2009), doi:10.1155/2009/439389.